

How does Cdc14 order exit from mitosis?

Meghna Kataria

University College London
and

The Francis Crick Institute

PhD Supervisor: Dr Frank Uhlmann

A thesis submitted for the degree of
Doctor of Philosophy
University College London

September 2016

Declaration

I, Meghna Kataria, confirm that the work presented in this thesis is my own. Where information has been derived from other sources, I confirm that this has been indicated in the thesis.

Abstract

Accurate progress through the cell cycle necessitates robust order and timing of events, the molecular basis for which is incompletely understood. During exit from mitosis, it is vital for cells to execute events in a precise sequence. Completion of chromosome segregation must precede chromatin decondensation, or indeed, cytokinesis.

In budding yeast, the ordering of mitotic exit events is imposed by the changing balance between Cdk kinase activity, which begins to decline upon anaphase entry, and increasing activity of the major Cdk-counteracting phosphatase, Cdc14. In early anaphase, Cdk activity is still high and little Cdc14 is active. Nonetheless, certain substrates, such as the spindle stabilizer Fin1, are dephosphorylated to facilitate early anaphase events, e.g. spindle elongation. It has been shown that Cdc14 has a high catalytic efficiency towards its early substrates, when compared to later substrates.

In this study, we seek a molecular understanding of mitotic exit by probing the biochemical characteristics of early Cdc14 substrate recognition. Through complementary *in vitro* and *in vivo* approaches, we find that Cdc14 is a dimer and the non-conserved C-terminal domain is not important for dimerization or substrate dephosphorylation. Cdc14 prefers phosphoserines over phosphothreonines, as well as a basic residue in the +3 position, even when presented in the context of Fin1, a highly efficient substrate. Further, it engages with this substrate via its non-catalytic N-terminal domain.

We also find that Fin1 possesses a higher affinity towards Cdc14 compared to other substrates, which is independent of its phosphorylation sites. Truncation analysis revealed that Fin1's C-terminus is important for this binding, and has a small impact on catalysis. Further, we have also established that early S-phase cyclin degradation is partly responsible for ensuring early dephosphorylation of this protein. In summary, multiple mechanisms collaborate to ensure efficient early substrate dephosphorylation.

Acknowledgements

First and foremost, I want to thank Frank for all the support and guidance through these years, and for being a great supervisor. I also want to express my gratitude to my thesis committee, Neil and Thomas, for their continued support.

Thanks to all of Chromosome Segregation Lab past and present for making the lab such fun and a great place to be. I'm indebted to Céline, Yasuto and Thomas for showing me the ropes and for always being helpful. In particular, thanks to my fellow cell cycle enthusiasts, my 'buds' and partners in crime Molly and Sandra for long scientific and non-scientific discussions interspersed with general hilarity, and support in and out of the lab. I could not have imagined completing this PhD any way other than being sandwiched between you two.

I also want to thank the peptide chemistry, structural biology and mass spectrometry facilities for all their help.

I'm grateful to friends in Delhi, Edinburgh and London who make me feel that I have three cities to call home.

Finally, my heartfelt gratitude to Alex, my family, Rohan, mom and dad, for being amazing in general and showering me with love, support and affection.

Table of Contents

Abstract	3
Table of Contents	5
Table of figures	9
List of tables	12
Abbreviations	13
Chapter 1. Introduction	16
1.1 The eukaryotic cell cycle	16
1.2 The budding yeast cell cycle	17
1.3 The cell cycle is a highly regulated process	18
1.3.1 Cyclin-dependent kinases are the master regulators of the cell cycle	19
1.3.2 Cdk activity is temporally regulated by phosphorylation	20
1.3.3 Cdks associate with a number of cyclins throughout the cell cycle and control various cellular events	20
1.4 Controlling ordered phosphorylation – a matter of quality or quantity?	23
1.4.1 Qualitative model for ordered substrate phosphorylation	23
1.4.2 A quantitative model for cell cycle regulation.....	25
1.5 A role for phosphatases in cell cycle regulation	27
1.5.1 Major phosphatases in eukaryotes	28
1.6 Cdc14 and budding yeast mitotic exit	30
1.6.1 Discovery of Cdc14 as a phosphatase	30
1.6.2 Cdc14 is a key regulator of exit from mitosis	31
1.6.3 Cdc14 is required for a number of mitotic exit events.....	32
1.6.4 Regulation of Cdc14 activity	33
1.7 Cdc14 and phosphatases in other organisms	37
1.7.1 <i>Schizosaccharomyces pombe</i> (fission yeast).....	39
1.7.2 Mammalian cells	40
1.7.3 <i>Other organisms</i>	44
1.8 Biochemical properties of Cdc14	45
1.8.1 Mechanism of catalysis.....	45
1.8.2 Structural properties.....	47
1.8.3 Phosphosite specificity of Cdc14	49
1.9 The quantitative model of exit from mitosis	51
1.10 Early substrate dephosphorylation	54
1.10.1 Clb5 degradation in early anaphase	55
1.10.2 Early substrate dephosphorylation – a role for docking sites?	57
1.11 Project aims	60
1.11.1 Biochemical features of Cdc14 that enable substrate recognition....	60
1.11.2 What factors influence efficient early substrate dephosphorylation?	61
Chapter 2. Materials and Methods	63
2.1 Yeast techniques	63
2.1.1 Yeast strains and growth conditions	63
2.1.2 Strain list	64
2.1.3 Cell synchronisation.....	65

2.1.4	Yeast transformation.....	65
2.1.5	Yeast mating and tetrad dissection.....	66
2.2	General biochemistry	66
2.2.1	Preparation of yeast extracts by protein precipitation.....	66
2.2.2	SDS-polyacrylamide gel electrophoresis (PAGE) and Western blotting	67
2.3	Other biophysical and biochemical techniques	68
2.3.1	Microscale thermophoresis (MST).....	68
2.3.2	Crosslinking and mass spectrometry.....	69
2.3.3	Peptide array analysis.....	70
2.3.4	Size exclusion chromatography coupled with multiple-angle laser light scattering (SEC-MALLS).....	70
2.3.5	Glycerol gradient sedimentation	71
2.3.6	Pull-down assays.....	71
2.4	Enzyme activity assays	72
2.4.1	<i>In vitro</i> Clb2-Cdc28 kinase assay	72
2.4.2	<i>In vitro</i> Cdc14 phosphatase assay.....	73
2.4.3	<i>para</i> -Nitrophenyl phosphate phosphatase (<i>p</i> -NPP) assay	73
2.5	Protein purification	74
2.5.1	Purification of His ₆ -Cdc14, GST-Cdc14, Fin1, Ask1 and Sli15 and Clb2-Cdc28.....	74
2.5.2	Purification of Cdc14 domains	74
2.5.3	Purification of Net1 ¹⁻⁶⁰⁰	76
2.6	Molecular biology and DNA manipulation	76
2.6.1	Genomic DNA preparation.....	76
2.6.2	Polymerase Chain Reaction (PCR)	77
2.6.3	Strain design.....	77
2.6.4	Agarose gel electrophoresis	78
2.6.5	Plasmid construction.....	78
2.7	Microscopy and cell biology	79
2.7.1	<i>In situ</i> Immunofluorescence (IF)	79
2.7.2	Cell cycle analysis by Flow Cytometry (FACS).....	79
2.8	Bioinformatic Analysis	80
Chapter 3.	Biochemical properties of Cdc14	81
3.1	Recombinant Cdc14 is a tight dimer in solution.....	82
3.1.1	Gradient sedimentation and gel filtration indicate that Cdc14 behaves as either a dimer or a trimer in solution.....	82
3.1.2	SEC-MALLS shows that Cdc14 is a dimer, with its C-terminal domain being dispensable for dimerization	85
3.2	Contribution of Cdc14 domains to substrate recognition and dephosphorylation.....	88
3.2.1	The non-catalytic N-terminal domain A interacts with Cdc14 substrates.....	88
3.2.2	Cdc14 ^{AB} is a hypomorphic Cdc14 allele, whilst the C-terminal domain is dispensable for Cdc14 function <i>in vivo</i>	90
Chapter 4.	Phosphosite-specific features of efficient Cdc14 substrates. 97	
4.1	Phosphosite composition of Cdc14 substrates dephosphorylated 'early' and 'late' into anaphase is similar	97

4.2 Phosphosite mutants of Fin1 reveal Cdc14 substrate specificity <i>in vivo</i>	100
4.2.1 Dephosphorylation of Fin1 ^{6TP} is markedly delayed <i>in vivo</i>	101
4.2.2 Fin1 ^{6TPxA} is dephosphorylated very early into anaphase	103
4.2.3 The ratio of kinase to phosphatase activities explains the dephosphorylation timings of Fin1 ^{WT} , Fin1 ^{6TP} , and Fin1 ^{6TPxA}	107
Chapter 5. Phosphosite-independent features that contribute to dephosphorylation of the early substrate, Fin1	112
5.1 Early degradation of Clb5 in part enables early dephosphorylation of the Clb5-specific substrate, Fin1	112
5.1.1 Mutation of the RxL motif within Fin1 does not hasten its dephosphorylation <i>in vivo</i>	112
5.1.2 Stabilization of Clb5 throughout the cell cycle leads to impaired Fin1 dephosphorylation	114
5.1.3 Disruption of the RxL motif of Fin1 restores its dephosphorylation timing in the Clb5 ^{Δdb} background	116
5.2 Fin1 causes a modest stimulation of Cdc14's phosphatase activity	118
5.3 Fin1 is a high affinity Cdc14 substrate	120
5.4 Crosslinking and mass spectrometry identify extensive interactions between Cdc14 and Fin1	123
5.5 Cdc14 binds to a number of Fin1 peptides <i>in vitro</i>	126
5.5.1 Cdc14 interacts with preferred Cdk consensus sites within Fin1 in addition to other sequence features <i>in vitro</i>	126
5.5.2 Fin1 dephosphorylation timing <i>in vivo</i> is remarkably resilient to mutagenesis	128
5.6 Binding of Fin1 to Cdc14 exerts a small effect on its efficient catalysis	132
5.6.1 Truncation analysis of Fin1	132
5.6.2 Cdc14 targets Fin1 ^{ΔC250} with reduced efficiency	136
5.6.3 Dephosphorylation timing of Fin1 ^{ΔC250} is same as that of the wild type protein	138
5.7 Probing Cdc14 - Fin1 interactions using Net1 as a tool	140
5.7.1 Net1 and Fin1 can outcompete each other for binding to Cdc14 ...	142
5.7.2 Net1 and Fin1 share distinct, but overlapping binding sites within Cdc14	145
Chapter 6. Discussion and future perspectives	147
6.1 Biochemical properties of Cdc14	147
6.1.1 Cdc14 is a dimeric protein	147
6.1.2 Implications of Cdc14 dimerization	148
6.2 What is the function of different Cdc14 domains?	149
6.2.1 Binding of Net1 and Fin1 to Cdc14 is mutually exclusive	150
6.2.2 Domain C is primarily a hub of regulatory input into Cdc14	151
6.3 Phosphosite composition of a substrate has a profound impact on phosphorylation/dephosphorylation equilibrium	152
6.3.1 Cdc14 is a serine-directed phosphatase	152
6.3.2 Which phosphatase dephosphorylates threonines <i>in vivo</i> ?	153

6.3.3 Phosphosite preferences of Cdk can also influence substrate dephosphorylation	155
6.3.4 Phosphosite-level knowledge of dephosphorylation reaction is needed.....	156
6.4 Phosphosite-independent factors in substrate dephosphorylation	157
6.4.1 The role of early degradation of Clb5 in substrate dephosphorylation	157
6.4.2 Role of Cdc14 docking site interactions in Fin1 dephosphorylation	158
6.5 From yeast to higher organisms	160
6.5.1 Substrate dephosphorylation in higher eukaryotes.....	160
6.5.2 Role of phosphatases and future avenues	161
Chapter 7. Appendix	163
7.1 Determination of stoichiometry and shape of Cdc14	163
7.1.1 Svedberg equation.....	163
7.1.2 S_{max} formula	163
7.2 List of early phosphopeptides	163
7.3 Michaelis-Menten equation	165
Reference List	166

Table of figures

Figure 1.1 – The budding yeast cell cycle.....	18
Figure 1.2 - Various cyclin-Cdk complexes are found throughout the cell cycle.	22
Figure 1.3 - The PSP superfamily.....	29
Figure 1.4 - Cdk/Cdc14 activity levels throughout the cell cycle.....	37
Figure 1.5 - Diverse roles of Cdc14 in different organisms.....	38
Figure 1.6 - Cdc14 catalysis mechanism.....	46
Figure 1.7 - Structure of ScCdc14.....	48
Figure 1.8 – Structural basis for pSer specificity of Cdc14.	50
Figure 1.9 - A quantitative model for Cdk substrate dephosphorylation during mitotic exit.....	53
Figure 1.10 - Balance of powers in early anaphase.....	55
Figure 1.11 – A kinase-centric hypothesis for early substrate dephosphorylation.	56
Figure 1.12 – Regulator-substrate interactions are often facilitated by short linear binding motifs.....	59
Figure 3.1 - Glycerol gradient sedimentation of Cdc14.....	83
Figure 3.2 - Size exclusion chromatography of Cdc14.	84
Figure 3.3 - Elution profiles of Cdc14 (A) and Cdc14 ^{AB} (B) determined through SEC-MALLS.....	87
Figure 3.4 - Domains of Cdc14.....	89
Figure 3.5 – Cdc14 domain interactions with the substrates Fin1 and Sli15. ...	90
Figure 3.6 – Comparison of phosphatase activities of wild type and truncated GST-tagged Cdc14 proteins.	91
Figure 3.7 – Cdc14 ^{AB} does not exhibit a growth defect.	92
Figure 3.8 – Dephosphorylation of substrates is delayed in Cdc14 ^{AB}	93
Figure 3.9 – Cdc14 ^{AB} is not mislocalized in the G1 phase.....	95
Figure 4.1 – Comparison of sequence logos derived from ‘early’, ‘late’ and ‘Cdk’ phosphopeptides.....	99

Figure 4.2 - Comparison of <i>in vivo</i> dephosphorylation timings of Fin1 ^{WT} and Fin1 ^{6TP}	103
Figure 4.3 – Fin1 ^{TPxA} is dephosphorylated very early in anaphase.	105
Figure 4.4 – Dephosphorylation timing of Fin1 ^{+3A} is unaffected.	106
Figure 4.5 – Fin1 phosphosite mutants interact efficiently with the immobilized phosphatase.	108
Figure 4.6 – Clb2-Cdc28 differs in its abilities to phosphorylate Fin1 ^{WT} , Fin1 ^{6TP} , and Fin1 ^{6TPxA}	109
Figure 4.7 – Cdc14 differs in its abilities to dephosphorylate Fin1 ^{WT} , Fin1 ^{6TP} , and Fin1 ^{6TPxA}	110
Figure 5.1 – Comparison of <i>in vivo</i> dephosphorylation of Fin1 ^{WT} and Fin1 ^{KNL-AAA}	114
Figure 5.2 – Comparison of Fin1 dephosphorylation in Clb5 ^{WT} and Clb5 ^{Δdb} strains.	116
Figure 5.3 – Comparison of Fin1 dephosphorylation in Clb5 ^{WT} and Clb5 ^{Δdb} strains.	117
Figure 5.4 – Fin1 causes a moderate stimulation of the phosphatase activity of Cdc14 <i>in vitro</i>	119
Figure 5.5 - Fin1 shows increased affinity to Cdc14 compared to Ask1.	121
Figure 5.6 – Crosslinking and mass spectrometric analysis of Fin1 and Cdc14.	124
Figure 5.7 – Peptide array analysis reveals Cdc14-binding peptides within Fin1.	126
Figure 5.8 – Examples of time courses from the mutagenesis screen for Fin1 mutants with altered dephosphorylation timings.	131
Figure 5.9 – Schematic depicting truncation mutants of Fin1.	134
Figure 5.10 – Pull-down of Fin1 truncation mutants by immobilized GST-Cdc14	135
Figure 5.11 – Comparison of catalytic efficiencies of Cdc14 towards Fin1 ^{WT} and Fin1 ^{ΔC250}	137
Figure 5.12 – Coimmunoprecipitation of Fin1 ^{WT} and Fin1 ^{ΔC250} with Cdc14. ...	138

Figure 5.13 – Comparison of *in vivo* dephosphorylation of Fin1^{WT} and Fin1^{ΔC250}.
..... 140

Figure 5.14 – Cdc14 point mutations that disrupt Net1 interaction. 142

Figure 5.15 – Fin1 and Net1 can compete for binding to Cdc14. 144

Figure 5.16 – Tungstate ions do not compete with Net1 or Fin1 for binding to
Cdc14..... 144

Figure 5.17 – Features of Fin1 and Net1 binding to Cdc14. 146

List of tables

Table 2.1 – Media composition	63
Table 2.2 – List of strains used in this thesis.....	64
Table 2.3 – List of antibodies used	68
Table 4.1 – Phosphosite composition of Fin1 alleles.....	101
Table 4.2 – A summary of the abilities of Clb2 and Cdc14 to target the three Fin1 variants.	111
Table 5.1 - List of all Fin1 mutants tested for changes in <i>in vivo</i> dephosphorylation timing.....	130
Table 7.1 – List of ‘early’ substrates used for the sequence logo in Fig. 4.1..	165

Abbreviations

Ab	Antibody
APC/C	Anaphase promoting Complex/Cyclosome
Ase	Anaphase spindle elongation
Ask	Associated with Spindles and Kinetochores
BSA	Bovine Serum Albumin
Bub	Budding Uninhibited by Benzimidazole
BS3	Bissulfosuccinimidyl suberate
Cdk	Cyclin Dependent Kinase
Cdc	Cell Division Cycle
Cdh	Cdc20 Homolog
DAPI	4',6-Diamidino-2- phenylindole
Dbf	Dumb Bell Former
Dbp	Dead Box Protein
DiFMUP	6,8-Difluoro-4-Methylumbelliferyl Phosphate
dNTP	Deoxynucleotide triphosphate
DNA	Deoxyribonucleic Acid
DTT	Dithiothreitol
ECL	Enhanced chemiluminescence
EDTA	Ethylene diamine tetraacetic acid
FACS	Fluorescence activated cell sorting
FEAR	Cdc fourteen early anaphase release
Fin	Filaments in between nuclei
G1/2	Gap phase $\frac{1}{2}$
GEF	Guanine Exchange Factor
GFP	Green fluorescent protein
Glc	Glycogen
GST	Glutathione S-Transferase
HA	Hemagglutinin
HRP	Horseradish peroxidase
k_{cat}	Turnover number

K_d	Dissociation constant
K_i	Constant of inhibition
K_M	Michaelis constant
kDa	kiloDalton
M	Mitosis
MAP	Mitogen Activated Protein
MEF	Mouse Embryonic Fibroblast
MEN	Mitotic Exit Network
min	minute
mM	milliMolar
ml	millilitre
MPF	Maturation Promoting Factor
MST	Microscale thermophoresis
NES	Nuclear Export Signal
Net	Nucleolar silencing Establishing factor & Telophase regulator
NLS	Nuclear Localization Signal
nm	nanometre
nM	nanomolar
OA	Okadaic Acid
Orc	Origin Recognition Complex
PCNA	Proliferating Cell Nuclear Antigen
PCR	Polymerase Chain Reaction
PEG	Polyethylene Glycol
PI	Propidium Iodide
pI	Isoelectric point
PIP	PCNA-interacting Protein
<i>p</i> -NPP	<i>para</i> -Nitrophenyl phosphate
PP	Protein Phosphatase
PSP	Protein Serine Phosphatase
PTP	Protein Threonine Phosphatase
rDNA	Ribosomal Deoxyribonucleic Acid

RNA	Ribonucleic Acid
RNase	Ribonuclease
rRNA	Ribosomal Ribonucleic Acid
rpm	revolutions per minute
s	seconds
S	Synthesis
SCF	Skp, Cullin, F-box
SDS	Sodium Dodecyl Sulfate
SDS-PAGE	Sodium Dodecyl Sulfate Polyacrylamide Gel Electrophoresis
SEC-MALLS	Size Exclusion Chromatography coupled with Multiple Angle Laser Light Scattering
SIN	Septation Initiation Network
Sld2	Synthetically Lethal with Dpb11-1
Sli	Synthetically Lethal with Ipl1
Smc	Structural Maintenance of Chromosomes
Slk	Synthetic Lethal Kar3p
ssDNA	single stranded DNA
TCEP	<i>tris</i> (2-carboxyethyl)phosphine
ts	temperature sensitive
V_{max}	Maximal velocity
wt	wild type
YP	Yeast Extract Peptone
YPD	Yeast Peptone Dextrose
μ l	microlitre
μ m	micrometer
μ M	micromolar
Zds	Zillion Different Screens

Chapter 1. Introduction

'Omnis cellula e cellula' – where a cell arises, a cell must have previously existed. These are the now famous words of Karl Virchow, published in 1858, and form the basic tenets of what we understand as Schleiden and Schwann's Cell Theory (Virchow, 1858).

Some 160 years since this pronouncement, our knowledge of the symphonic rhythms of cell division has expanded considerably. It is clear that each cell, whether a starfish egg, a human embryo, or anything in between and beyond, must adhere to the same basic rules.

Cell division entails a task of enormous complexity and has been entrusted to many 'master regulators'. We are only beginning to understand the molecular features of their intricate input, by which they appear to imbue the cell with intelligence.

1.1 The eukaryotic cell cycle

The division of a cell into two daughters is arguably one of the common denominators of all forms of life. In order to accomplish this gargantuan task, every eukaryotic cell undergoes an archetypical series of events, called the cell division cycle.

The fundamental aim of this process is to ensure error-free duplication of the genomic content and other organelles, followed by accurate segregation of these to give rise to two 'daughter' cells.

Whilst the details may vary, the overall logic of the cell cycle and many of its molecular aspects are remarkably conserved through billions of years of evolution.

1.2 The budding yeast cell cycle

Saccharomyces cerevisiae, or budding yeast is a small, single-celled fungal eukaryote that proliferates as a haploid. Owing to its genetic tractability, ease of growth and shared use of cell cycle circuitry with its counterparts higher up in the scale of complexity, it has emerged as an immensely useful tool in cell cycle research. Indeed, studies in budding yeast have been instrumental in illustrating its governing principles (Hartwell, Culotti, Pringle and Reid, 1974). Moreover, the master regulatory proteins have also been found to be structurally and functionally conserved in all rungs of the evolutionary ladder (Morgan, 2007).

In order to divide, budding yeast first takes stock of its surrounding cues and, if they are found satisfactory, it 'decides' to undergo cell division (Fig. 1.1). It enters a period of growth called the gap phase or G1. Next, it duplicates its DNA during the 'synthesis' or S-phase. The beginning of DNA replication is phenotypically concomitant with the emergence of a bud. In fact, progression through the cell cycle witnesses a commensurate growth of the bud. Following a very short second gap phase called G2, the cell then enters the mitotic M-phase. Here, the duplicated and condensed genetic material lines up along the equatorial plane of the mother and daughter cells (metaphase), which is then segregated into two equal halves to the two cells in one fell swoop (anaphase). Budding yeast undergoes a 'closed' mitosis, that is, it does not break down the nuclear membrane, keeping the nucleoplasm and the cytoplasm separate. The following step is telophase during which the now virtually equal cells decondense their DNA. Finally, the cells physically separate their cytoplasm and cell walls to create two new cells - a process called cytokinesis.

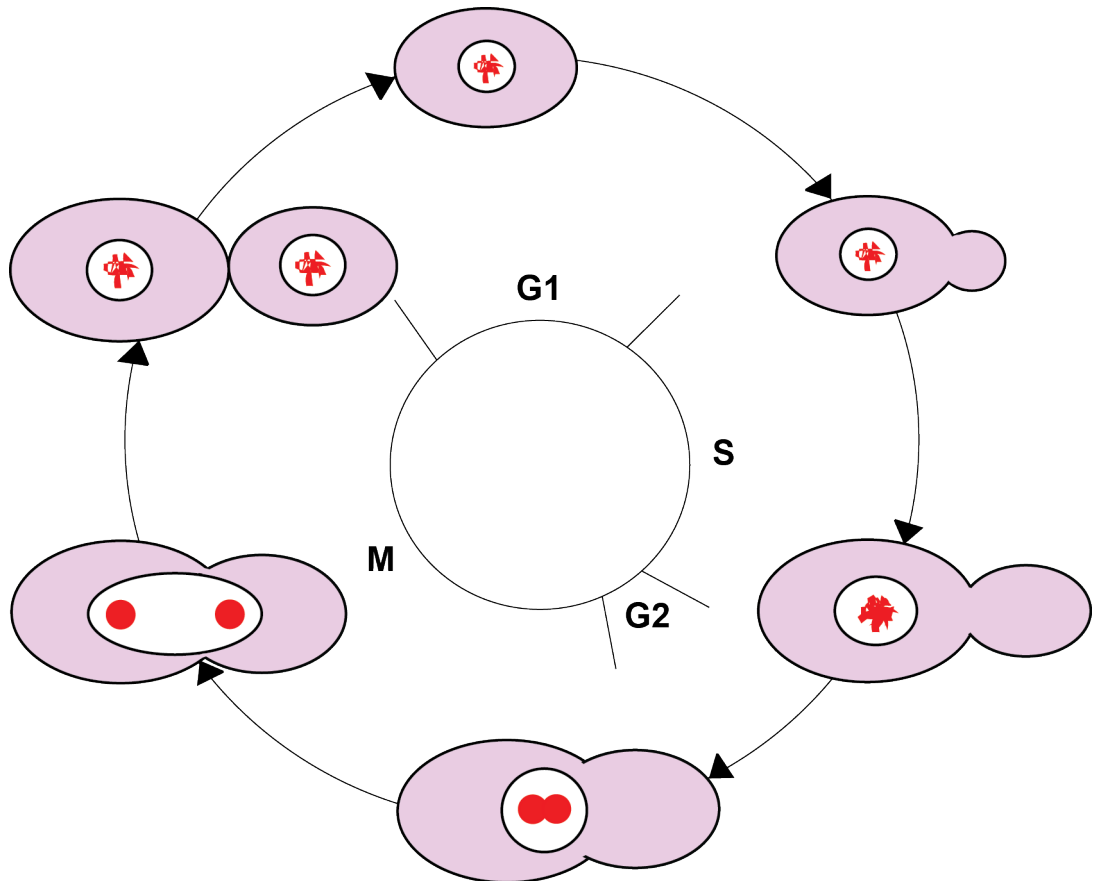


Figure 1.1 – The budding yeast cell cycle.

The cells enter the cell cycle in the G1-phase, following which they duplicate their DNA during S-phase. After another short G2-phase, they enter the M-phase, where they properly align and segregate this duplicated DNA by dividing it equally between the mother and daughter cells.

Whilst there are many differences between budding yeast and higher eukaryotes, such as the emergence of ‘open’ mitosis in the latter, in which the nuclear envelope is dissembled before mitosis and reassembled after chromosome segregation, the order of these phases is well conserved.

1.3 The cell cycle is a highly regulated process

As is to be expected, a process of such vast complexity has warranted equally exquisite molecular controls that ensure its fidelity, as the cost of not doing so can be catastrophic to the perpetuation of life. Indeed, failure to properly segregate

chromosomes can lead to aneuploidy, a hallmark of cancer cells. A striking feature of this process is how it appears to follow a predetermined schedule: S-phase follows M-phase and the two do not normally coincide, for instance. What decides the order and course of events? This question has fascinated researchers for decades.

1.3.1 Cyclin-dependent kinases are the master regulators of the cell cycle

Despite it being known since 1971 that a Maturation Promoting Factor (MPF) controls entry into M-phase in oocytes and metazoan eggs (Masui and Markert, 1971), its identity remained elusive for nearly 20 years. The discovery that it is comprised of a heterodimeric enzyme hailed the dawn of a new era in cell cycle research. This enzyme is composed of a cyclin-dependent kinase (Cdk) subunit in complex with a partnering cyclin. Cdk alone exists in an auto-inhibited state, which is relieved by cyclin binding (Gautier et al., 1988; Draetta et al., 1989). Through the cell cycle, whilst the kinase subunit remains largely constant, the identity and abundance of the cyclin changes, with each exhibiting periodic waves of synthesis and destruction. Thus, MPF represents only one of the many cyclin-Cdk flavours. This behaviour forms the basis of a robust timer that 'switches' events on in the right order and the right time during the cell cycle (Murray and Kirschner, 1989; Minshull, Blow and Hunt, 1989).

What constitutes these biochemical 'switches'? Phosphorylation of hydroxyl-containing residues - serines and threonines - on protein substrates by cyclin-Cdk complexes was found to be the engine propelling the cell cycle forwards. Although the chemistry of the reaction had been discovered by Fisher and Krebs in the 1950s (Krebs and Fischer, 1956; Fischer and Krebs, 1955), it only gradually became clear that phosphorylation constitutes one of the most important aspects of cell cycle regulation, and indeed cellular physiology.

Cyclin-Cdk complexes phosphorylate (S/T)-P-x-(K/R)-containing consensus sites on proteins, with the +3 basic residue being preferred but not essential for catalysis (Nigg, 1991; Songyang et al., 1994; Holt et al., 2009). These phosphorylation events change the

behaviour of the protein and hence promote a particular phase of the cell cycle. For instance, they can enhance protein-protein interactions or alter the biochemical activity of the modified protein. Whilst the road from phosphorylation to a cytological event has not always been straightforward, it is well understood in some instances. The molecular details of licensing and firing of replication origins during S-phase by phosphorylation are well understood (Fragkos, Ganier, Coulombe and Méchali, 2015).

1.3.2 Cdk activity is temporally regulated by phosphorylation

Although the Cdk-cyclin complex represents an active form of the enzyme, its activity can be further post-translationally modified by phosphorylation of the kinase subunit. An evolutionarily conserved tyrosine residue on Cdk (Y19 in budding yeast) gets phosphorylated by the conserved tyrosine kinase Wee1 (Swe1 in budding yeast), which severely inhibits associated kinase activity of many cyclin-Cdk complexes. This inhibition is relieved by dephosphorylation by the conserved phosphatase, Cdc25. Both Wee1 and Cdc25 are themselves subjected to regulatory input. Tyrosine phosphorylation of Cdk constitutes an important control mechanism and regulates G2-M transition in many organisms by enabling timely, switch-like activation of the kinase at this stage.

Another residue within Cdk, T169 in budding yeast, gets phosphorylated by Cdk-activating kinases. For many cyclin-Cdk complexes, this phosphorylation is associated with an increase in kinase activity.

1.3.3 Cdks associate with a number of cyclins throughout the cell cycle and control various cellular events

Budding yeast contains only one major Cdk, called Cdc28, which sequentially associates with nine different cyclins through the cell cycle. In fact, each cell cycle stage is characterized by the presence of particular Cdc28-cyclin combinations, which in turn initiate the transcription of the cyclins necessary for the following stage (Fig. 1.2A).

Three G1 cyclins, Cln1-3, fulfil the G1 function of bud site selection, licensing of spindle pole body (the yeast centrosome equivalent) duplication, phosphorylation of

the B-type cyclin inhibitor Sic1 and transcription of the two B-type S-phase cyclins, Clb5 and Clb6. Towards the end of G1, Cln1 and Cln2 are degraded by the proteasome following ubiquitylation by the E3 ubiquitin ligase SCF^{Grr1} (Barral, Jentsch and Mann, 1995). Clb5 and Clb6 then promote S-phase by phosphorylation of different proteins, which leads to efficient initiation of DNA replication. At this stage, the two duplicated sister chromatids are held together by the topological embrace of a protein 'glue' - a cohesion ring (Uhlmann, 2016). Next, Clb1-4 are transcribed, promoting entry into M-phase. This phase is characterized by formation of the spindle, which captures duplicated and condensed chromosomes in metaphase (Morgan, 2007; Bloom and Cross, 2007a). Following amphitelic attachment of each sister chromatid to the opposite spindle pole, the spindle assembly checkpoint (SAC) is satisfied. If this step is not completed, the checkpoint keeps the cells arrested in metaphase with high kinase activity (Musacchio, 2015). SAC satisfaction leads to activation of another E3 ubiquitin ligase, the Anaphase Promoting Complex/Cyclosome (APC/C). This complex causes destruction of securin, the binding partner and inhibitor of the protease separase. Unrestrained, separase then cleaves the cohesion ring, leading to segregation of sister chromatids to the opposite poles (Uhlmann, Lottspeich and Nasmyth, 1999). The APC/C also destroys all B-type cyclins, with the exception of Clb6, which is degraded earlier (Jackson, Reed and Haase, 2006). This decline in kinase activity at anaphase heralds the onset of exit from mitosis.

Higher eukaryotes have evolved considerably more complex cyclin-Cdk control systems (Fig. 1.2B). Although they contain more than 10 different Cdks, in most contexts, only Cdk1 and Cdk2 appear to be important for mitosis, with the others providing ancillary support. These sequentially associate with cyclins D (in the absence of Cdk4 and 6) and E during G1/S phases, cyclin A during S-phase, followed by cyclin B over the course of M-phase. Each flavour of cyclin also contains multiple members within its family (Morgan, 2007; Hochegger, Takeda and Hunt, 2008). Despite this complexity, the overall sequence of events and principles of control remain the same between these organisms.

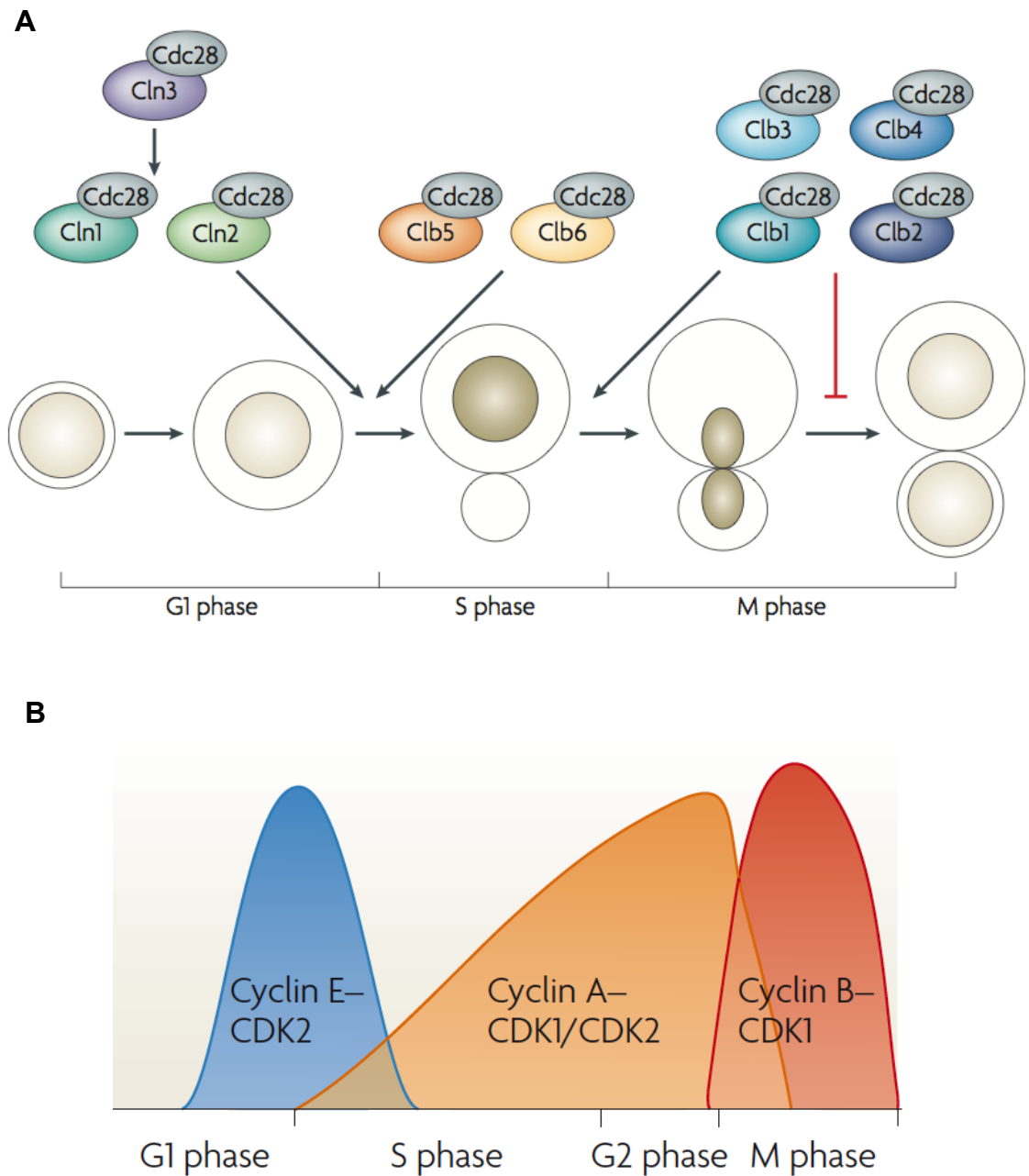


Figure 1.2 - Various cyclin-Cdk complexes are found throughout the cell cycle.

A. In budding yeast, the kinase Cdc28 associates with Cln1-3, followed by Clb5, 6, Clb3, 4 and Clb1, 2. **B.** In higher vertebrates, Cdk1 and Cdk2 control the cell cycle. These sequentially associate with cyclins E, A and B. Adapted from Bloom and Cross (2007) and Hocheeger, Takeda and Hunt (2008) respectively.

1.4 Controlling ordered phosphorylation – a matter of quality or quantity?

Does the presence of distinct forms of cyclins during different stages of the cell cycle imply their functional specialization? Or, can they stand in for each other?

1.4.1 Qualitative model for ordered substrate phosphorylation

The former hypothesis, described as the ‘qualitative model’, holds that different cyclins, when complexed with the kinase, imbue the latter with altered substrate specificities. Further, the model posits that their sequential rise and fall is the primary determinant of the timing and order of different cell cycle phases.

Lending confidence to this theory are the following observations. Working in mammalian systems, a number of studies found that cyclin A, the S-phase cyclin, bound to and efficiently phosphorylated some of its substrates by employing a specific docking motif – the RxL or Cy motif (Krek et al., 1994; Adams et al., 1996). Structural analysis of cyclin A-Cdk2 bound to p107 found that it engaged with this motif via a complementary ‘hydrophobic patch’, centred about the conserved MRAIL sequence on the cyclin (Johnson, Brown, Noble and Endicott, 1999). By systematic analysis of Cdk substrates, a similar trend was discovered in the budding yeast S-phase cyclin Clb5 (Loog and Morgan, 2005). It was shown to be highly efficient in phosphorylating about 15 proteins compared to Clb2, an effect contingent upon their RxL motifs. These include replication factors such as Orc6 (Wilmes et al., 2004), and the APC/C specificity factor, Cdh1.

Similarly, whilst examining the G1 cyclin Cln2 and its substrates, recent studies have also identified an LLPP motif, which greatly enhances Cln2-mediated phosphorylation of Ste5 and Ste20 (Bhaduri and Pryciak, 2011), components of the yeast Mitogen-Activated Protein (MAP) Kinase pathway, via a specific docking site on the cyclin surface (Bhaduri et al., 2015).

In order to gain insights into whether specificity is a feature of other cyclin-substrate interactions in budding yeast, another study immunoprecipitated individually-tagged cyclin subunits, and subjected the interacting proteins to mass spectrometry (Archambault et al., 2004). This led to the identification of a handful of substrates that only associated with a particular cyclin. A similar approach was taken by another study, which assayed stage-specific interactors of tagged human cyclins E1, A2 and B1. Whilst they too found a number of specific interacting proteins, they also observed a significant degree of overlap between cyclin A2 and B1 interactors (Pagliuca et al., 2011).

However, these observations alone do not prove the qualitative model entirely. For instance, although it is true that both of the above mentioned studies identify some specific cyclin targets, one cannot ignore the issue of protein abundance. Cyclins (and some substrates too) are only present at specific stages of the cell cycle, in the absence of others. Thus, interactions might be partly explained by availability. Further strengthening this interpretation is another survey of the ability of different cyclin-Cdk complexes to phosphorylate proteins from a *Xenopus* cDNA library. Here, the authors found that a vast majority of substrates could be phosphorylated by several cyclin-Cdks (Errico et al., 2010).

Indeed, genetic analyses have also revealed redundancies in cyclin functions. For instance, G1 cyclins within budding yeast were initially thought to perform an indispensable function, with a triple *cln1Δ cln2Δ cln3Δ* strain proving inviable (Richardson, Wittenberg, Cross and Reed, 1989). Deletion of the B-type cyclin inhibitor Sic1 (Tyers, 1996) or overexpression of Clb5 (Epstein and Cross, 1992) were both later found to rescue this inviability, suggesting that, given the right context, cyclins can indeed be interchangeable.

A parallel principle was found to apply to the severe S-phase delay shown by *clb5Δ clb6Δ* cells, which could not be rescued by the advanced expression of mitotic Clb2 from the Clb5 promoter (Schwob and Nasmyth, 1993). Concomitant deletion of Swe1,

that preferentially inhibits Clb2 over other cyclins by the inactivating Y19 phosphorylation of the kinase, restored the S-phase timing (Hu and Aparicio, 2005).

In many mammalian cells, deletion of all Cdks other than Cdk1 can drive the cell cycle through normal S-phase and mitosis (Santamaría et al., 2007; Hochegger et al., 2007). Similarly, barring cyclin B and, in some cases, cyclin A, all others appear to be redundant (Santamaría et al., 2007; Kalaszczynska et al., 2009; Kozar et al., 2004; Geng et al., 2003; Hochegger et al., 2007).

1.4.2 A quantitative model for cell cycle regulation

The observations outlined herein along with insights from a seminal piece of work by Fisher and Nurse (1996) has led to the proposition of a ‘quantitative model’, which posits that increasing kinase activity thresholds are required for entry into successive cell cycle phases – an idea which is not mutually exclusive with the qualitative model. Using fission yeast, they demonstrated that the mitotic cyclin, Cdc13, in complex with the sole Cdk, Cdc2, could impart directionality to the cell cycle and promote orderly progression into S- and M-phases in the absence of all other cyclins (Fisher and Nurse, 1996). Furthermore, ablation of the complex in G2 caused rereplication as the kinase activity was presumably never allowed to build up to high level required for M-phase. Hence, a lower activity threshold needs to be traversed to trigger S-phase, whereas higher level leads to entry into mitosis (Stern and Nurse, 1996).

Further work has lent credence to this model. The authors generated a translational fusion of Cdc13-Cdc2 under the control of the Cdc13 promoter and other regulatory elements, which garnered periodicity to the presence of the fusion protein by ensuring its destruction during mitotic exit. This module was sufficient to drive a normal cell cycle (at least under the parameters tested) in the absence of all endogenous cyclins and the Cdk. The ability of this strain to promote timely and orderly cell cycle progression was further explained by mathematical modelling of kinase activity throughout the cell cycle and showed that different activity thresholds promote different stages (Tyson and Novak, 2011). Moreover, use of a kinase allele whose activity can be modulated by the

ATP analogue 1-NM-PP1 demonstrated the existence of S- and M-phase specific kinase activity thresholds. More convincingly, release of G2-arrested cells into media containing various concentrations of the ATP analogue (and hence differing amounts of kinase activities) caused inappropriate entry into stages proportional to the new activity levels, or even overlap of stages (Coudreuse and Nurse, 2010). These cell cycle acrobatics demonstrate the lack of an inherent order inbuilt in the machinery.

In accordance with these observations, manipulation of Clb2-associated kinase activities to supra-physiological levels causes an acceleration of mitosis in budding yeast, indicating that overall kinase activity levels promote cell cycle progression (Oikonomou and Cross, 2011).

Is a quantitative rise in kinase activity responsible for ordering the cell cycle in unperturbed conditions? In budding yeast, it has been observed that whilst the sum of cyclin concentrations is roughly constant throughout the cell cycle, their abilities to activate Cdks are not, with the mitotic cyclin Clb2 being the best kinase activator, followed by the S-phase cyclin Clb5. Clns were found to be the poorest Cdk activators (Kõivomägi et al., 2011). Thus, one can indeed view progression from G1 to M-phase as a period of increasing kinase activity. Similarly, in metazoans, S-phase promoting cyclin E-Cdk2 has lower activity than mitotic cyclin B-Cdk1 (Hochegger, Takeda and Hunt, 2008).

How does one reconcile the 'qualitative' and 'quantitative' models of cycle regulation? In the light of low overall kinase activity, the docking motifs perhaps exist as a failsafe, having evolved to make phosphorylation of some key targets highly likely. However, one can conservatively argue their existence does not constitute proof to the contrary, that other cyclins cannot take over the task of phosphorylating these in a timely fashion. Genetic experiments do suggest that greater overall catalytic efficiency perhaps makes up for the advantage that binding motifs provide.

1.5 A role for phosphatases in cell cycle regulation

That kinase activity promotes cell cycle progression is incontrovertible. However, thus far, tacit has been the assumption that phosphorylation of substrates would require a 'reset' button, reversing the effects of phosphorylation and enabling the cell to carry out another round of division. In theory, this can be brought about by degradation of phosphoproteins. Given that hundreds, if not thousands of proteins are phosphorylated during the cell cycle (Ubersax et al., 2003; Holt et al., 2009; Dephoure et al., 2008) this would constitute an ineffective strategy, requiring an added layer of control of mass transcription, translation and degradation. Phosphatases provide an effective solution to this problem.

The existence of proteins with phosphatase activity has long been known. Initially identified as a protein with "prosthetic group" (phosphoryl group) removing activity and referred to as PR enzyme (Cori and Cori, 1945), was the phosphatase we contemporaneously refer to as protein phosphatase 1 (PP1). Whilst research into kinases prospered, our knowledge of phosphatases languished as it was assumed that cell cycle regulation primarily occurs by oscillating kinase activity in a backdrop of constant and non-specific phosphatase activity. This kinase evangelism was perhaps fuelled by the inability to define kinase-style consensus motifs that phosphatases act on (Kennelly and Krebs, 1991).

We now understand the importance of the cell cycle regulation that phosphatases provide. Recent work has highlighted their exquisite regulation, along with consensus motif preferences. In particular, their role during mitotic exit is crucial. As described in 1.3.3, at this stage, satisfaction of the spindle assembly checkpoint leads to activation of the APC/C, in complex with Cdc20 as the co-activating protein, which causes destruction of cyclins at the metaphase-anaphase transition. In all organisms tested, Cdk downregulation is insufficient to remove phosphates on proteins – phosphatase activity is also required for exit from mitosis.

Broadly, this activity leads to a number of events associated with mitotic exit, such as proper segregation of sisters to the opposite poles, disassembly of the mitotic spindle, decondensation of chromosomes, reformation of the nuclear membrane (in vertebrates), eventually culminating in cytokinesis, the physical separation of the cells.

1.5.1 Major phosphatases in eukaryotes

Phosphatases comprise a broad group of enzymes, with the potential to regulate a myriad of cellular processes. They can be divided into two categories based on sequence homology and mode of catalysis: serine/threonine specific and tyrosine specific.

As the name suggests, protein serine/threonine phosphatases (PSPs) target phosphoryl groups on the polar residues serines and threonines. They can be subdivided into three different families: phosphoprotein phosphatases (PPP), metal-dependent phosphatases (PPM) and aspartate-based phosphatases (Fig.1.3). Members of the PPP and aspartate-based phosphatases have well defined roles in cell cycle regulation.

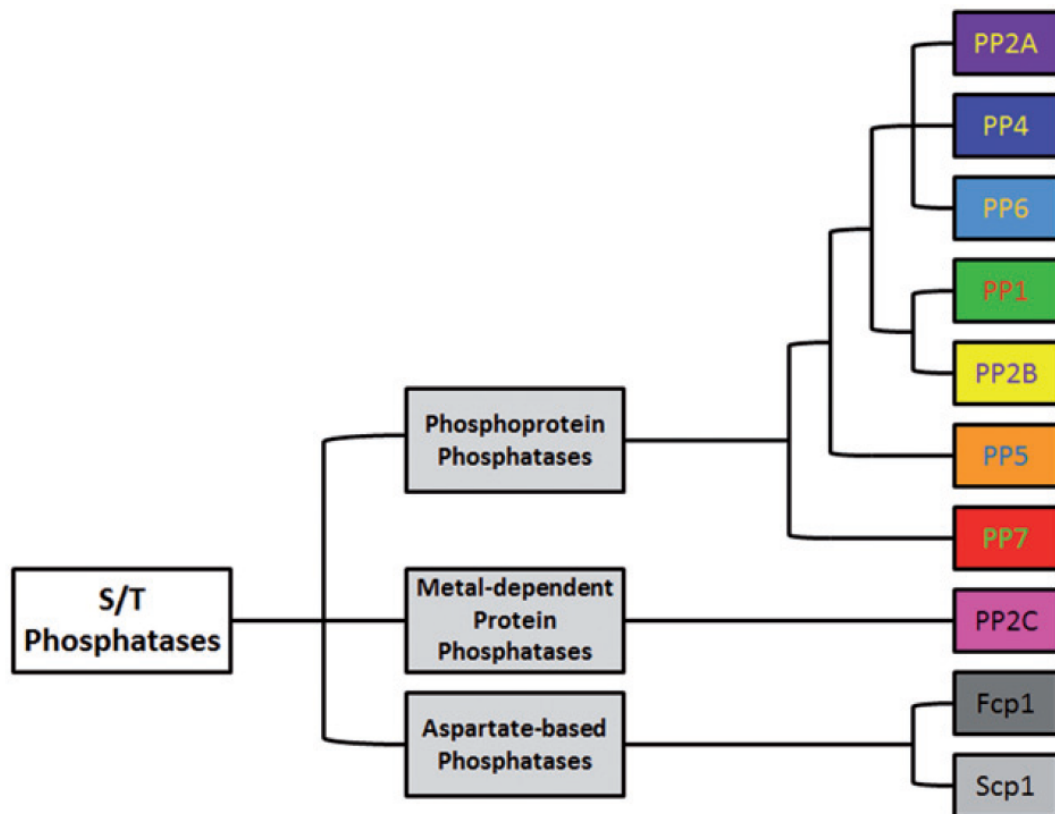


Figure 1.3 - The PSP superfamily.

PSPs can be broadly divided into three classes each of which has its own members, catalytic mechanism, requirement of divalent cations, etc. From (Wlodarchak and Xing, 2016).

Protein phosphatase 2A (PP2A) is one of the best known members of this family. It is highly conserved from yeast to man. Overall, an active enzyme consists of three different subunits: a scaffold subunit (A), a catalytic (C), and a regulatory subunit (B). The B subunit family can often control the subcellular location of the holoenzyme, and even provide substrate specificity. This family consists of many heterogeneous members (each with its own isoforms), not all of which are found in every organism. Of these, B55 (Cdc55 in budding yeast) and B56 have roles in cell cycle control.

The PPP family also contains PP1 (called Glc7 in budding yeast), a protein that has been implicated in a wide variety of cellular processes, such as regulation of the spindle assembly checkpoint (Musacchio, 2015). It consists of a catalytic subunit that can

associate with hundreds of regulatory subunits, which guide its location, activity and enzymatic preferences.

Finally, the aspartate-based family consists of the protein Fcp1, which dephosphorylates the C-terminal tail of RNA polymerase II (Kimura, Suzuki and Ishihama, 2002). Recently, its role in mitotic exit has also been discovered (discussed in section 1.7.2).

The protein-tyrosine phosphatase (PTP) superfamily also consists of a wide array of phosphatases, which can act on substrates ranging from transmembrane proteins to fatty acids – a repertoire too diverse for detailed discussion presently. It has also been divided into two families on the basis of catalytic mechanism: cysteine-based and aspartate-based. The former family consists of the well-known phosphatase Cdc25 that responsible for dephosphorylating a conserved tyrosine (Y19 in budding yeast) on Cdk, which leads to activation of the enzyme and propels cells into mitosis (Strausfeld et al., 1991).

The other famous member of the cysteine-based PTP family is Cdc14, which belongs to a category called dual-specificity phosphatases, so named owing to their ability to dephosphorylate phosphoserines and phosphothreonines, and at least *in vitro*, phosphotyrosines. Nowhere is this enzyme better studied than in mitotic exit of budding yeast, where it has an essential role.

1.6 Cdc14 and budding yeast mitotic exit

1.6.1 Discovery of Cdc14 as a phosphatase

Cdc14 was first discovered in a genetic screen by Hartwell and colleagues for temperature sensitive mutations that cause a cell cycle arrest. The *cdc14-3^{ts}* cells, when shifted to a high temperature, arrested with long mitotic spindles and a 2C DNA content – the late stages of mitosis (Culotti and Hartwell, 1971). This proffered some

clues as to the stage at which its function is required, though it was initially thought to be important for DNA replication only (Hogan and Koshland, 1992; Kroll, Hyland, Hieter and Li, 1996).

The subsequent cloning of the gene and sequence analysis yielded similarities to other protein tyrosine phosphatases (Wan, Xu and Grunstein, 1992), which we now know to be the case because of their shared family. It was not until the 1990s that Cdc14 was definitively confirmed to possess phosphatase activity (Taylor, Liu, Baskerville and Charbonneau, 1997), placing it in the dual-specificity phosphatases sub-class of PTPs.

The next discovery, that Cdc14 is required to directly downregulate Cdk activity, thus ushering on exit from mitosis (Visintin et al., 1998), brought home its importance as a major regulator of the cell cycle. It also explained why *cdc14^{ts}* cells arrested in mitosis with high kinase activity.

1.6.2 Cdc14 is a key regulator of exit from mitosis

How does Cdc14 promote exit from mitosis? The answer is multi-pronged. Firstly, it leads to downregulation of Cdk activity. A peculiarity of budding yeast is that, the metaphase-to-anaphase transition does not lead to total abrogation of Cdk activity. Whilst all cyclins are completely degraded in other eukaryotes at this stage, budding yeast only witnesses complete destruction of the S-phase cyclin Clb5 by APC^{Cdc20} (Shirayama, Tóth, Gálová and Nasmyth, 1999; Lu et al., 2014). This initial activator of the APC, however, only leads to a partial decline of the mitotic cyclin Clb2 levels, to about 50% of their G2/M values (Yeong, Lim, Padmashree and Surana, 2000). Degradation of the persisting Clb2 pool is mediated by Cdh1 in telophase when the latter becomes active (Schwab, Lutum and Seufert, 1997; Yeong et al., 2000). It is Cdc14 that dephosphorylates key residues within Cdh1, thereby activating it and seeing cyclin destruction through (Jaspersen, Charles and Morgan, 1999).

Next, Cdc14 promotes the transcription of the yeast p27^{Kip1} homolog and B-type cyclin inhibitor Sic1, by promoting the nuclear localization of its zinc finger transcription

factor Swi5. It does so by dephosphorylating and thereby restoring its nuclear localization sequence (NLS). Cdc14 also directly dephosphorylates Sic1 (Visintin et al., 1998), which, along with other mechanisms, renders mitotic exit irreversible (López-Avilés, Kapuy, Novak and Uhlmann, 2009).

1.6.3 Cdc14 is required for a number of mitotic exit events

Abolishing Cdk activity is far from the only role of Cdc14. As phosphorylation mediates certain events during interphase, the same is true for Cdc14-mediated dephosphorylation, a subset of whose functions we have come to understand over the past few years.

Anaphase onset is not only characterized by the dramatic splitting of the sister chromatids to the opposite poles of the cell, but also by a period of low dynamic instability associated with the elongating spindle. This enhanced spindle stability aids the process of doling out of the DNA to the mother and daughter cells. Cdc14, by directly dephosphorylating the DASH protein Ask1 and the spindle stabilizer (and PP1 regulator (Akiyoshi, Nelson, Ranish and Biggins, 2009)) Fin1 early during anaphase aids this process (Higuchi and Uhlmann, 2005; Woodbury and Morgan, 2006).

Next, now that anaphase onset has begun and the sister chromatids are moving to the opposite poles, kinetochores face a tension-less state, which could trigger inappropriate spindle assembly checkpoint signaling. This outcome is prevented by Cdc14-mediated dephosphorylation of the Chromosome Passenger Complex component INCENP (Sli15 in budding yeast), causing relocation of the complex on to the elongating microtubules, away from the kinetochores. This action provides a mechanism for silencing the SAC for good (Mirchenko and Uhlmann, 2010; Pereira, 2003).

Elaborate mechanisms also exist within the cell that ensure replication of the genetic material strictly once per cell cycle. Late into anaphase, replication proteins such as Cdc6, Orc2 and Orc6 are dephosphorylated by Cdc14 (Bloom and Cross, 2007b; Zhai, Yung, Huo and Liang, 2010). Removal of phosphates stabilizes Cdc6 (Walter et al.,

2016), whilst making the other proteins competent for origin activation and pre-replicative complex assembly. This function of Cdc14 explains why a number of genetic interactions had been noted between the protein and the process of DNA replication, as mentioned previously. A vital aspect of Cdc14-facilitated origin relicensing is that it must occur late in anaphase, when Cdk activity has dropped sufficiently so as to prevent replication during mitotic exit.

Cytokinesis, the physical pinching off of the cells into two, is the last step of cell division. Here too, following the execution of earlier mitotic exit events, a cytoplasmic pool of Cdc14 dephosphorylates key targets. Inn1 dephosphorylation, for instance, causes its relocalization to the bud-neck where it promotes formation of the primary septum (Palani et al., 2012). Similarly, dephosphorylation of Iqg1 also recruits it to the site of cell division for regulation of the acto-myosin ring (Miller et al., 2015).

By no means an exhaustive list, these are but a small sampling of Cdc14 substrates. Recent proteomic studies, employing Cdc14 overexpression in metaphase-arrested cells (Kuilman et al., 2015) or comparison with *cdc14-1^{ts}* cells (Kao et al., 2014), have revealed a plethora of new Cdc14 substrates. What can easily be appreciated though is the need for Cdc14 to act temporally to promote a multitude of processes in the right order, thus resetting the cell to a biochemically G1 state.

1.6.4 Regulation of Cdc14 activity

Unsurprisingly, given the importance of Cdc14 and the diverse roles it performs within the cell, its activity is tightly regulated throughout the cell cycle even though its levels remain constant.

1.6.4.1 Cdc14 is sequestered by Net1 from G1 to M-phase

A two-hybrid screen for Cdc14 interactors identified the nucleolar protein Net1 as a key inhibitor of Cdc14 (Visintin, Hwang and Amon, 1999). Subsequent biochemical analyses revealed that this large 1,189 amino acid-long, 128 kDa protein is a potent and specific competitive inhibitor of Cdc14. The constant of inhibition, K_i was found to be 3

nM (using tyrosine-phosphorylated Myelin Basic Protein as a Cdc14 substrate) at least in a sub-physiological ionic strength buffer (100 mM KCl). Increasing the KCl concentration to the slightly more physiological value of 120 mM led to a K_i of 74 nM (Traverso et al., 2001a), indicating the salt sensitivity of this interaction.

Net1 binds to and tethers Cdc14 in the nucleolus, thus inhibiting its activity from G1 through to anaphase onset. At this stage, phosphorylation of Net1 and probably Cdc14, mediated by Cdc5 (the yeast Polo-like kinase) and Clb2-Cdc28 reduce the affinity of the proteins for each other (Yoshida and Toh-e, 2002; Shou et al., 2002; Visintin, Stegmeier and Amon, 2003). Unfettered, Cdc14 begins to be released, bringing about dephosphorylation of substrates and exit from mitosis.

The temporal window encompassing Cdc14 release is thus restricted to precisely when its activity is required – avoiding futile cycles of phosphorylation and dephosphorylation outside this period.

What promotes Cdc14 release from Net1? A series of two distinct signaling cascades, named FEAR (**F**ourteen **E**arly **A**naphase **R**elease) and MEN (**M**itotic **E**xit **N**etwork) pathways, promote two sequential waves of release of Cdc14 upon anaphase onset.

1.6.4.2 FEAR pathway causes Cdc14 release in early anaphase

Early into anaphase, securin cleavage leads to the activation of separase. Separase, along with concerted action of the proteins Slk19 and Spo12, leads to Zds1/Zds2-mediated downregulation of PP2A^{Cdc55} activity, which, up until now, had been keeping Net1 dephosphorylated (Rossio and Yoshida, 2011; Queralt and Uhlmann, 2008; Stegmeier, Visintin and Amon, 2002; Sullivan and Uhlmann, 2003). Thus Clb2-Cdc28 and Cdc5 gain the upper hand and are now able to phosphorylate Net1 on key sites, causing its dissociation from Cdc14 (Azzam, 2004). How these components come together biochemically to promote Cdc14 release is poorly understood.

FEAR-mediated Cdc14 release is thought to be only “partial” and is cytologically restricted to the nucleus; for “fully” released Cdc14, particularly into the cytoplasm, the second, Ras-like MEN signaling pathway is required.

1.6.4.3 MEN pathway causes sustained release of Cdc14 from mid- to late-anaphase

Mutations that abrogate MEN signaling lead to a late anaphase arrest, highlighting its importance in Cdc14 release. At the top of this cascade is the GTPase protein Tem1, which is stimulated by declining Cdk activity and rising Cdc14 activity (Jensen et al., 2002). It activates the protein kinases Cdc15 and Dbf2-Mob1, which sustain the phosphorylation of Net1, thereby keeping Cdc14 released (Asakawa, Yoshida, Otake and Toh-e, 2001; Bardin, Boselli and Amon, 2003; Lee et al., 2001; Mah, Jang and Deshaies, 2001). Cdc14 also dephosphorylates and activates Cdc15, thereby sanctioning its own freedom (Jaspersen and Morgan, 2000). Tem1 is negatively regulated by the GTPase activating protein complex Bub2-Bfa1, which is further phosphorylated and inactivated by Cdc5 (Hu et al., 2001).

At this stage, Cdc14 is also granted admittance to the cytoplasm by Dbf2-Mob1-mediated phosphorylation and abrogation of its nuclear localization signal (Mohl et al., 2009), thus probably allowing its nuclear export signal (NES) to predominate (Bembenek et al., 2014).

Later in anaphase, following the Cdh1-mediated degradation of Cdc5 (Visintin et al., 2008) - which removes the Net1 phosphorylation signal - and dephosphorylation and activation of Bfa1 (Pereira, Manson, Grindlay and Schiebel, 2002; Baro et al., 2013) (a negative regulator of MEN), Cdc14 is resequenced into the nucleolus.

Curiously, there has been one report of a substrate, Dsn1 – a part of the MIND complex at kinetochores – being dephosphorylated by Cdc14 in metaphase, when the latter’s activity is thought to be inhibited (Akiyoshi and Biggins, 2010).

Why has Cdc14 release evolved to be rather complicated? One explanation proffered is that every protein requirement ensures that a separate, earlier biological event has been completed. For instance, the requirement for separase for FEAR activation ensures satisfaction of the spindle assembly checkpoint, concomitant cohesin cleavage, and hence commitment to exit from mitosis. Similarly, the MEN GTPase Tem1, found on the spindle pole body, can only meet its activating GEF (Guanine Exchange Factor) Lte1, present in the daughter bud, when the dividing nucleus partitions correctly along the mother-bud axis, enters the daughter and brings the two proteins together (Bardin, Visintin and Amon, 2000). Thus, it only leads to the release of Cdc14 under strict conditions of accurate partitioning of the spindle, which have been called the 'spindle positioning checkpoint'.

Differences between levels and localization notwithstanding, FEAR or MEN-released Cdc14 are not biochemically distinct. In fact, globally, one can envision the following picture of mitotic exit: one of Cdk activity levels falling concomitant with steadily increasing Cdc14 activity released through these pathways (Fig. 1.4).

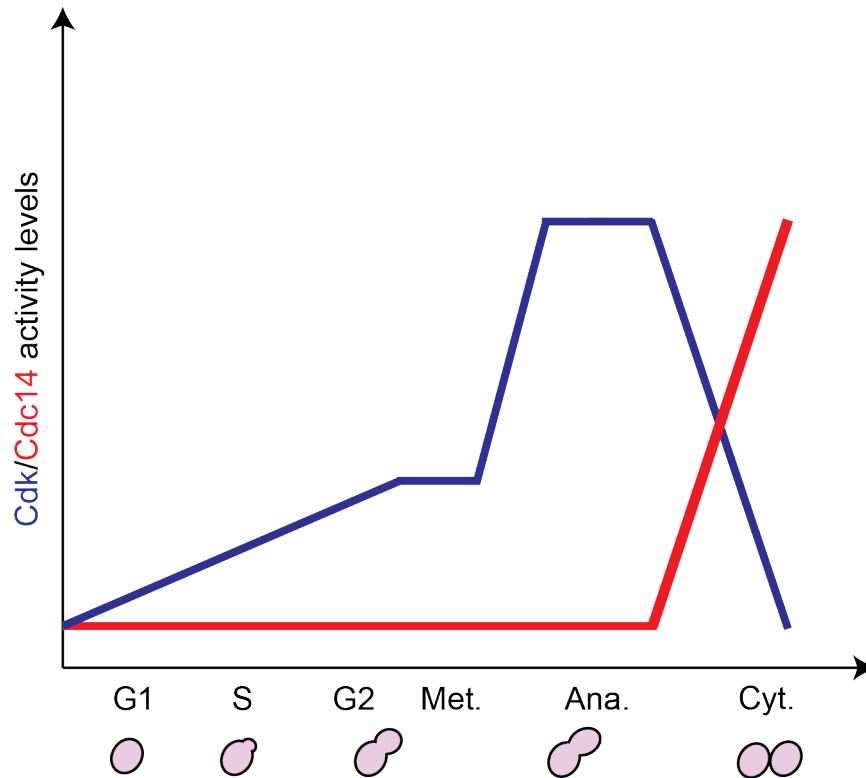


Figure 1.4 - Cdk/Cdc14 activity levels throughout the cell cycle.

Cdk1 activity (blue) experiences a dynamic change throughout the cell cycle, reaching a maxima at anaphase and falling to its G1 levels after anaphase. Cdc14 activity (red) remains constrained through most of the cell cycle, rising gradually from anaphase onset.

1.7 Cdc14 and phosphatases in other organisms

Cdc14 orthologs are found in a wide variety of species, with considerable conservation of the overall structure (discussed in section 1.8.2). Given the importance of the phosphatase in budding yeast cell cycle, does it perform the same functions within other organisms too? Overall, it appears that the mitotic exit function of the Cdc14 has not been conserved through evolution. Instead, different organisms have varying reliance on the phosphatase to promote a number of other cellular functions (Fig. 1.5). Mitotic exit promotion has been taken up by other phosphatases, the identity and substrates of which, barring a few, remain at large in many organisms.

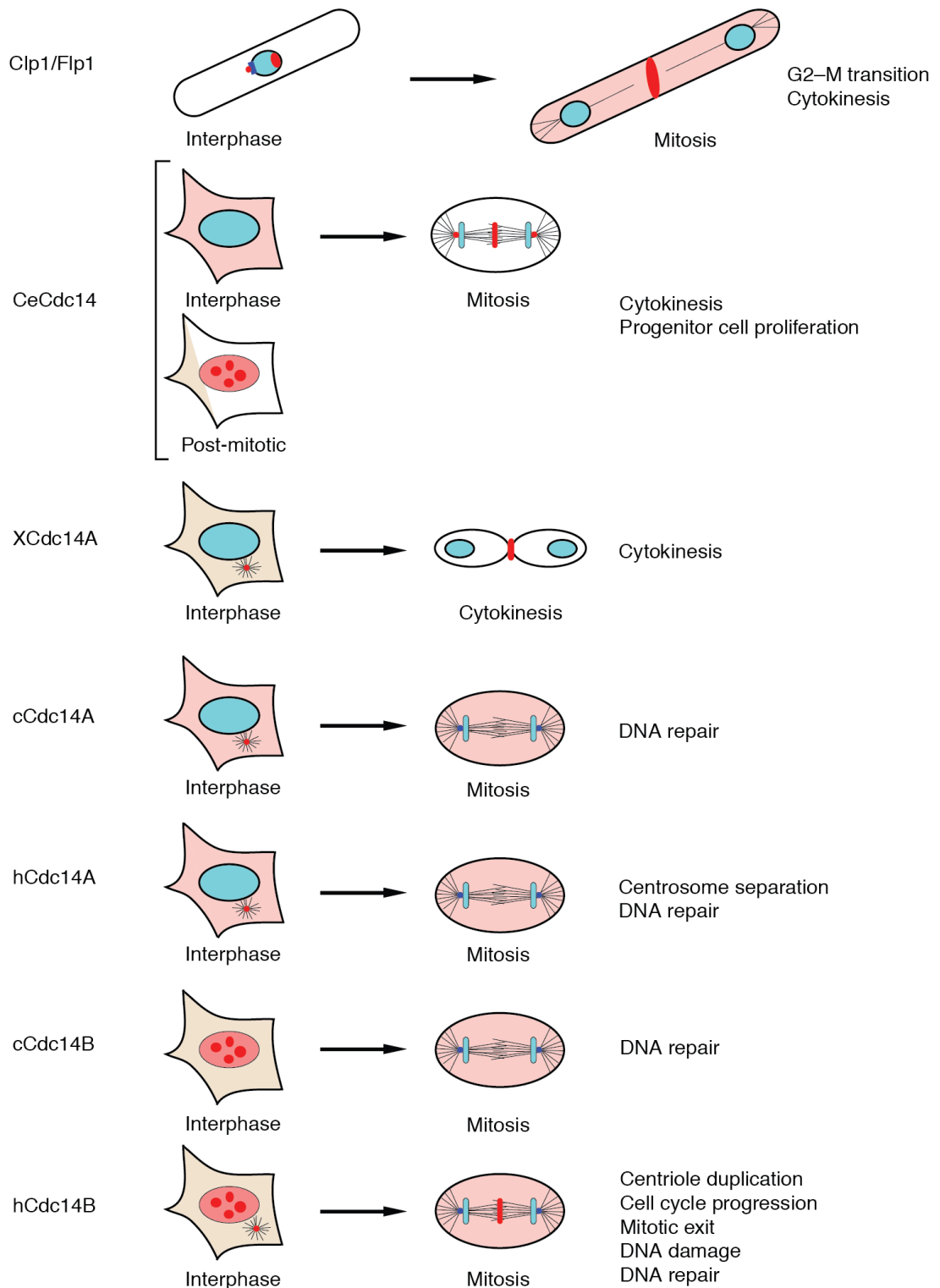


Figure 1.5 - Diverse roles of Cdc14 in different organisms.

Functions of *S. cerevisiae* (ScCdc14) *S. pombe* (Clp1), *C. elegans* (CeCdc14), *X. Leavis* (XCdc14A), *G. gallus* (cCdc14A/B) and human (hCdc14A/B) are depicted, with Cdc14 localization in red. Adapted from Mocciaro and Schiebel (2010).

Nonetheless, the principle that exit from mitosis requires Cdk-opposing phosphatase activity(ies) is a defining feature of eukaryotic life.

1.7.1 *Schizosaccharomyces pombe* (fission yeast)

The fission yeast homolog of Cdc14, Clp1/Flp1 was found to be inessential for executing exit from mitosis (Cueille et al., 2001). Similar to its budding yeast counterpart, Clp1 is nucleolar during most of interphase. However, it is released at the G2/M transition in a Cdk1 phosphorylated, inactive form, spreading to the nucleus and the cytoplasm at the same time. Following a decline in Cdk activity in anaphase, it autocatalytically removes these phosphorylations and self-activates (Wolfe, McDonald, Yates and Gould, 2006).

Clp1 was shown to dephosphorylate and inactivate the Cdk-activating phosphatase Cdc25 both *in vivo* and *in vitro* (Wolfe and Gould, 2004), thereby contributing to Cdk downregulation. Similarly, it has also been implicated in dephosphorylation of Ase1, a microtubule-bundling spindle midzone protein, thus contributing to anaphase spindle dynamics (Fu et al., 2009). Later in mitosis, a signalling cascade analogous to MEN, called the Septation Initiation Network (SIN) enables localization of Clp1 to the actomyosin ring, where it regulates septum formation. Accordingly, although *clp1Δ* cells are viable, they display frequent defects in cytokinesis (Celton-Morizur et al., 2004). In these regards, Clp1 and ScCdc14 display some overlap in their cellular functions.

Which phosphatases promote mitotic exit in fission yeast? A recent study found the existence of a 'relay' driving mitotic exit, wherein upon anaphase onset, active PP1 sequentially activates PP2A-B55, which then initiates PP2A-B56 activation. Disruption of this regulatory cascade leads to errors in chromosome segregation (Grallert et al., 2014). As these events correlate with mitotic exit, it is tempting to speculate that these are bona fide mitotic exit phosphatases. However, the knowledge of which substrates they dephosphorylate and how these relate to cytological events still eludes us. Proteomic studies have identified many PP2A-B55 substrates (Bernal et al., 2014), but they tend to cluster in processes controlling cellular metabolism.

1.7.2 Mammalian cells

1.7.2.1 *Mitotic exit function of Cdc14 is not conserved in mammals*

In mammalian cells, Cdc14 is found in three, structurally similar isoforms: Cdc14A, Cdc14B and Cdc14C. Overall, the three isoforms appear to have distinct expression profiles in tissues and even subcellular locations. For instance, Cdc14A is found to be primarily centrosomal (Mailand et al., 2002) whilst Cdc14B appears nucleolar during interphase (Li et al., 1997). During mitosis, they appear delocalized from these locations, similarly to their budding yeast counterpart. Mechanisms controlling this delocalization or indeed their locations are not well understood.

Substrates and processes regulated by Cdc14A and B have mostly been discovered on a case-by-case basis, with findings as to the functions of these phosphatases often being inconsistent. For instance, one study found that overexpression of Cdc14A in U2OS cells led to unscheduled centrosome amplification and supernumerary spindles, along with chromosome missegregation and cell death (Mailand et al., 2002). Overexpression of Cdc14B had no effect in these cells. However, Cdc14B knockdown using siRNA in HeLa cells caused extensive centrosome duplication, with overexpression causing a prolonged S-phase (Wu et al., 2008).

Similar studies taking overexpression/knockdown approaches have implicated the proteins in a myriad of other cellular processes such as regulation of Cdk activity by dephosphorylating Wee1 and altering its stability (Ovejero, Ayala, Bueno and Sacristan, 2012) or Cdc25 dephosphorylation which inhibits its activity (Vazquez-Novelle et al., 2010), dephosphorylation of ERK3 leading to its stabilization (Tanguay, Rodier and Meloche, 2010), promotion of mitotic exit by dephosphorylation and degradation of the histone deacetylase Sirt2 (Dryden et al., 2003), etc.

In contrast, other studies taking a homozygous knockout approach have failed to replicate these cell cycle phenotypes. Instead, these studies have implicated Cdc14 phosphatases in DNA repair processes. For instance, Cdc14A or Cdc14B single

knockout cells showed no cell cycle delay and were competent in mounting a DNA damage response, but showed elevated levels of background DNA damage and reduced DNA damage repair (Mocciaro et al., 2010), associating the phosphatases with this process.

Accordingly, Mouse Embryonic Fibroblasts (MEFs) homozygous null for Cdc14B displayed DNA repair defects which were found to be redundantly controlled by Cdc14A (Lin et al., 2015). Otherwise, these cells were found to have normal cell cycle profiles, contradicting previous studies that linked Cdc14B with mitotic processes. In a similar vein, contrary to previous reports, Cdc14B homozygous knockout RPE-TERT cells exhibited no discernible mitotic phenotype when scored for events such as chromosome segregation, mitotic exit, and cytokinesis (Berdougo, Nachury, Jackson and Jallepalli, 2014).

Taken together, an overall theme in Cdc14 studies has emerged: misexpression or knockdown studies tend to have a cell cycle phenotype whilst knockout studies do not. How to reconcile these observations? It is worth mentioning that Cdc14A and B double knockout cells still await analysis, thus redundancy between the proteins cannot be ruled out, as is known to be the case for proteins such as the mammalian Cdc25 paralogs (Ferguson, White, Donovan and Piwnicka-Worms, 2005). It is also possible that knockout cell lines do not recapitulate previous observations as the procedure leads to selection of cells that have adapted to the loss of the proteins via different mechanisms. Extrapolating from observations in *Caenorhabditis elegans*, a study found that RNAi of Cdc-14 caused many cytokinetic defects in embryos, which causes embryonic lethality in the long run (Gruneberg, Glotzer, Gartner and Nigg, 2002). However, another study was successful in generating Cdc-14 null worms, perhaps alluding to the existence of compensatory mechanisms (Saito et al., 2004). In contrast, comparison of acute and well as long-term Cdc14 knockout performed in human cells by Berdougo and colleagues (2014) found no differences in phenotypes.

In summary, the involvement and precise functions of Cdc14 proteins are far from clear in mammals, but they do not appear to be major players in mitotic exit.

1.7.2.2 PP2A is a mammalian mitotic exit phosphatase

Nonetheless, regulation by phosphatases has been shown to be a central requirement of mitotic exit in mammals.

Potapova et al., (2006) found that chemical inhibitor-mediated downregulation of Cdk activity at metaphase in HeLa cells led to mitotic exit and cytokinesis. This was accompanied by loss of phosphorylation of Cdh1, indicating activation of phosphatase(s). Other studies found that treatment of cells with okadaic acid (OA) (an inhibitor of PP1 and PP2A depending on the concentration used, with the IC_{50} of PP2A being 100-fold lower) lessened bulk substrate dephosphorylation (Skoufias et al., 2007; McCloy et al., 2015). Similarly, OA treatment or siRNA of B55 α or B55 δ , too led to preservation of mitotic phosphorylations (Manchado et al., 2010; Schmitz et al., 2010).

These observations have led to the conclusion that certain isoforms of PP2A-B55 contribute to mitotic exit in higher animals. But, how is its activity regulated to coincide with mitotic exit? Findings in various model organisms have led to the following picture: PP2A-B55 activity is firstly downregulated at mitotic entry, which enables efficient Cdk activation via dampening of Wee1 activity. Cdk1 phosphorylates and activates the conserved kinase Greatwall (also known as MASTL in humans), which then goes on to phosphorylate two highly unstructured, small protein inhibitors called Ensa and Arpp19 (Mochida, Maslen, Skehel and Hunt, 2010; Ma et al., 2016; Vigneron et al., 2009; Burgess et al., 2010; Gharbi-Ayachi et al., 2010). These act as 'unfair substrates' for PP2A, as the enzyme exhibits very high K_m and low k_{cat} towards them, in effect being inhibited by the proteins (Williams et al., 2014).

Following anaphase, cyclin proteolysis leads to the downregulation of Cdk activity and causes dephosphorylation and inactivation of Greatwall by PP1, Fcp1 and PP2A-B55 itself (Heim, Konietzny and Mayer, 2015; Ma et al., 2016; Monica et al., 2015). With the

kinase input ablated, Ensa/ARPP19 can now be dephosphorylated by PP2A or by Fcp1 (Williams et al., 2014; Hégarat et al., 2014), thereby relieving PP2A-B55 inhibition. Unconstrained, the phosphatase can now dephosphorylate its substrates.

By combining mass spectrometry- and modelling-based approaches, a recent study has been able to delineate hundreds of PP2A-B55 α substrates during an induced mitotic exit *in vivo* (Cundell et al., 2016), controlling processes such as spindle dynamics and nuclear envelope reassembly. Accordingly, a previous study also identified the spindle midzone protein Prc1 (human Ase1 homolog) as a PP2A-B55 α substrate during mitotic exit (Cundell et al., 2013). However, this study and others did not detect complete substrate dephosphorylation by PP2A-B55 alone, as adjudged by western blotting with a pan-Cdk antibody. This observation points to the complicity of other phosphatases in bringing about mitotic exit.

Accordingly, PP1 has also been proposed as a major mitotic exit phosphatase. In an analogous regulatory circuit to PP2A, PP1 also gets activated during mitotic exit due to Cdk downregulation. Autodephosphorylation of an inactivating residue, followed by dephosphorylation and dissociation of a small protein inhibitor, Inhibitor-1 generates active PP1 (Wu et al., 2009). Indeed, substrate dephosphorylation following PP1 activation has been observed in some studies (such as Manchado et. al., 2010). Whether this is primarily due to PP1-mediated activation of PP2A-B55, or due to its more direct role in opposing Cdk phosphorylations remains an open question.

Overall, one can say that no one phosphatase has been identified whose inhibition leads to a complete block of mitotic exit. It is possible that this is due to siRNA-related technical reasons. The other possibility is that many phosphatases collaborate to bring about mitotic exit in mammalian cells and that redundancy is built into the system.

1.7.3 Other organisms

The contribution of Cdc14 in bringing about mitotic exit is not much clearer in other organisms. *Xenopus laevis* contains two Cdc14 homologs, XCdc14A and XCdc14B, which share considerable sequence identities with the human hCdc14A and hCdc14B respectively (Mocciaro and Schiebel, 2010; Krasinska et al., 2007). Of these, only XCdc14A has been studied in some detail. The ectopically expressed protein localizes to the centrosome during interphase, but is found at the midbody in mitosis where it has been implicated in cytokinesis (Krasinska et al., 2007), but has not been found to have a more general role in mitotic exit.

Recent studies have started to unravel this knot: one reported the existence of an oscillating phosphatase activity that was required for the second meiotic exit in PP2B/Calcineurin-released *Xenopus* egg extracts (Mochida and Hunt, 2007), the identity of which was later revealed to be PP2A-B55 δ (Mochida, Ikeo, Gannon and Hunt, 2009). This is in accordance with an earlier report that biochemically assayed for phospho-H1 directed phosphatase activity from fractionated extracts (Ferrigno, Langan and Cohen, 1993), indicating that PP2A-B55 δ activity indeed controls mitotic exit.

However, based on further experiments, one is forced to conclude that PP2A-B55 δ is only a part of the mitotic exit story: whilst immunodepletion of this B isoform in interphase led to a complete block of mitotic exit (when induced by Cdk inhibition), doing so in mitotic extracts had a very small affect (Mochida et al., 2009), arguing that other phosphatases might be doing the bulk of the heavy lifting.

A similar theme has emerged in *Drosophila*. Although PP2A-B55 has been suggested to be important (Mayer-Jaekel et al., 1993), an RNAi screen directed against multiple phosphatases found that many, in fact collaborate to bring about mitotic exit (Chen et al., 2007). The details of requirement of each will have to be teased out further. In both *Drosophila* and *Xenopus*, the Greatwall-Ensa/Arpp19 regulation operates, showing that this level of phosphatase control is highly conserved.

More generally, that mitotic exit requires phosphatases is unequivocal, even though their identities and regulation vary between organisms.

1.8 Biochemical properties of Cdc14

1.8.1 Mechanism of catalysis

As mentioned previously, Cdc14 phosphatases belong to a family of dual-specificity phosphatases that can dephosphorylate both phosphoserine (pSer)/phosphothreonine (pThr) and phosphotyrosine (pTyr) residues. Although the overall dephosphorylation mechanism is conserved with other PTPs, their unique active site, defined by the consensus HC-(x)₅-R, allows accommodation of both types of residues (Tonks, 2006).

The active site contains the catalytic cysteine, Cys283 in budding yeast, which mounts a nucleophilic attack on the phosphorous atom of the incoming phosphorylated substrate (Fig. 1.6A). This leads to the formation of a thiol-phosphate intermediate, a step stabilized by the general acid Asp253 which donates a proton to the dephosphorylated protein. At this stage, the newly dephosphorylated substrate dissociates. Next, a water molecule leads to hydrolysis of the thiophosphate enzyme intermediate, again mediated by the general base Asp253, that accepts a proton from the water molecule (Fig. 1.6B) (Wang et al., 2004). Following this step, the phosphate moiety dissociates from the enzyme (Fig. 1.6C).

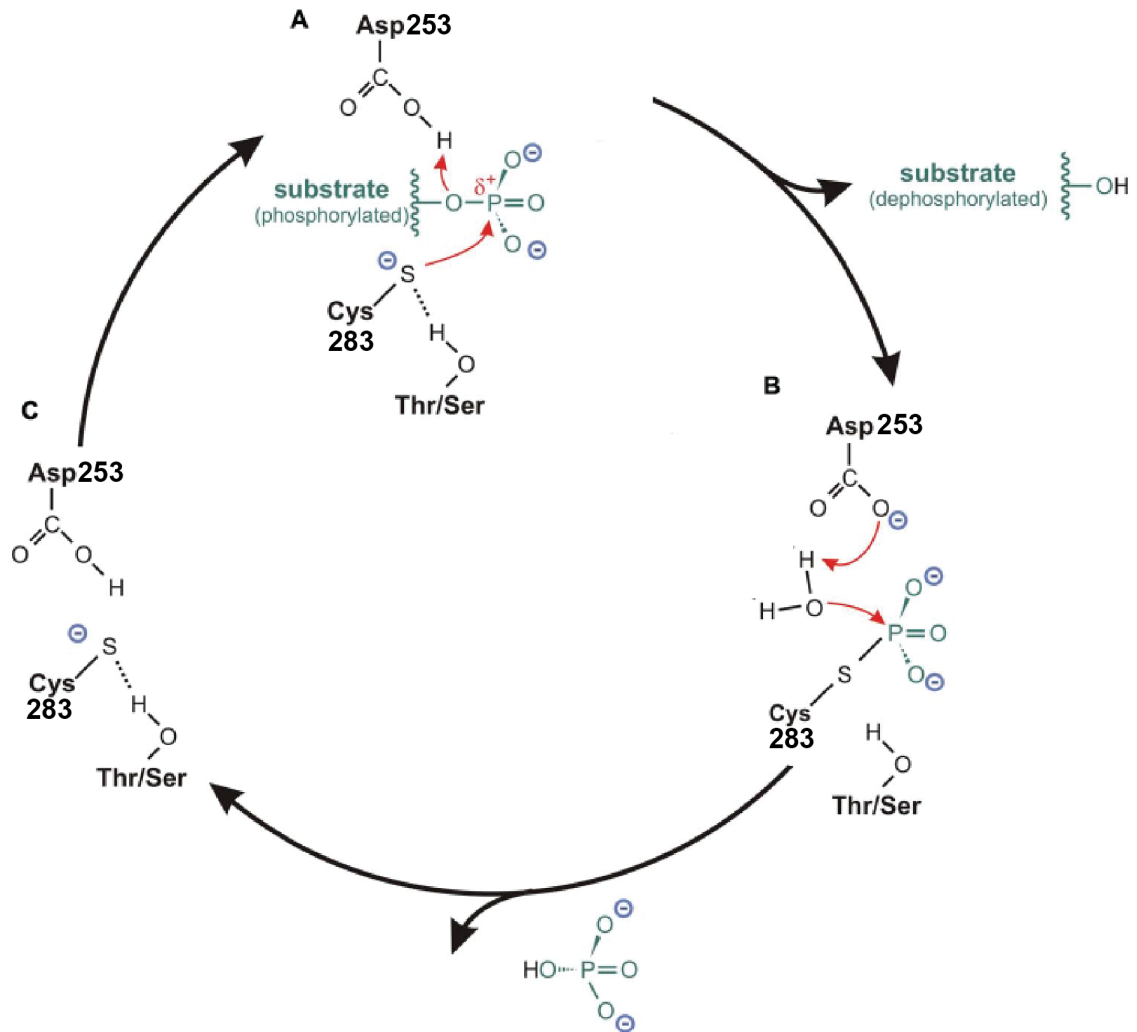


Figure 1.6 - Cdc14 catalysis mechanism.

A. Phosphate of the substrate experiences a nucleophilic attack by the thiol-containing Cys283, leading to **B.** an enzyme-phosphate intermediate and dissociation of the substrate. **C.** The general acid Asp253 and a water molecule lead to regeneration of the enzyme. Adapted from (Hobiger and Friedrich, 2015).

Structures of human Cdc14B indicate that although the Cdc14 catalytic pocket can easily accommodate pSer residues, it lacks the depth required for pTyr residue dephosphorylation (Gray, Good, Tonks and Barford, 2003). Accordingly, even though it is competent in pTyr-targeted activity *in vitro* (Taylor et al., 1997), *in vivo*, Cdc14 is thought to target pSer/pThr residues.

1.8.2 Structural properties

S. cerevisiae Cdc14 is a 551 amino acid long, 62 kDa protein. Curiously, it was found to be oligomeric *in vitro* via a number of biophysical and biochemical techniques (Taylor et al., 1997). The significance of this property is unknown.

As alluded to previously, all of our structural knowledge of the enzyme stems from a crystal structure of a portion of the human Cdc14 isoform, Cdc14B (Gray et al., 2003). A spontaneously truncated form of this protein was found to readily crystallize. Determination of its structure divulged the reason: this part contained a well-ordered, bipartite structure composed of two equivalently sized, globular domains arranged in tandem: the N-terminal domain A and the domain B, but lacked the C-terminal domain. Domains A and B compose the catalytic core of the enzyme. Sequence alignment with Cdc14 orthologs from diverse species has revealed that whilst these domains are evolutionarily well conserved and exhibit considerable sequence homology, the C-terminal domain is variable in both length and residue composition (Mocciaro and Schiebel, 2010).

Domain B adopts a classical dual-specificity phosphatase fold and contains the phosphatase consensus site along with all the residues required for catalysis. It forms the lion's share of the active site of the enzyme, with some contribution from domain A. The two domains are connected by a linker alpha helix which lies at the base of the active site (Fig. 1.7).

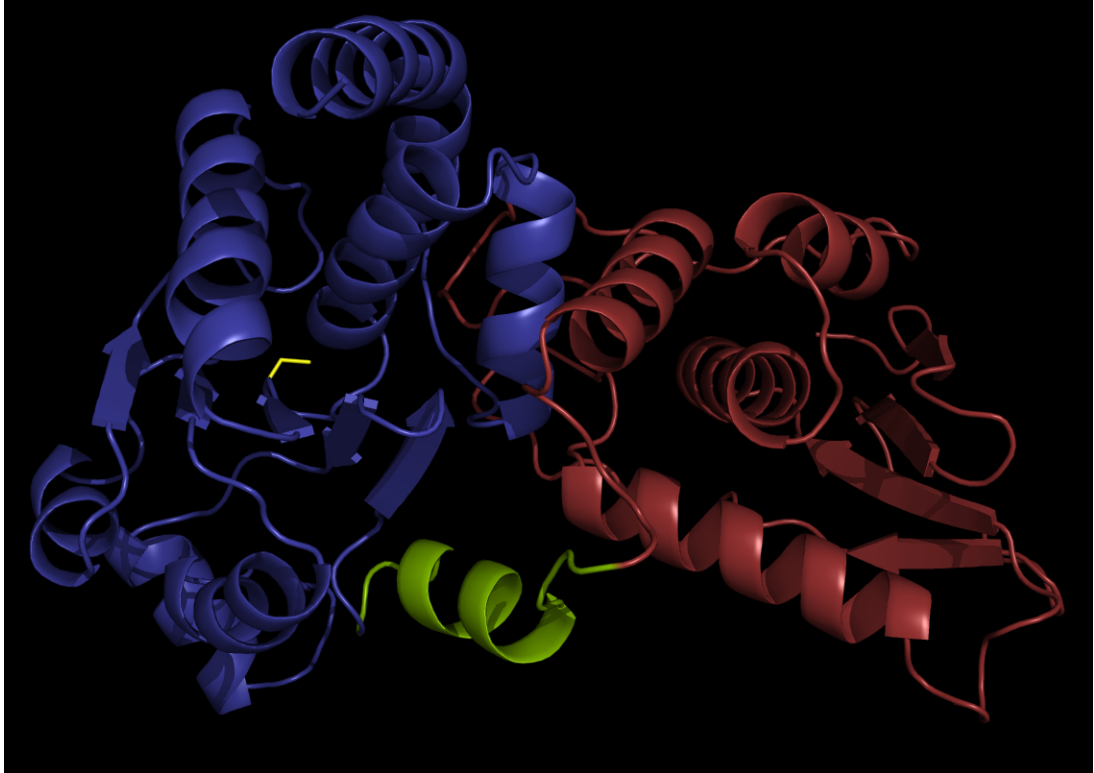


Figure 1.7 - Structure of ScCdc14.

A homology model of ScCdc14 was constructed using SWISS-MODEL (Schwede, Kopp, Guex and Peitsch, 2003), with hCdc14B structure as a template. Domain A is shown in red, and domain B in blue. The linker alpha helix is depicted in green. The catalytic Cys283 is shown in a stick representation in yellow.

Even though the two domains possess little in the way of sequence identity between each other (11%), domain A, too, was found to adopt a DSP-like fold (Gray et al., 2003). Crucially however, it lacks a phosphate-binding cradle and all the residues necessary for catalysis (Gray et al., 2003). Nonetheless, it contributes two residues, Phe47 and Tyr132 in budding yeast, that select for a Pro at the +1 position. Finally, the linker helix was found to possess a number of acidic residues facing inwards into the active site (Gray et al., 2003), and these could contribute to incoming phosphopeptide selection.

Comparison of the apo- and phosphopeptide-bound Cdc14B structures further revealed that there was no significant structural change or movement induced by binding of the substrate. Thus, unlike many other phosphatases, Cdc14 does not undergo conformational changes in response to phosphopeptide binding.

At present, domain C remains the only part of Cdc14 about which we have no structural information. Analysis using the secondary structure prediction software PSIPRED (McGuffin, Bryson and Jones, 2000), revealed that domain C contains no elements that are reliably predicted as structured, perhaps explaining its recalcitrance to crystallization. Deletion of this domain *in vitro* leads to slightly compromised phosphatase activity of the enzyme (Taylor et al., 1997). It is nonetheless thought to perform a regulatory role: it possesses a NES (spanning residues 359-367) (Bembenek et al., 2014) and a NLS at the very C-terminus of the protein. As mentioned previously, phosphorylation of the NLS late in anaphase by MEN kinases is thought to be the mechanism enabling Cdc14 release into the cytoplasm (Mohl et al., 2009).

Can domain B function by itself as a phosphatase? Aside from some contribution to +1 Pro specificity, does domain A exert any influence on substrate specificity? How does domain C contribute to these processes *in vivo* and *in vitro*? These questions remain to be answered.

1.8.3 Phosphosite specificity of Cdc14

The structure of Cdc14 has shed light on its preference for Cdk substrates i.e. pSP/pTP. Are there any other subtleties of enzyme-phosphosite interactions that further delineate substrate specificity?

The first question that comes to mind is: does Cdc14, like Cdk (Suzuki et al., 2015), prefer phosphoserines? A recent study examining this question found that ScCdc14, and indeed those from fission yeast and humans, have a very strong preference for serines over threonines (Bremmer et al., 2012). Substitution of pSer for pThr of a Cdc6-derived peptide, for instance, led to a drop in the catalytic efficiency of the enzyme towards it by three orders of magnitude, caused by a decrease in both k_{cat} and K_m . Steric hindrance, caused by a clash between the methyl side-chain of threonine and Ala316 of the Cdc14 active site (Fig 1.8), was cited as the reason behind this pSer selectivity. Although mutagenesis of Ala316 to Gly relieved some of this specificity *in vitro*

(Bremmer et al., 2012), it came at the cost of a massive reduction in overall catalytic ability of the enzyme, making detailed analysis difficult.

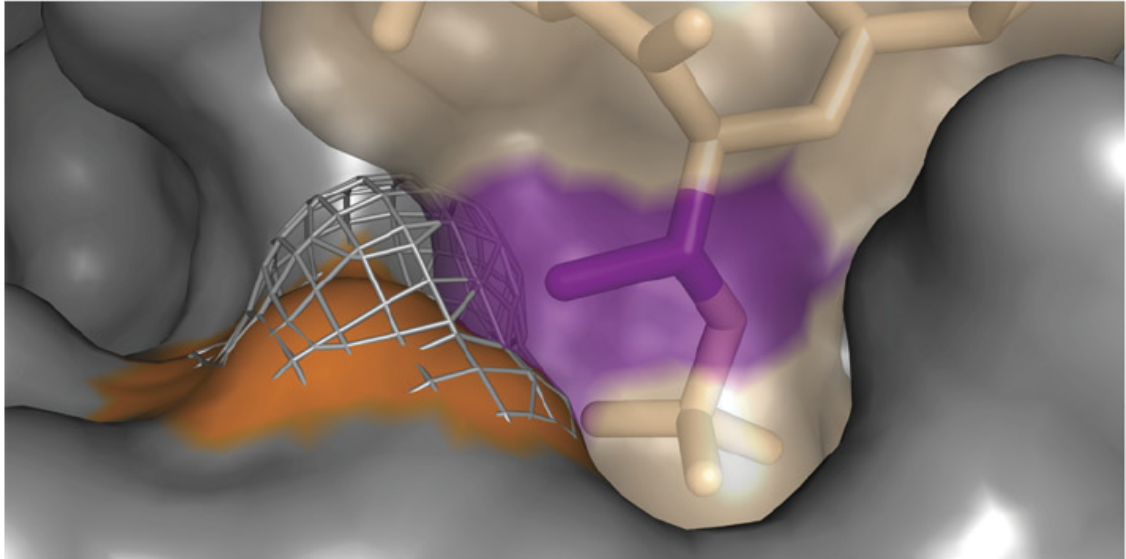


Figure 1.8 – Structural basis for pSer specificity of Cdc14.

An *in silico* model showing Cdc14 active site (in grey) containing the conserved Ala316 (in mesh), that might serve as a steric hindrance to the binding and subsequent catalysis of the methyl group (in purple) containing threonine side chain (in stick representation). Adapted from Bremmer et. al., (2012).

It is still unknown how, if at all, this selectivity translates *in vivo*. Given that 22% of Cdk phosphorylated substrates are threonines (based on (Holt et al., 2009)), and indeed a considerable proportion of dephosphorylation events dependent on Cdc14 are also on pTPs (Kao et al., 2014; Kuilman et al., 2015), makes this question pertinent.

Further, during the course of this project, a new publication posited that the ‘full’ Cdk consensus site, (S/T)-P-x-(K/R), containing a +3 lysine or arginine, is preferred by Cdc14 (Eissler et al., 2014). Surprisingly, molecular dynamic studies of this peptide and the Cdc14 active site showed that the positively charged lysine at the +3 position, instead of forming salt bridges with the acidic residues of the Cdc14 linker alpha helix as predicted, interacted with Phe47 and Tyr44 within the active site, engaging in cation- π interactions, i.e. electrostatic interactions between the delocalized electron cloud of these aromatic residues and the positively charged nitrogen ion of the lysine (Eissler et al., 2014). Basic residues downstream of the +3 position were predicted to interact with

the linker helix. These ideas, however, remains to be experimentally verified. These preferences were found to extend to enzymes from other species as well. However, in the crystal structure of hCdc14B bound to a peptide, ApSPR, the +3 Arg was not found to be structured, possibly because it engaged in a number of different interactions, leading to some doubt as to the precise nature of +3 residue interactions. As before, the importance of this position *in vivo*, within the context of an endogenous substrate (rather than a peptide) needs to be determined.

Finally, the -1 position of the Cdc14-bound peptide was found to be solvent directed in the crystal structure, making no significant contacts with the enzyme, perhaps indicating a lack of selectivity at this position by the phosphatase (Gray et al., 2003).

Another study found that Cdc14 disfavored catalysis of sites phosphorylated by the meiosis-specific serine/threonine kinase, Ime2. These sites are defined by the consensus RP-x-(S/T) - a subset of Cdk sites. This aversion of Cdc14 was proposed to protect phosphorylation of certain proteins, such as Cdh1 and the Mcm2-7 complex, thereby preventing complete exit from the meiotic program and DNA rereplication between the first and second meiotic divisions upon Cdc14 release (Holt, Hutt, Cantley and Morgan, 2007). The mechanistic details driving this specificity are unknown.

Outside the catalytic center, whether Cdc14 possesses other substrate specificities is still an open question.

1.9 The quantitative model of exit from mitosis

Observations from the previous two sections bring to light two important features of Cdc14: the fact that it is biochemically geared to target Cdk substrates, yet it does so at different times during mitotic exit. In other words, there is a measure of temporality to the dephosphorylation of substrates, which correlates with the order in which their function is required.

What brings about this order? Whilst a number of explanations were put forward, a study has examined this question in depth and proposed the ‘quantitative model of exit from mitosis’ (Bouchoux and Uhlmann, 2011). Representative substrates that were dephosphorylated *in vivo* with ‘early’ (Fin1), ‘intermediate’ (Sli15) and ‘late’ (Orc6) timings were chosen. The ability of both Clb2-Cdc28 and Cdc14 to act on them was examined *in vitro*. The kinase, in part, showed similar catalytic efficiencies towards the substrates. Cdc14 exhibited markedly varied catalytic efficiencies towards them. However, the only parameter that correlated with the timing of dephosphorylation *in vivo* was the activity ratio of the phosphatase to kinase. It was found to be very high for Fin1, lower for Sli15, and lesser still for Orc6. This shows that both decreasing kinase activity, and concomitantly increasing phosphatase activity are in a constant tussle within the cell. At different stages during mitotic exit, depending on the unique sensitivity of each substrate to this ratio, will the phosphatase gain the upper hand and lead to complete substrate dephosphorylation. By extension, this will lead to the promotion of a particular cellular function in a specific order (Fig 1.9).

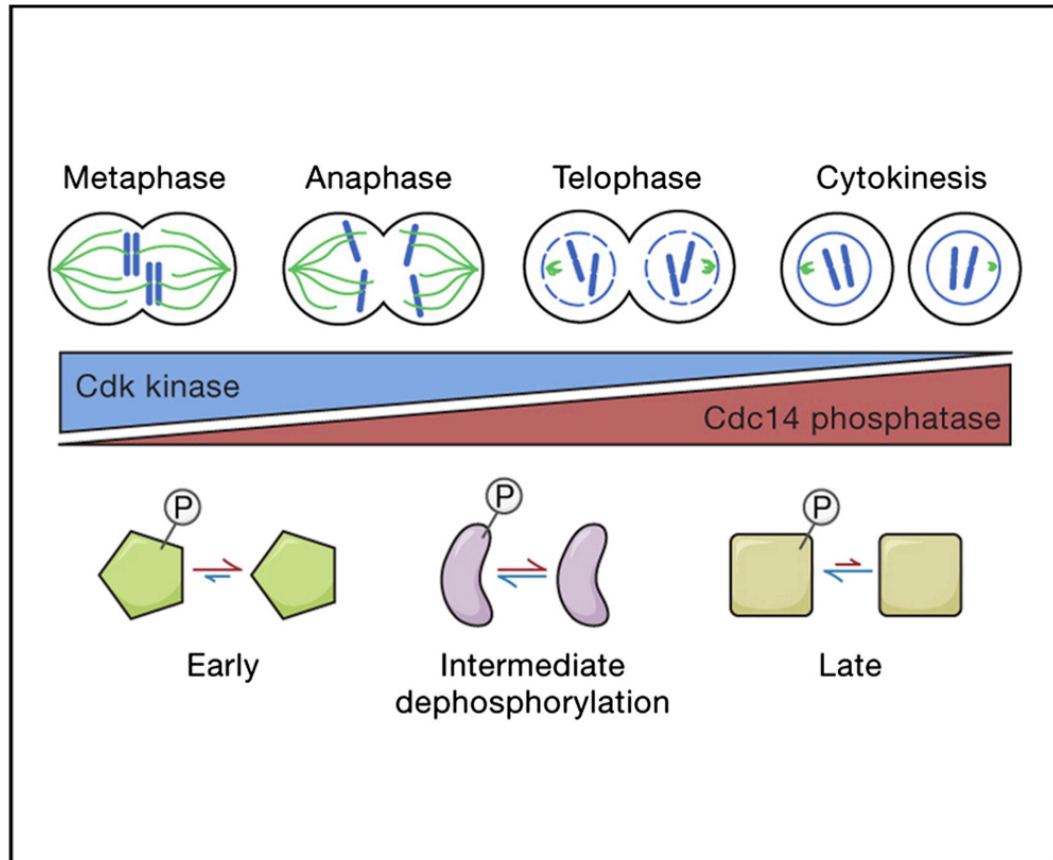


Figure 1.9 - A quantitative model for Cdk substrate dephosphorylation during mitotic exit.

Cdk substrates are dephosphorylated in an ordered manner depending on the ratio of Cdk to Cdc14 phosphatase activity during mitotic exit. At this stage, Cdk activity is declining due to the actions of the APC, and Cdc14 activity is rising due to the successive actions of the FEAR and MEN pathways. From Bouchoux and Uhlmann (2011).

Intuitively, it makes sense as neither reaction exists in isolation within the cell. Further, studies examining this relationship found that increasing Clb2-associated kinase activity led to a dose-dependent delay in mitotic exit events (Drapkin et al., 2009), with analogous findings in human cells (Wolf, Wandke, Isenberg and Geley, 2006).

However, there are other factors that can influence the dephosphorylation timing. In budding yeast that undergoes closed mitosis, localization of a substrate might become important. Cdc14 is not permitted access to the cytoplasm until later in mitosis, where a number of substrates (such as the cytokinetic machinery) lie. Accordingly, forced localization of Cdc14 to the nucleus by its fusion with a strong ectopic NLS promoted

mitotic exit but not cytokinesis (Kuilman et al., 2015). The representative substrates tested in the Bouchoux & Uhlmann (2011) study were all nuclear, showing that within this compartment, the quantitative model holds. One can thus assume that when Cdc14 is released into the cytoplasm, the same rules would be applicable, albeit later into the cell cycle.

Substrate competition can also play a part, especially in early anaphase, when small quantities of active enzyme face a vast molar excess of phosphorylated substrates. *In vitro*, competition with earlier, more efficient substrates was found to delay the dephosphorylation of the late substrate Orc6 (Bouchoux and Uhlmann, 2011).

Finally, whilst many substrates within the cell are soluble and can exhibit free diffusion, a number of them are found as components of fixed complexes wherein free diffusion is not possible. Thus, it is possible that the catalysis reaction would deviate from the generally assumptions of Michaelis-Menten kinetics.

1.10 Early substrate dephosphorylation

Shifting our focus back to early anaphase, the following situation emerges: newly released Cdc14 faces a large stoichiometric excess in its choice of substrates.

This stage also witnesses a number of critical events, such as securin degradation that promotes cohesion cleavage and sister chromatid separation. A study found that Cdk phosphorylation of residues close to securin's degron motifs inhibited APC action on the protein, which was relieved by Cdc14 dephosphorylation (Holt, Krutchinsky and Morgan, 2008).

Similarly, a role for Cdc14 in enabling complete compaction and segregation of the rDNA locus has been proposed (Sullivan, Higuchi, Katis and Uhlmann, 2004; D'Amours, Stegmeier and Amon, 2004), by enabling anaphase-specific recruitment of the condensing complex (D'Amours, Stegmeier and Amon, 2004).

As such, despite high kinase activity at this stage, Cdc14 needs to dephosphorylate some key targets, for which the reaction equilibrium must lie decidedly towards dephosphorylation (Fig. 1.10) for some substrates. What are the factors controlling efficient early substrate dephosphorylation? Possible explanations will be dealt with herewith.

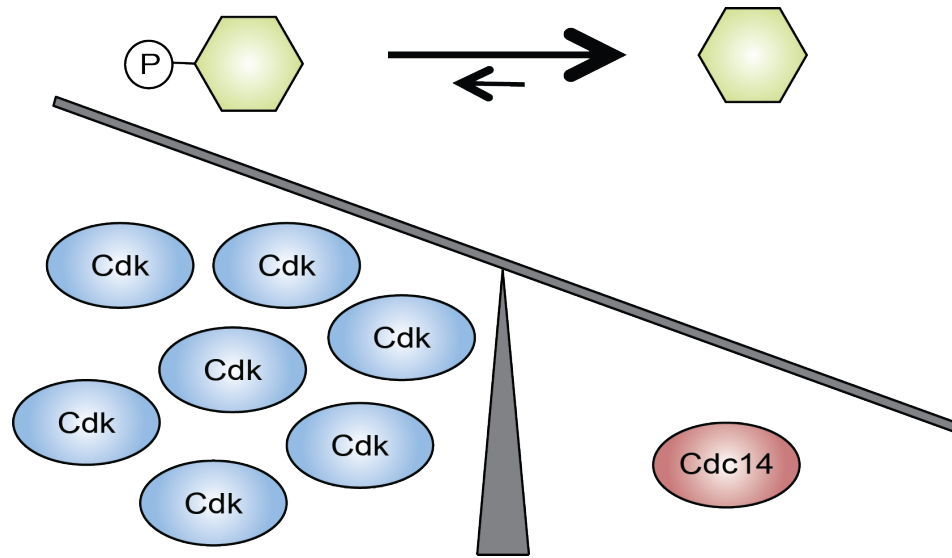


Figure 1.10 - Balance of powers in early anaphase.

Early anaphase witnesses a large excess of Cdk activity over Cdc14 activity, which still leads to the dephosphorylation of some early substrates.

1.10.1 Clb5 degradation in early anaphase

As mentioned previously, budding yeast exhibits a biphasic pattern of Cdk inactivation, beginning with complete degradation of the S-phase cyclin Clb5 and only partial degradation of the mitotic cyclin Clb2. Furthermore, Clb5 also efficiently phosphorylates a subset of Cdk substrates – those containing the RxL motif.

These observations have led to the hypothesis that the early degradation of Clb5 is a major factor responsible for early dephosphorylation of its RxL-containing substrates (Sullivan, Holt and Morgan, 2008; Jin et al., 2008) (Fig. 1.11) - an idea that harks back to the ‘unregulated phosphatases’ roots of the field.

Yet, it has been appreciated that the dephosphorylation of RxL-containing Cdh1, Orc6 and Sic1 occurs late into mitosis, well after Clb5 has been degraded. The remaining mitotic cyclin, Clb2 is a stronger activator of Cdc28 than Clb5 (Kõivomägi et al., 2011) and its role in maintaining phosphorylation in early anaphase cannot be ignored. Indeed, qualitative aspects aside, the main factor pertinent to a substrate is the quantitative input it receives from a kinase.

Nonetheless, a systematic study examining this question remains to be performed. Additionally, the dependence of early Cdc14 substrates, some of which are RxL-bearing, on early Clb5 degradation is as yet unknown.

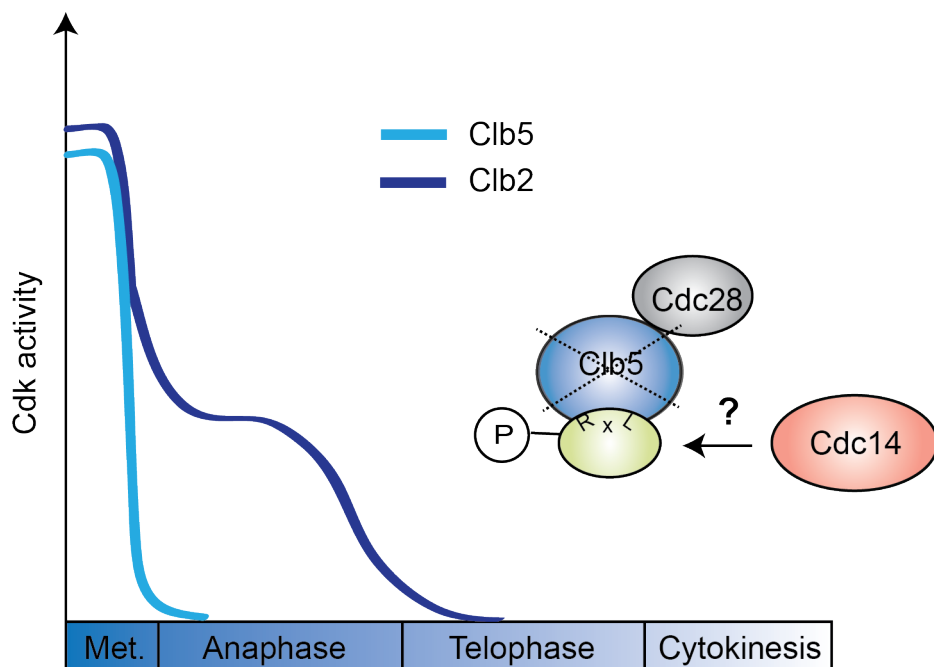


Figure 1.11 – A kinase-centric hypothesis for early substrate dephosphorylation.

One hypothesis of early substrate dephosphorylation is that early degradation of Clb5 enables the kinase's preferred substrates to be dephosphorylated by Cdc14.

1.10.2 Early substrate dephosphorylation – a role for docking sites?

1.10.2.1 *Use of docking sites is ubiquitous amongst cell cycle regulators*

Another possibility is that a subset of early substrates is able to overcome the fierce competition for phosphatase attention in early anaphase by ‘finding’ the phosphatase using remote docking sites.

Docking site-mediated interactions are a ubiquitous feature of the cell cycle and indeed, cellular regulation. They facilitate processes such as efficient Cln2- or Clb5-driven phosphorylation (Bhaduri and Pryciak, 2011; Loog and Morgan, 2005), multisite substrate phosphorylation by Cks1 (Kõivomägi et al., 2013; McGrath et al., 2013), substrate degradation by Cdc20/Cdh1 (Glotzer, Murray and Kirschner, 1991; Pflieger and Kirschner, 1992) and association with regulatory proteins of PP1 (Egloff et al., 1997). These regulator-substrate interactions are often mediated by short, linear interaction motifs, ten or fewer residues in length, typically found in intrinsically unstructured protein regions (Davey, Cyert and Moses, 2015). They tend to possess weak, low micromolar-range affinity for the substrate (Van Roey et al., 2014) allowing for dynamic interactions.

For instance, even though Cln2 is a poor activator of Cdc28, possessing 2.4% of the catalytic efficiency of Clb2-Cdc28 (calculated from (Kõivomägi et al., 2011)), it can nonetheless promote efficient and timely phosphorylation of LLPP motif-containing proteins (Bhaduri and Pryciak, 2011). In this way, it promotes progression of cells through Start and commitment to the cell cycle.

Modular combination of docking sites within the same substrate can also allow for coordination of different events. Efficient phosphorylation is promoted by the RxL motif, and efficient degradation by the cyclosome via D-box and ABBA motifs – all contained within Clb5 (Lu et al., 2014). Figure 1.12 summarizes a few examples of docking sites employed by some important cell cycle regulators.

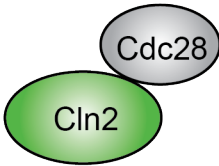
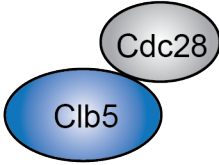
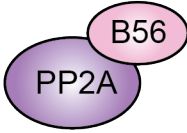
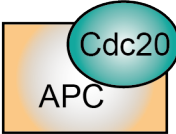
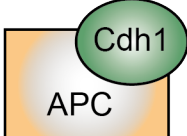
	Substrate motif	Important target(s)
	LLPP (Bhaduri & Pryciak, 2011)	Ste5, Ste20
	RxL (Johnson et al., 1999)	Orc6, Cdh1, Ase1
	(F/I/L/P/V/W/Y)xpTP (McGrath et al., 2013)	Cdc6, Swe1, Sic1
	LxxIxE (Wang et al., 2016)	Mad3
	D-box (Glotzer et al, 1991) ABBA motif (Lu et al., 2016)	Clb5, securin Clb5, Acm1, Bub1
	KEN box (Pfleger & Kirschner, 1992)	Cdc20, Cdc5, Ase1
	RVxF (Egloff et. al., 1997)	Fin1, Spc105, Sds22
	PxIxIT (Boustany & Cyert, 2002)	Crz1
	D-site (Bardwell et al., 2001)	Ste7
	S(pS/pT)(P/x) (Elia et al., 2003)	Net1, Scc1, Cdc14

Figure 1.12 – Regulator-substrate interactions are often facilitated by short linear binding motifs.

Given these examples, it seems reasonable to suggest that early Cdc14 substrates may possess docking sites for the phosphatase that promote timely and efficient dephosphorylation of a critical subset of targets.

1.10.2.2 *Fin1 – a candidate Cdc14 docking-site possessor?*

Bouchoux & Uhlmann (2011) found that Fin1 is not only one of the earliest substrates of Cdc14 but that the phosphatase also possesses a high catalytic efficiency towards it. When compared to some of the later substrates, it is an order of magnitude higher. This high catalytic efficiency also correlates with efficient interaction of Fin1 with the phosphatase, especially when compared to intermediate and later substrates. The fact that this interaction stays largely intact even when the Fin1 is not phosphorylated, points to phosphosite-independent interactions – a docking motif, perhaps.

Although the function of Fin1 is not well understood, the importance of its timely phosphoregulation is clear, with overexpression of non-phosphorylatable mutant being lethal.

Fin1 is a 31 kDa highly basic protein (with a pI of 10), which is predicted to be mostly unstructured, barring two coiled-coils at its C-terminus that enable self-association. They also enhance microtubule binding (van Hemert et al., 2003; Woodbury and Morgan, 2007). Absent in G1 due to APC^{Cdh1} activity, Fin1's abundance rises during S-phase. It is phosphorylated by Clb5-Cdc28, which is known to enhance its association to the localization anchor 14-3-3 proteins Bmh1 and Bmh2 *in vitro* and *in vivo* (Mayordomo and Sanz, 2002).

During interphase, a small pool of Fin1 is also bound to the budding yeast PP1, Glc7 at kinetochores, where it enhances PP1 activity towards unknown targets and regulates the mitotic checkpoint (Akiyoshi et al., 2009). At anaphase onset, Cdc14-mediated

dephosphorylation of Fin1 on Cdk residues drives its localization to the spindle pole body and the elongating spindle. Here, it is thought to stabilize the spindle through the microtubule-binding activity of its N-terminal region (Woodbury and Morgan, 2006; 2007), prevent checkpoint signaling by upregulating PP1 levels at the spindle (Akiyoshi et al., 2009) and enable clearance of the checkpoint protein Bub1 at kinetochores (Bokros et al., 2016). During late anaphase, APC^{Cdh1} begins degradation of Fin1.

Whilst *fin1*Δ cells do not have a phenotype, expression of the non-phosphorylatable Fin1 is lethal, and causes rampant chromosome mis-segregation (Woodbury and Morgan, 2006), which is partly contingent upon its binding to Glc7 via RVxF-type motifs (Bokros et al., 2016).

Thus, efficient dephosphorylation of Fin1 by Cdc14 could be regulating both spindle integrity and the spatial dynamics of the mitotic checkpoint in anaphase.

1.11 Project aims

1.11.1 Biochemical features of Cdc14 that enable substrate recognition

As mentioned in section 1.8.2, Cdc14 is thought to be multimeric *in vitro*. To further understand the importance of this property and its relevance to substrate recognition and dephosphorylation, the precise stoichiometry of Cdc14 needs to be determined. Also, an understanding of which domain(s) of Cdc14 enable this oligomerization would provide a direct way of comparing monomeric and dimeric proteins, and testing their properties with regards to substrate recognition and subsequent catalysis.

Further, Cdc14 contains three tandemly arranged domains, two of which are evolutionarily conserved. However, the importance of each domain in substrate and inhibitor recognition presents a gap in our knowledge.

In chapter 3, I have outlined my results concerning Cdc14 stoichiometry, and the importance of the three domains for substrate recognition and catalysis *in vitro* and *in vivo*.

1.11.2 What factors influence efficient early substrate dephosphorylation?

Having studied properties of the phosphatase, I wanted to focus my attention on features within substrates that enable efficient catalysis. One readily appreciated fact about Cdc14 is that there is a huge spread in its catalytic efficiencies towards substrates. What features is Cdc14 'reading' and subsequently 'integrating' within substrates that change its behaviour towards them? I have used Fin1 as a model substrate to answer these questions because of our prior knowledge of catalytic efficiencies of both the kinase and the phosphatase towards it. Most importantly, not only was Fin1 found to be a highly efficient Cdc14 substrate, it also exhibits strong interactions with the phosphatase compared to other, less efficient substrates. These observations make it likely that Fin1 possesses unique features that enable its early and proficient dephosphorylation by Cdc14.

Further, I have divided the question of substrate recognition and catalysis into two parts. First, the place of Cdc14 action is the site(s) of phosphorylation within a protein. Thus, it is possible that differences within these could define windows of dephosphorylation timings for substrates. Chapter 4 describes my systematic analysis of the importance of various motifs within phosphosites and their impact on dephosphorylation, both *in vivo* and *in vitro*. Using Fin1, I have attempted to provide a full description of kinase and phosphatase reactions, and found that they together determine equilibrium phosphorylation/dephosphorylation.

Second, I have considered the possibility that phosphosites are only part of this equation; 'remote' features within substrates could also enable efficient dephosphorylation. In this regard, I attempted to define a Cdc14 docking site within Fin1 that enables its efficient dephosphorylation. Multiple biochemical and biophysical techniques were employed, but I was unable define a short linear motif within the

protein of the kind described for other binary enzyme-substrate interactions. Nonetheless, I was able to discover a number of features of Cdc14-Fin1 binding. Further, I have also examined a kinase-centric model of early dephosphorylation of Fin1. These results are presented in chapter 5.

Finally, in chapter 6, I have discussed the relevance and implications of these findings, and how they relate to our current view of the cell cycle and beyond.

Chapter 2. Materials and Methods

2.1 Yeast techniques

2.1.1 Yeast strains and growth conditions

All budding yeast strains used in this study were of W303 background. The strains were grown in YP (Yeast Extract Peptone) media, which was supplemented with 2% (w/v) glucose (YPD – YP Dextrose) or, 2% (w/v) raffinose/galactose with 0.05% (w/v) glucose (YP-Raff/Gal).

For selection of transformants, YNB (Yeast Nitrogen Agar) plates, supplemented with 60 µg/ml of the following amino acids (except for the one used for selection) were used: adenine, isoleucine, leucine, lysine, histidine, phenylalanine, tyrosine, tryptophan, and 50 µg/ml threonine.

Cells were sporulated on sporulation media (table 2.1).

Medium name/ Abbreviation	Composition
YP	Yeast Extract Peptone – 1.1% w/v yeast extract, 2.2% w/v bacto-peptone and 0.0055% w/v adenine-HC
YNB	Yeast Nitrogen Base – 0.8% w/v yeast nitrogen base
YP agar	1.1% w/v yeast extract, 2.2% w/v bacto-peptone and 0.0055% w/v adenine-HC, 2% w/v agar
YNB agar	0.8% w/v yeast nitrogen base, 2% w/v agar
Sporulation media	100 mM CH ₃ COONa, 20 mM NaCl, 25 mM KCl, 1.5mM MgSO ₄ and 1.5% w/v agar

Table 2.1 – Media composition

2.1.2 Strain list

Strain name	Genotype	Mating Type
MK14	Fin1 Δ 263 - 3PK::TRP, Ask1-9myc::URA	a
MK16	Dsn1-3Pk::HIS, Ask1-9myc::LEU, Fin1-3 HA::URA Mut A	a
MK17	Dsn1-3Pk::HIS, Ask1-9myc::LEU, Fin1-3HA::URA KNL	a
MK18	Dsn1-3Pk::HIS, Ask1-9myc::LEU, Fin1-3HA::URA Mut B	a
MK19	Dsn1-3Pk::HIS, Ask1-9myc::LEU, Fin1-3HA::URA Mut C	a
MK20	Dsn1-3Pk::HIS, Ask1-9myc::LEU, Fin1-3HA::URA Mut D	a
MK21	Dsn1-3Pk::HIS, Ask1-9myc::LEU, Fin1-3HA::URA Mut E	a
MK22	Dsn1-3Pk::HIS, Ask1-9myc::LEU, Fin1-3HA::URA Mut F	a
MK23	Dsn1-3Pk::HIS, Ask1-9myc::LEU, Fin1-3HA::URA Mut G	a
MK24	Dsn -3Pk::HIS, Ask1-9myc::LEU, Fin1-3HA::URA Mut H	a
MK25	Dsn1-3Pk::HIS, Ask1-9myc::LEU, Fin1-3HA::URA Mut I	a
MK26	Dsn1-3Pk::HIS, Ask1-9myc::LEU, Fin1-3HA::URA Mut J	a
MK27	Dsn1-3Pk::HIS, Ask1-9myc::LEU, Fin1-3HA::URA Mut K	a
MK28	Dsn1-3Pk::HIS, Ask1-9myc::LEU, Fin1-3HA::URA Mut L	a
MK29	Dsn1-3Pk::HIS, Ask1-9myc::LEU, Fin1-3HA::URA Mut M	a
MK30	Dsn1-3Pk::HIS, Ask1-9myc::LEU, Fin1-3HA::URA Mut N	a
MK31	Dsn1-3Pk::HIS, Ask1-9myc::LEU, Fin1-3HA::URA Mut O	a
MK32	Dsn1-3Pk::HIS, Ask1-9myc::LEU, Fin1-3HA::URA Mut P	a
MK33	Dsn1-3Pk::HIS, Ask1-9myc::LEU, Fin1-3HA::URA Mut Q	a
MK34	Dsn1-3Pk::HIS, Ask1-9myc::LEU, Fin1-3HA::URA Mut R	a
MK35	Dsn1- 3Pk::HIS, Ask1-9myc::LEU, Fin1-3HA::URA Mut S	a
MK36	Dsn1-3Pk::HIS, Ask1-9myc::LEU, Fin1-3HA::URA Mut T	a
MK37	Dsn1-3Pk::HIS, Ask1-9myc::LEU, Fin1-3HA::URA Mut U	a
MK38	Dsn1-3Pk::HIS, Ask1-9myc::LEU, Fin1-3HA::URA +3A	a
MK39	Dsn1-3Pk::HIS, Ask1-9myc::LEU, Fin1-3HA::URA	a
MK40	Dsn1-3Pk::HIS, Ask1-9myc::LEU, Fin1-3HA::URA 6TP	a
MK41	Dsn1-3Pk::HIS, Ask1-9myc::LEU, Fin1-3HA::URA 6TPxA	a
MK42	Yen1-3PK::TRP, Fin1-3HA::URA, Ask1-9myc::LEU	a
MK46	Ask1-9myc::LEU, Fin1-3HA::URA, Cdc14-6Pk ::TRP	a
MK47	Ask1-9myc::LEU, Fin1-3HA::URA, Cdc14 (1-374)-6Pk ::TRP	a
MK67	Dsn1-3Pk::HIS, Ask1-9myc::LEU, Fin1 Δ C250::URA	a
MK72	Clb5 Δ db::His, FIn1-3HA::URA, Ask1-9myc::TRP	a
MK79	GAL-Cdc20::LEU, Fin1-3HA::URA	a

Table 2.2 – List of strains used in this thesis.

2.1.3 Cell synchronisation

For arresting cells in the G1 phase of the cell cycle, yeast cells of the 'a' mating type were grown to early log phase ($OD_{600} = 0.15$), and then treated with synthetically derived mating pheromone α -factor (manufactured by the Peptide Chemistry Laboratory, The Francis Crick Institute Lincoln's Inn Fields Laboratory) at a final concentration of 2.5 $\mu\text{g/ml}$. Cultures were treated with α -factor once an hour, for a total time of 2.5 hours. Following synchronisation, the cells were released into the appropriate medium (devoid of α -factor), by collecting the cells on a membrane filter using a filtration device, and extensively washing (>10 times the culture volume) the cells with YP media. For re-arrest in the G1 phase of the following cell cycle, 7.5 $\mu\text{g/ml}$ of α -factor was added to the cells 70 minutes post-release.

For arresting cells in metaphase, yeast strains that had the endogenous Cdc20 promoter replaced by a galactose inducible promoter were constructed. The strains were grown in YP containing raffinose and galactose, each at a final concentration of 2% (w/v). For achieving the metaphase arrest by Cdc20 depletion, the cultures were extensively washed and resuspended in media lacking galactose (containing raffinose as the only energy source) for 2.5 hours at OD_{600} of 0.2. Next, the cells were released to progress through the cell cycle by adding galactose at a final concentration of 2% (w/v) and arrested in G1 by α -factor addition at a concentration of 2.5 $\mu\text{g/ml}$ at the time of release.

2.1.4 Yeast transformation

Yeast transformation was performed using PCR reactions for tagging genes with an epitope, gene mutagenesis, or with enzyme-linearized plasmid DNA for exchanging promoters of genes.

Briefly, 50-100 ml of mid-log phase cells ($OD_{600} = 0.1 - 0.5$) were pelleted and washed with 1 ml distilled water, followed by 1 ml TEL (10 mM Tris/HCl pH 7.5, 100 mM EDTA, 100 mM LiOAc). The cells were finally resuspended in 50 μl TEL. This cell suspension was added to a mixture of 1 μg linearized plasmid DNA or 8 μl PCR

product mixed with 2 μ l of 10 mg/ml single stranded salmon sperm carrier DNA. Three hundred μ l of TEL-P (TEL containing 40% PEG 4000) was added to the mixture, and vortexed briefly. The cells were incubated at 25°C for 2 - 4 hours, following which they were heat-shocked for 15 minutes at 42°C. After pelleting, the cells are resuspended in 1 ml 1 M sorbitol and plated on selective media.

Positive clones were checked for the appropriate integration by PCR, western blot analysis, diagnostic PCRs and/or Sanger sequencing.

2.1.5 Yeast mating and tetrad dissection

Mating was induced by incubation of the opposite mating type yeast strains on YPD plates at 25°C for 8 hours. Diploids were selected on appropriate selective media and grown again on YPD for 24 hours. For sporulation, they were plated on a sporulation plate for 2 - 3 days. Spores were then resuspended in 1 M sorbitol and treated with Lyticase (Sigma-Aldrich) at 30°C for 10 minutes to digest the asci. The four released spores from each ascus were dissected using Singer-MSM micromanipulator and incubated at 25°C until colony formation.

2.2 General biochemistry

2.2.1 Preparation of yeast extracts by protein precipitation

Protein extracts were prepared by precipitation with trichloroacetic acid (TCA), washed with 1 M Tris-base and resuspended in 100 μ l 2 x SDS buffer (100 mM Tris-HCl pH 6.8, 200 mM DTT, 4% SDS, 0.1% bromophenol blue, 20% glycerol). 200 μ l of 0.5 mm glass beads (Biospec Products) were added and cells were lysed using a FastPrep at 5.5 m/s for 1 minute. Extracts were then spun down to separate them from the glass beads. Collected supernatant was boiled at 95°C for 2 minutes and cleared by briefly centrifuging at 13,000 rpm.

2.2.2 SDS-polyacrylamide gel electrophoresis (PAGE) and Western blotting

Protein samples were resolved on acrylamide/bis-acrylamide gels (37.5:1, 30% solution), with 375 mM Tris-HCl pH 8.8 and 0.1% SDS. Proteins were migrated at 50 mA using SDS-PAGE running buffer (25 mM Tris, 250 mM glycine and 0.1% SDS) in electrophoresis tanks from CBS scientific, CA. A broad range pre-stained protein marker (New England Biolabs) was added to determine protein migration.

Separated proteins were transferred onto pre-equilibrated nitrocellulose membranes using a wet-transfer tank (Bio-Rad). Transfer buffer contained 3.03 g/l Tris base, 14.1 g/l glycine, 0.05% SDS and 20% v/v methanol, and was carried out either at 250 mA for 12 hours or 400 mA for 2 hours in a cold room.

The membrane was blocked with a 5% skimmed milk solution (Marvel) in PBST for 30 minutes - 1 hour at room temperature. Membranes were then incubated with the primary antibodies diluted in PBST containing 5% milk for 1-2 hours at room temperature or at 4°C overnight. The antibodies concentrations were as indicated in table 2.3. Membranes were washed for 3 x 10 minutes with PBST before being incubated with α -mouse, α -rabbit or α -rat horseradish peroxidase (HRP) coupled secondary antibodies in PBST containing 5% milk for 30 minutes - 2 hours at room temperature. Membranes were washed a further three times before adding ECL (Amersham) according to the manufacturer's instructions, and then were either exposed to an ECL film, or photographed using an ImageQuant las 4000 (GE Healthcare).

Antigen	Description	Dilution	
		WB	IF
Clb2	Santa Cruz, sc9071 (0.2 mg/ml) - Rabbit	1/500- 1/1000	
Orc6	In house, clone SB49 (1.1 mg/ml) - Mouse	1/1000	
Sic1	Santa Cruz, sc50441 (0.2 mg/ml) - Rabbit	1/500	
Tub1	Clone YOL1/34, AbD Serotec (1 mg/ml) - Rat	1/1000	1/200
Tat1	Sigma-Aldrich (1.5 mg/ml) - Mouse	1/10000	
HA	Clone 12CA5, Abcam (1 mg/ml) - Mouse	1/5000	
myc	In house, clone 9E10 (1.2 mg/ml) - Mouse	1/5000	
Pk	Clone SV5-Pk1 AbD Serotec - Mouse	1/5000	1/200
MultiMab No. 9477	Cell Signalling - Rabbit	1/1000	
Mouse IgG	GE Healthcare – HRP-coupled secondary	1/5000	
Rabbit IgG	GE Healthcare – HRP-coupled secondary	1/5000	
Rat IgG	GE Healthcare – HRP-coupled secondary	1/5000	
Rat IgG	Sigma – Cy3-Coupled secondary		1/500
Rabbit IgG	Chemicon – FITC-coupled secondary		1/200

Table 2.3 – List of antibodies used

2.3 Other biophysical and biochemical techniques

2.3.1 Microscale thermophoresis (MST)

Purified Cdc14 tagged with superfolder green fluorescent protein (Pédélecq et al., 2005), was mixed with increasing concentrations of a binding partner (Fin1 or Ask1) in a final

buffer of 50 mM Tris/HCl pH 7.5, 250 mM NaCl, 10% glycerol, 0.5 mM TCEP, 0.05% Tween-20, containing GFP-Cdc14 at a final concentration of 200 nM.

After incubating the mixtures in the dark at room temperature for 30 minutes, each mixture was loaded into glass capillaries (Monolith NT.115 Standard Treated Capillaries) by capillary action. All measurements were performed at 60% MST power, 9% blue LED-power on the Monolith NT.115 Blue/Red instrument. Dissociation constants were determined by fitting MST data using the MO Affinity Analysis software into an equation based on law of mass action.

2.3.2 Crosslinking and mass spectrometry

Purified Fin1 and Cdc14 mixed together in a final concentration of 9.82 μ M and 3.42 μ M respectively, in a buffer containing 50 mM HEPES pH 7.5, 250 mM NaCl, 10% glycerol and 0.5 mM TCEP for 10 minutes and room temperature. Next, the proteins were cross-linked using the hydrophilic crosslinker BS3 (Bissulfosuccinimidyl suberate) at the indicated concentrations for 45 minutes at room temperature. The reactions were quenched using ammonium bicarbonate at the final concentration of 50 mM for 30 minutes at room temperature. Optimum cross-linking efficiency was determined by varying BS3 concentration and crosslinking time, as adjudged by SDS-PAGE.

Following resolution by SDS-PAGE (or precipitation by 8 M urea), the reactions were resuspended in 8 M urea and 50 mM TCEP to reduce disulfide bonds, for 30 min at 37 °C. Next, they were alkylated with 100 mM iodoacetamide for 30 min at room temperature and protected from light. The solutions were then diluted with 50 mM ammonium bicarbonate to reduce the urea concentration to 1 M. The samples were digested with sequencing grade trypsin at a ratio of 1:50 (enzyme:protein) and left overnight at 37 °C. Digested peptides were next acidified to 2 % (v/v) formic acid to stop the enzymatic activity. Peptides were desalted using a C₁₈ SepPak, 50 mg bed volume and dried under vacuum. Following this step, peptide mixtures were re-suspended in 35 μ l 0.1 % trifluoroacetic acid, with 10 μ l per injection into an LTQ-Orbitrap Velos instrument for data collection. Each run was a 3 h gradient elution with

collision-induced dissociation being the selected activation method. Data processing was performed using the xQuest/xProphet bioinformatics suite (currently v2.1.1)

2.3.3 Peptide array analysis

Fin1 peptide array was first activated by incubation in 50 ml of 50% methanol, 10% acetic acid for one hour. All steps were carried out at room temperature unless otherwise stated. Following activation, the peptide array was extensively washed with 50 ml PAB (25 mM Tris/HCl pH 7.5, 50 mM NaCl, 0.1% Tween-20) three times for 10 minutes (per wash). The array was then blocked for 2 hours in 50 ml PAB + 2.5% skimmed milk (Marvel). For the antibody only control, 4 μ l of the anti-HA antibody (table 2.3) was added to 25 ml PAB + 2.5% skimmed milk, and the array incubated in it for 2 hours. Following three washes with PAB, the array was incubated in 1.25 μ l of anti-mouse HRP-conjugated secondary antibody (table 2.3) added to 25 ml PAB + 2.5% milk for an hour. As before, the membrane was washed three times in PAB, developed using ECL and exposed to an ECL film.

For the protein binding experiment, activation and blocking steps were followed as described above. Following these, purified His-HA-Cdc14 was added to PAB + 2.5% skimmed milk at a final concentration of 1 μ g/ml, and the array was incubated in this solution overnight at 4 °C. The following day, the array was washed three times with PAB. Next, primary and secondary antibody binding steps, and membrane development were carried out as described above.

2.3.4 Size exclusion chromatography coupled with multiple-angle laser light scattering (SEC-MALLS)

Purified protein samples (100 μ l, at a concentration of 45 μ M each) were subjected to size-exclusion chromatography in conjunction with MALLS at 16 different light angles using the DAWN-HELEOS II photometer coupled to an OPTILAB-TrEX differential refractometer (Wyatt Technology) at room temperature in a buffer containing 50 mM Tris/HCl pH 7.5, 500 mM NaCl, 10% glycerol, 0.5 mM TCEP. The data were analysed using ASTRA software version 6.1.

2.3.5 Glycerol gradient sedimentation

In order to determine the sedimentation coefficient of recombinant Cdc14, sedimentation analysis was performed. A glycerol gradient of 15 – 35% was prepared in 50 mM Tris/HCl pH 7.5, 250 mM NaCl, 0.5 mM TCEP. The gradient was prepared by manually layering individually prepared buffers with the appropriate glycerol concentration, in steps of 2.5% glycerol. For instance, 500 μ l of 35% glycerol buffer was pipetted to the bottom of the tube, followed by 500 μ l of 32.5% glycerol buffer, and so on. Finally, 100 μ l of Cdc14, at a concentration of 0.5 μ g/ μ l in the same buffer was carefully overlaid on the top of the gradient. In parallel, an identical gradient was prepared, and a protein standard mixture containing Thyroglobulin, Bovine Serum Albumin and Catalase (GE Healthcare), each at a concentration of 0.5 μ g/ μ l, was overlaid on top.

Next, the gradients were centrifuged at 42,000 rpm (equivalent to 117,000 g) for 16 hours at 4°C in a swinging-bucket rotor (TLS-55) in Optima MAX-XP ultracentrifuge (Beckman Coulter, Inc.), with a deceleration of 0 to avoid disturbing the equilibrated proteins.

Finally, 200 μ l fractions were carefully pipetted, and an aliquot analysed by SDS-PAGE and stained by the Coomassie stain InstantBlue (Expedeon).

2.3.6 Pull-down assays

2.3.6.1 *Glutathione S-Transferase (GST) pull-down*

In order to assay protein-protein interactions, purified GST-tagged proteins were immobilized on 10 μ l of Glutathione Sepharose 4B (GE Healthcare) beads equilibrated in the appropriate binding buffer for an hour. Next, the beads were washed four times with 500 μ l of binding buffer to remove excess unbound protein.

The prey protein(s), in the appropriate binding buffers (50 mM Tris pH 7.5, 100 mM NaCl, 10% glycerol, 0.5 mM TCEP, unless otherwise indicated), were added to the

immobilized GST-tagged bait protein at the final concentration of 1 μ M for 5 minutes at 25°C. Next, the beads were washed four times in 700 μ l buffer to remove unbound proteins. Finally, the beads were boiled in 30 μ l of 2x SDS sample buffer, and the eluate was separated by SDS-PAGE, and Coomassie stained. Band intensities of the input and pulled down proteins were quantified by densitometry using ImageQuant software (GE Healthcare).

2.3.6.2 Nickel pulldown

A similar protocol was followed to assay interactions between hexahistidine-tagged bait proteins with their preys. Ten μ l of Ni-NTA beads (Qiagen) were equilibrated in the appropriate binding buffer (containing 20 mM imidazole to prevent non-specific interactions), following which, they were chelated to His₆-tagged protein for an hour. After three washes of 500 μ l each, the prey protein(s) were added to the Ni-NTA-bound bait proteins for 5 minutes at 25°C in 50 mM Tris pH 7.5, 200 mM NaCl, 10% glycerol, 0.5 mM TCEP. The beads washed four times in 700 μ l buffer and boiled in 30 μ l of 2x SDS sample buffer. The proteins were separated by SDS-PAGE and stained with Coomassie. Band intensities of the input and pulled down proteins were quantified by densitometry using ImageQuant software (GE Healthcare).

2.4 Enzyme activity assays

2.4.1 *In vitro* Clb2-Cdc28 kinase assay

A buffer containing 50 mM Tris/HCl pH 7.5, 150 mM NaCl, 10 mM MgCl₂, 100 μ M ATP and 0.5 mg/ml BSA, 33 nM (or as indicated) purified Clb2-Cdc28 kinase was used to phosphorylate 1.66 μ M purified substrate protein at 30 °C for 1 hour, or as indicated. The reaction was then stopped by addition of EDTA at a final concentration of 15 mM if used for subsequent phosphatase assays. Otherwise, the reactions were stopped by adding 2x sample buffer, resolved using SDS-PAGE and stained using Coomassie.

2.4.2 *In vitro* Cdc14 phosphatase assay

Fully phosphorylated protein substrates (see above) were diluted to a protein concentration of 640 nM, in a buffer containing 50 mM Tris/HCl pH 7.5 and 100 mM NaCl, containing 6.4 nM (or as indicated) purified Cdc14. The reactions were incubated at 30°C for the indicated amounts of time and stopped using 2x sample buffer. They were resolved by SDS-PAGE and stained using Coomassie.

If used in a kinetic assay, reaction aliquots were removed at 15 second intervals from the time of commencement and stopped by resuspension in 2x sample buffer maintained at 95 °C. The reactions were resolved on an SDS-PAGE gel, which was then transferred on to a nitrocellulose membrane. Phosphorylation was detected by western blotting using the MultiMab antibody (no. 9477) at a dilution of 1/1000. In order to ensure that the western blot signal was in the linear range of signal, the blots were developed using an ImageQuant LAS 4000 (GE Healthcare) imager. Band intensity was then quantified using the ImageQuant TL software (GE Healthcare). After conversion into concentration of substrate hydrolysed, the data was fitted into an integrated form of the Michaelis-Menten equation outlined in section 7.3 and catalytic efficiencies were calculated.

2.4.3 *para*-Nitrophenyl phosphate phosphatase (*p*-NPP) assay

Phosphatase activity was assessed using the colorimetric *p*-NPP assay, based on dephosphorylation of the non-specific substrate *p*-nitrophenyl phosphate.

All assays were performed in 50 mM Tris/HCl pH 7.5, 100 mM NaCl, 0.5 mM TCEP, containing 20 mM *p*-nitrophenyl phosphate (Calbiochem). The reactions were started by mixing the Cdc14, or its variants, and a pre-prepared reagent mixture, leading to a final volume of 100 µl, and were incubated at 37°C for the indicated amount of time. Development of colour was monitored using the BioTek microplate reader at 410 nm. A_{410} was converted to µmol of substrate hydrolysed by applying Beer's Law and using the molar extinction coefficient of 18,000 M⁻¹ cm⁻¹.

2.5 Protein purification

2.5.1 Purification of His₆-Cdc14, GST-Cdc14, Fin1, Ask1 and Sli15 and Clb2-Cdc28

His₆-Cdc14 and GST-Cdc14, along with mutants based on these proteins, Fin1 (including all mutants), Ask1 and Sli15 were purified following overexpression in *Escherichia coli*. In case of Clb2-Cdc28, the complex was purified following overexpression in *S. cerevisiae*. Purification protocols described in Bouchoux and Uhlmann (2011) were followed.

2.5.2 Purification of Cdc14 domains

2.5.2.1 GST-Cdc14^A and GST-Cdc14^C

Purifications of these constructs followed the same protocol. Cloned plasmids were transformed into BL21 (DE3) pLys.S *Escherichia coli* cells by electroporation. An overnight culture of the cells was backdiluted to OD₆₀₀ 0.1, and grown for another few hours in a 37°C incubator with shaking at 250 rpm, until they reached mid-log phase (OD₆₀₀ = 0.6). Next, the cultures were transferred to an incubator maintained at 19°C. The cultured were allowed to cool for an hour, following which IPTG was added at a final concentration of 0.05 mM. Protein production was induced overnight for 16 hours. The following day, cells were harvested by pelleting in a centrifuge at 4200 rpm. Cell pellets were flash frozen in liquid nitrogen.

The cell pellets were resuspended in 20 ml of buffer A (50 mM Tris/HCl pH 7.5, 10% glycerol, 0.5 mM TCEP) supplemented with 500 mM NaCl, 0.2% Triton X-100, 0.2 mM PMSF, 1 EDTA-free protease inhibitor tablet (Roche), 1 µl Benzonase Nuclease (Sigma-Aldrich). The cells were lysed by sonication on ice (30 s on, 1 min rest, repeated 3 times). The extracts were clarified by centrifugation at 40,000 rpm in a MLA-80 rotor in an ultracentrifuge at 4 °C.

Clarified supernatant was bound to 1 ml Glutathione-Sepharose 4B beads (GE Healthcare), which had been extensively equilibrated in buffer A (+ 500 mM NaCl, 0.2% Triton X-100). Binding was carried out at 4 °C for 2 hours by end-on-end rotation. The beads were then washed extensively in the above buffer, and protein was eluted by addition of buffer A containing 20 mM reduced glutathione (Sigma-Aldrich). Peak fractions containing the protein were pooled, clarified at 13,000 rpm in a table-top centrifuge and applied to a Superdex 200 10/300 HR column, equilibrated in buffer A (+ 250 mM NaCl). Peak fractions were pooled, aliquoted and flash frozen in liquid nitrogen.

2.5.2.2 GST-Cdc14^{AB}

Cloned plasmids were transformed into BL21 (DE3) pLys.S *Escherichia coli* cells by electroporation. An overnight culture of the cells was backdiluted to OD₆₀₀ 0.1, and grown for another few hours in a 37°C incubator with shaking at 250 rpm, until they reached mid-log phase. Next, the cultures were transferred to an incubator maintained at 19°C. The cultured were allowed to cool for an hour, following which IPTG was added at a final concentration of 0.5 mM. Protein production was induced overnight for 16 hours. The following day, cells were harvested by pelleting in a centrifuge at 4200 rpm. Cell pellets were flash frozen in liquid nitrogen.

The cell pellets were resuspended in 20 ml of buffer A (50 mM Tris/HCl pH 7.5, 10% glycerol, 0.5 mM TCEP) supplemented with 500 mM NaCl, 0.2% Triton X-100, 0.2 mM PMSF, 1 EDTA-free protease inhibitor tablet (Roche), 1 µl Benzonase Nuclease (Sigma-Aldrich). The cells were lysed by sonication on ice (30 s on, 1 min rest, repeated 3 times). The extracts were clarified by centrifugation at 40,000 rpm in a MLA-80 rotor in an ultracentrifuge at 4 °C.

Clarified supernatant was bound to 1 ml Glutathione-Sepharose 4B beads (GE Healthcare), which had been extensively equilibrated in buffer A (+ 500 mM NaCl, 0.2% Triton X-100). Binding was carried out at 4 °C for 2 hours by end-on-end rotation. The beads were then washed extensively in the above buffer, and protein was eluted by

addition of buffer A containing 20 mM reduced glutathione (Sigma-Aldrich). Peak fractions containing the protein were pooled, clarified at 13,000 rpm in a table-top centrifuge and applied to a Superdex 200 10/300 HR column, equilibrated in buffer A (+ 500 mM NaCl). Peak fractions were pooled, aliquoted and flash frozen in liquid nitrogen.

2.5.3 Purification of Net1¹⁻⁶⁰⁰

For purification of His₆-Net1¹⁻⁶⁰⁰ *E. coli* transformation, protein induction and lysis protocols described in section 2.5.1 were followed, with the only difference being that buffer A was additionally supplemented with 20 mM imidazole. Next, clarified protein supernatant was applied to 1 ml Ni-NTA beads (Qiagen) which had been pre-equilibrated in buffer A (+ 500 mM NaCl, 0.2% Triton X-100, 20 mM imidazole). Binding was carried out at 4 °C for an hour by end-on-end rotation. The beads were then washed extensively in the above buffer, and protein was eluted by addition of buffer containing 300 mM imidazole.

An aliquot of each fraction was assayed using SDS-PAGE for presence of Net1¹⁻⁶⁰⁰; peak fractions containing the protein were pooled, clarified at 13,000 rpm in a table-top centrifuge and applied to a Superdex 200 10/300 HR column, equilibrated in buffer A (+ 500 mM NaCl). Peak fractions were pooled, aliquoted and flash frozen in liquid nitrogen.

2.6 Molecular biology and DNA manipulation

2.6.1 Genomic DNA preparation

Yeast genomic DNA for PCR genotyping was prepared from freshly streaked patches of the strain of interest. Cells was resuspended in 100 µl 200 mM LiOAc, 1% SDS solution, and incubated at 70°C for 10 min. After incubation, 300 µl of 100% ethanol was added, and DNA was collected by centrifugation at 13,000 rpm for 3 min. DNA pellets were

dried for 3 minutes at 65°C and dissolved in 100 µl TE. Cell debris was spun down by brief centrifugation at 13,000 rpm for 1 min, and 1 µl supernatant was used for the PCR.

2.6.2 Polymerase Chain Reaction (PCR)

PCR reactions were carried out in 25 or 50 µl reactions containing Taq (Qiagen), Expand High Fidelity (Roche), or ClonAmp (ClonTech) polymerases with buffers supplied by the manufacturers, 0.5 µM of each primer, and, if necessary 0.2 mM dNTPs. All PCRs were performed on a Peltier Thermal Cycler (MJ Research). PCR products were resolved by agarose gel electrophoresis to confirm the size of the fragments.

2.6.3 Strain design

2.6.3.1 Epitope tagging

Epitope tagging of endogenous genes was performed by gene targeting using PCR products (Bähler et al., 1998; Knop et al., 1999).

Forward and reverse primers with homology to the 3' end of the gene of interest and the 3' UTR respectively were used. These also contained an 18-mer sequence homologous to the vector used for tagging. These were used to amplify the vector by PCR, with the subsequent product containing the epitope tag, a marker, and a 50-mer sequence at each end homologous to the region of marker insertion.

Transformants were subsequently selected on plates by using auxotrophic markers (derived from either *Kluyveromyces lactis* or *Schizosaccharomyces pombe*) to minimize the odds of integration at the marker locus.

2.6.3.2 Gene mutagenesis

For Fin1 gene mutagenesis, a cassette containing full-length Fin1 tagged with three repeats of the HA epitope, followed by the *URA4* selection marker from *S. pombe* was cloned into the pCR™ 2.1 Topo vector using the TA cloning kit (Invitrogen). Next, appropriate mutations were introduced using the Q5 Mutagenesis Kit (New England

Biolabs). Finally, the entire cassette, containing the mutations, was amplified by PCR, and transformed into the strain(s) of interest. Integration of the mutation into the endogenous protein was confirmed by sequencing.

2.6.4 Agarose gel electrophoresis

DNA samples were loaded on a 0.8-2% agarose gel (depending on the size of the DNA fragment) in 6x loading buffer (0.25% w/v bromophenol blue, 0.25% w/v xylene cyanol, 30% (v/v) glycerol). Agarose gels were prepared in 1x Tris-acetate EDTA buffer (TAE) (40 mM Tris base, 1 mM EDTA pH 8.0, 0.115% v/v acetic acid), to which GelRed (Biotium) was added to a final concentration of 0.5 µg/ml. Electrophoresis was carried out in TAE at 80-20 V in electrophoresis tanks (Anachem).

2.6.5 Plasmid construction

2.6.5.1 Transformation of chemically competent bacteria with plasmid

DNA

Chemically competent *Escherichia coli* (DH5α) cells were thawed on ice. Five µl of the appropriate cloning reaction was added to 50 µl of competent cells, and the mix was incubated on ice for 30 minutes. Following a heat shock at 42°C for 1 minute, and 2 minute-long cool down period on ice, 950 µl of LB media was added to the cells. They were allowed to recover in a shaking incubator for 1 h, and then plated on LB agar plates containing the appropriate antibiotic and left to grow overnight at 37°C.

2.6.5.2 Isolation of plasmid DNA from E. coli

Plasmid DNA was purified using the Qiagen Miniprep kit according to the manufacturer's instructions.

2.6.5.3 Sanger sequencing

Each sequencing reaction was set up using 200 ng of DNA, 3.2 pmol of sequencing primer, 8 µl of BigDye Terminator Cycle Sequencing Ready Reaction Mix, made up to 20 µl with water. Following thermal cycling, unincorporated dideoxynucleotides were

removed by ethanol precipitation and the sequencing reactions were loaded on to automated sequencing machines (Applied Biosystems) at the Equipment Park at The Francis Crick Institute.

2.7 Microscopy and cell biology

2.7.1 *In situ* Immunofluorescence (IF)

Two ml of log-phase cells were resuspended in 1 ml ice-cold 1% formaldehyde buffer (IF1), and fixed overnight at 4°C. The cells were then washed in the same buffer lacking formaldehyde. Next, the cells were resuspended in a sorbitol-based buffer, IF2. The cells were finally resuspended in 200 µl of spheroplasting solution (IF2 containing 2 µl 2-mercaptoethanol and 2 µl Liticase per ml of solution). Following this, the spheroplasted cells were washed once, and subsequently resuspended in IF2. Five µl of cells were loaded on polylysine-coated wells on 15-well slides (MP Biomedicals). The slides were blocked with a blocking buffer (0.5% Bovine Serum Albumin, BSA, in PBS) after fixing cells in methanol and acetone.

The following antibodies were used: α-Tub1 (clone YOL1/ 34, AbD Serotec), α-Pk (clone SV5-Pk1, AbD Serotec), along with FITC and Cy3-dye labeled secondary antibodies (Sigma and Chemicon, respectively) (see table 2.3 for antibody concentrations). Cells were counterstained with the DNA binding dyes 4',6-diamidino-2- phenylindole (DAPI), or Hoescht, present in the mounting media ProLong Gold at a concentration of 100 ng/ml. Fluorescent images were acquired using an Axioplan 2 imaging microscope (Zeiss) equipped with a 100x (NA = 1.45) Plan-Neofluar objective and an ORCA-ER camera (Hamamatsu).

2.7.2 Cell cycle analysis by Flow Cytometry (FACS)

To determine cell cycle progression by monitoring the DNA content, 1 ml of cells was fixed in ethanol for 2 - 24 hours at 4°C, RNase treated in 50 mM Tris-HCl pH 7.5 with

0.1 mg/ml RNase A for 2 - 24 hours at 37°C, and resuspended in propidium iodide-containing buffer (200 mM Tris-HCl pH 7.5, 211 mM NaCl, 78 mM MgCl₂, 50µg/ml propidium iodide). Cells were sonicated (Sanyo, Soniprep 150) before being analyzed on a FACScan or a FACSCalibur (Becton Dickinson). DNA content profiles were prepared using FlowJo.

2.8 Bioinformatic Analysis

As described in section 4.1, lists of phosphopeptides containing early (section 7.2), late (Kuilman et. al., 2015) and Cdk substrates (Holt et al., 2009) were assembled. Next, to ensure equivalent lengths of each phosphopeptide centered about the phosphorylated residue, the list was expanded using MotixX (Chou and Schwartz, 2002) to a length of 22 residues using the *S. cerevisiae* genome sequence as a reference. Using WebLogo3 (Crooks, Hon, Chandonia and Brenner, 2004), a sequence logo of each was generated.

Chapter 3. Biochemical properties of Cdc14

As discussed in chapter 1, the question of stoichiometry of Cdc14 has not been adequately resolved. Analysis using orthogonal techniques has indicated that the protein exists either as a dimer or a higher order multimer. According to estimates obtained by gel filtration and glycerol gradient centrifugation of the purified protein, it is a 2.6-mer in solution (Taylor et al., 1997).

Protein oligomerization is a recurring theme in biological systems. Amongst major mitotic exit phosphatases, Cdc14 is an outlier, in that it represents the sole class that is thought to function as a monomer. Indeed, the monomer contains all the residues required for full catalytic activity.

In order to deepen our understanding of the mechanisms of actions of Cdc14, and to resolve the disparities regarding the nature of the phosphatase, I aimed to examine the stoichiometry of Cdc14. An important question is whether oligomerization is physiologically relevant. How might the stoichiometry of Cdc14 impinge on substrate recognition, or indeed substrate dephosphorylation? It is possible that this potential oligomerization enhances the kinetics of dephosphorylation by increasing the local concentration of the phosphatase that a substrate experiences. Alternatively, it could also generate novel binding interfaces for substrates (Marianayagam, Sunde and Matthews, 2004).

In support of a role for oligomerization of Cdc14 *in vivo* is the fact that the active site phosphatase mutant, Cdc14^{C283S} suppresses the temperature sensitivity of *cdc14-1*, (Taylor et al., 1997), indicating a degree of collaborative action between the alleles.

3.1 Recombinant Cdc14 is a tight dimer in solution

3.1.1 Gradient sedimentation and gel filtration indicate that Cdc14 behaves as either a dimer or a trimer in solution

I performed glycerol gradient sedimentation coupled with size exclusion chromatography to ascertain the stoichiometry of purified Cdc14 in solution.

Sedimentation of proteins through a glycerol gradient is based on the principle that a protein moves through the gradient based on its size, with heavier proteins sedimenting faster – thus oligomeric Cdc14 would move through the gradient faster than monomeric Cdc14 (Fig. 3.1A). This is measured in sedimentation coefficient, $S_{20,w}$, i.e. sedimentation through water at 20 °C, where S is the Svedberg unit with a value of 10^{-13} s (Erickson, 2009).

Using BSA, catalase and thyroglobulin as protein standards whose properties are known, Cdc14 was found to have a sedimentation coefficient of 7.5 S (Fig 3.1B & 3.1C).

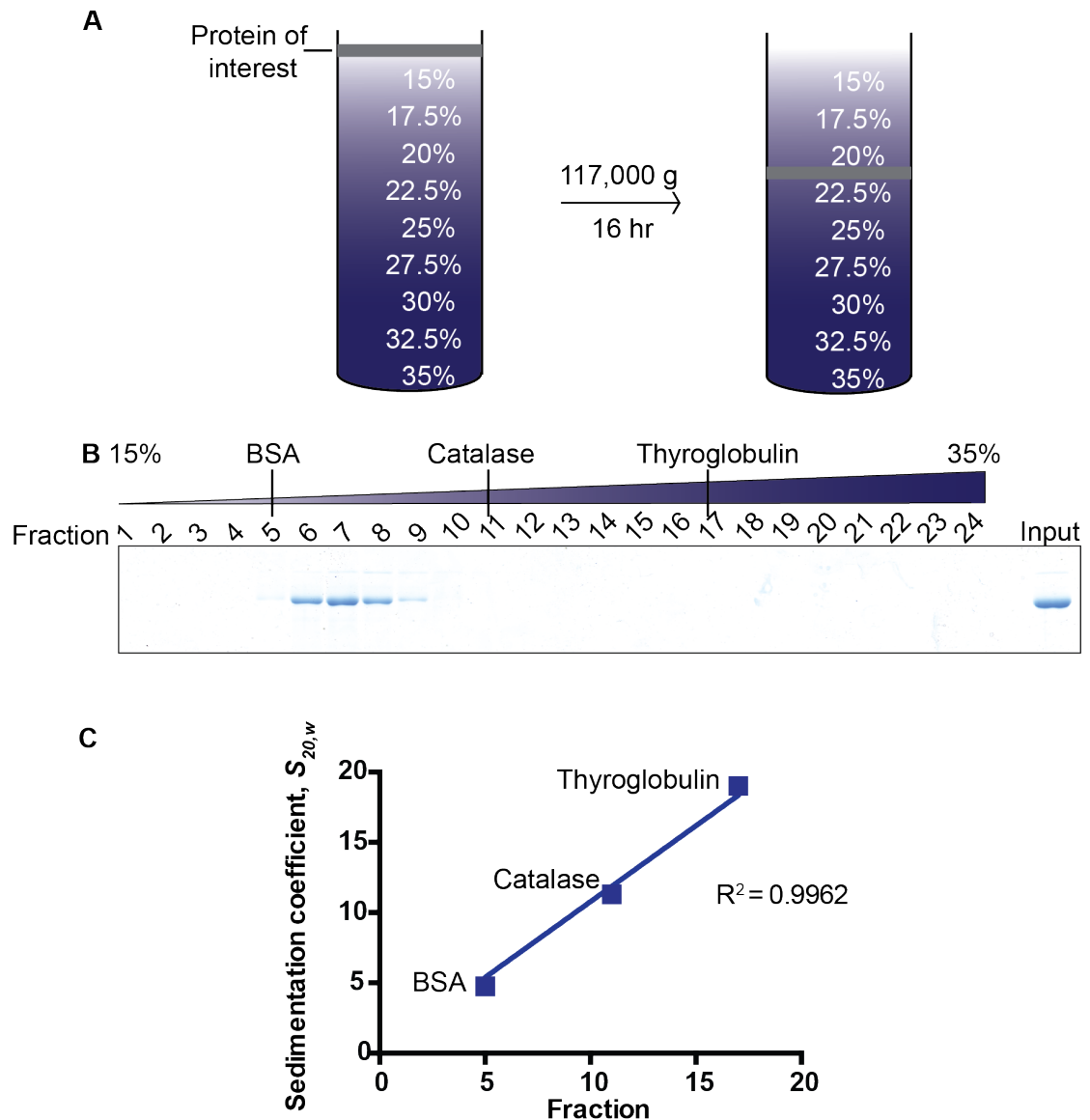


Figure 3.1 - Glycerol gradient sedimentation of Cdc14.

A. Schematic of the principle behind glycerol gradient sedimentation. **B.** SDS-PAGE gel showing the Cdc14-containing fractions relative to protein markers.

C. Peak fractions containing the protein markers plotted against their sedimentation coefficients.

This value provides some initial clues as to the nature of Cdc14. It can be used to calculate the ratio S/S_{max} , where S_{max} is the maximum possible sedimentation coefficient of a protein, a value derived from the molecular mass of a protein when it is assumed to be a smooth sphere without a hydration shell (Erickson, 2009). For Cdc14, this ratio is 1.31. Comparison to S/S_{max} values of proteins with known structures allows one to deduce that Cdc14 is a globular, rather than an elongated protein.

Next, I performed gel filtration chromatography on the protein to determine its Stokes radius, R_s , the radius of a smooth, theoretical sphere that would elute from the column at the given size. As before, thyroglobulin, ferritin and catalase were used as protein standards (Fig. 3.2). Compared to these standards, the Stokes radius of Cdc14 was found to be 5.3 nm.

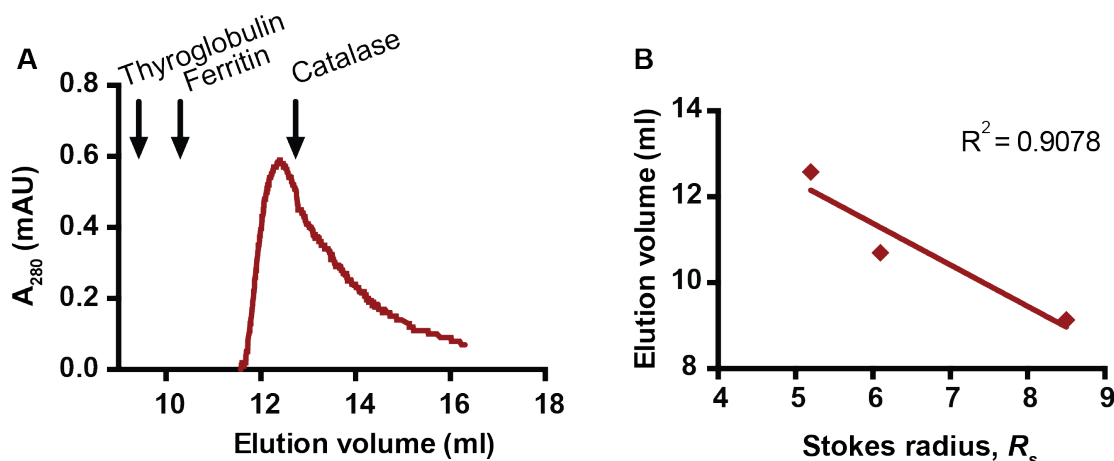


Figure 3.2 - Size exclusion chromatography of Cdc14.

A. UV spectrum (A_{280}) showing the elution volume of Cdc14 relative to protein markers. **B.** Elution volume of protein markers plotted against their Stokes radii to determine Cdc14's Stokes radius.

Using these values, it was then possible to determine Cdc14's molecular mass, M , by applying the Svedberg equation - a function of S and R_s . (see section 7.1 for a detailed description of the Svedberg equation). Molecular mass of Cdc14 was calculated to be 169,300 Da, which is in close agreement with the previously calculated value of 169,000 Da using a similar methodology (Taylor et al., 1997). Based on a calculated monomeric molecular weight of 64,069 Da, Cdc14 appears to exist as a 2.64-mer in solution, i.e. a dimer or a trimer.

Given these results, it can be concluded that Cdc14 is most likely oligomeric rather than monomeric in solution; however, its exact stoichiometry still remains uncertain.

3.1.2 SEC-MALLS shows that Cdc14 is a dimer, with its C-terminal domain being dispensable for dimerization

In the absence of a clear answer from the above experiments, I used Size Exclusion Chromatography coupled with Multiple Angle Laser Light Scattering (SEC-MALLS) as an orthogonal technique to assess the stoichiometry of Cdc14 in solution. In this technique, laser beams are passed through a protein in solution at various angles. When the particle encounters the light, it scatters the incident photons, which are then picked up by a detector. This technique can be used to detect the hydrodynamic profile of the particles in solution, thus providing a method for the calculation of their molecular weight.

Cdc14 was purified to homogeneity as before, and diluted to a concentration of 2.9 $\mu\text{g}/\mu\text{l}$ (or 45 μM) and eluted through a hydrophilic gel filtration column coupled to a multiple angle light scattering instrument. The analysis was performed in a high NaCl buffer (500 mM) because of the proclivity of the protein to precipitate at lower ionic strengths at the high concentrations required for SEC-MALLS.

The analysis yielded a single peak containing Cdc14. The calculated molecular weight was 121,000 Da (Fig. 3.3A), which is close to a dimeric value of 128 kDa. Thus, Cdc14 is a tight dimer in solution. The fact that this interaction is detectable in this supra-physiological ionic strength implies the existence of either very strong ionic interactions, and/or hydrophobic interactions between the dimers.

Now that it has been ascertained that Cdc14 is a dimer in solution, the following question arises: which domain of Cdc14 enables this dimerization? The Barford group crystallized a truncated form of one of the human Cdc14 homologues, Cdc14B (Pro44 – His386) (Gray et al., 2003). This protein contains the conserved N-terminal domain A and the catalytic domain B (with \approx 60% homology to its yeast counterparts), whilst lacking the variable, non-conserved C-terminal domain. It was found to crystallize as a

monomer. Therefore, I wondered if the C-terminal domain of the *S. cerevisiae* Cdc14 could be driving multimerization.

To test this hypothesis, I constructed a plasmid encoding Cdc14^{AB}, spanning residues 1-374, which contained solely domains A and B of the protein but lacked domain C. I then purified the protein to homogeneity and analysed it using SEC-MALLS in the same buffer conditions. Surprisingly, it too eluted as a dimer of 78 kDa (close to its calculated dimeric weight of 90 kDa) (Fig. 3.3B). Thus, the C-terminal domain is dispensable for dimerization.

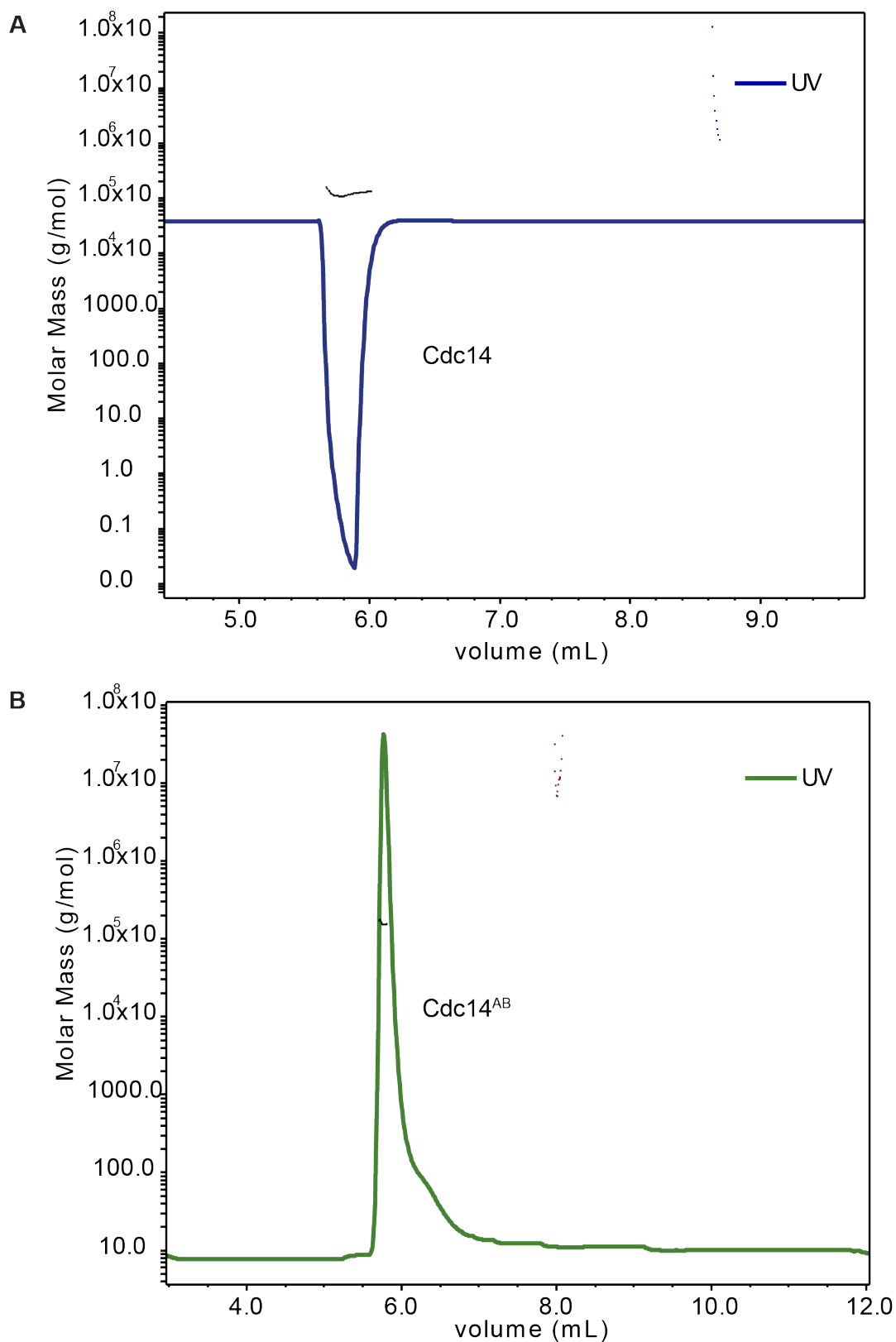


Figure 3.3 - Elution profiles of Cdc14 (A) and Cdc14^{AB} (B) determined through SEC-MALLS.

The horizontal black lines correspond to the SEC-MALLS calculated molecular masses of the proteins across the entire peak.

This experiment indicates that the dimerization cues are contained within domains A or B (or both). I thus attempted to further narrow down a dimerization domain by truncation analysis, but met with limited success. Whilst domain A alone could be purified to homogeneity (discussed in the next section 3.2.1), the protein was only stable in the presence of an N-terminal GST tag. As GST is known to weakly dimerize itself (Fabrini et al., 2009), GST-tagged domain A was unsuitable for such analysis.

3.2 Contribution of Cdc14 domains to substrate recognition and dephosphorylation

3.2.1 The non-catalytic N-terminal domain A interacts with Cdc14 substrates

As Cdc14 is organized into three discrete domains, I next wanted to assess the contribution of each of them to substrate recognition and dephosphorylation. To this end, I cloned and purified GST-tagged individual domains of Cdc14. The domain boundaries were guided by the structure of human Cdc14B and its sequence alignment with the yeast homolog (Fig. 3.4A and 3.4B).

Domain A included the linker alpha helix that connects it to the catalytic domain B. This helix is acidic in nature and might aid substrate recognition by binding to positively charged residues downstream of the target phosphosite. Domain B proved to be recalcitrant to purification, with all constructs tried being insoluble; thus, domain AB was constructed in its stead.

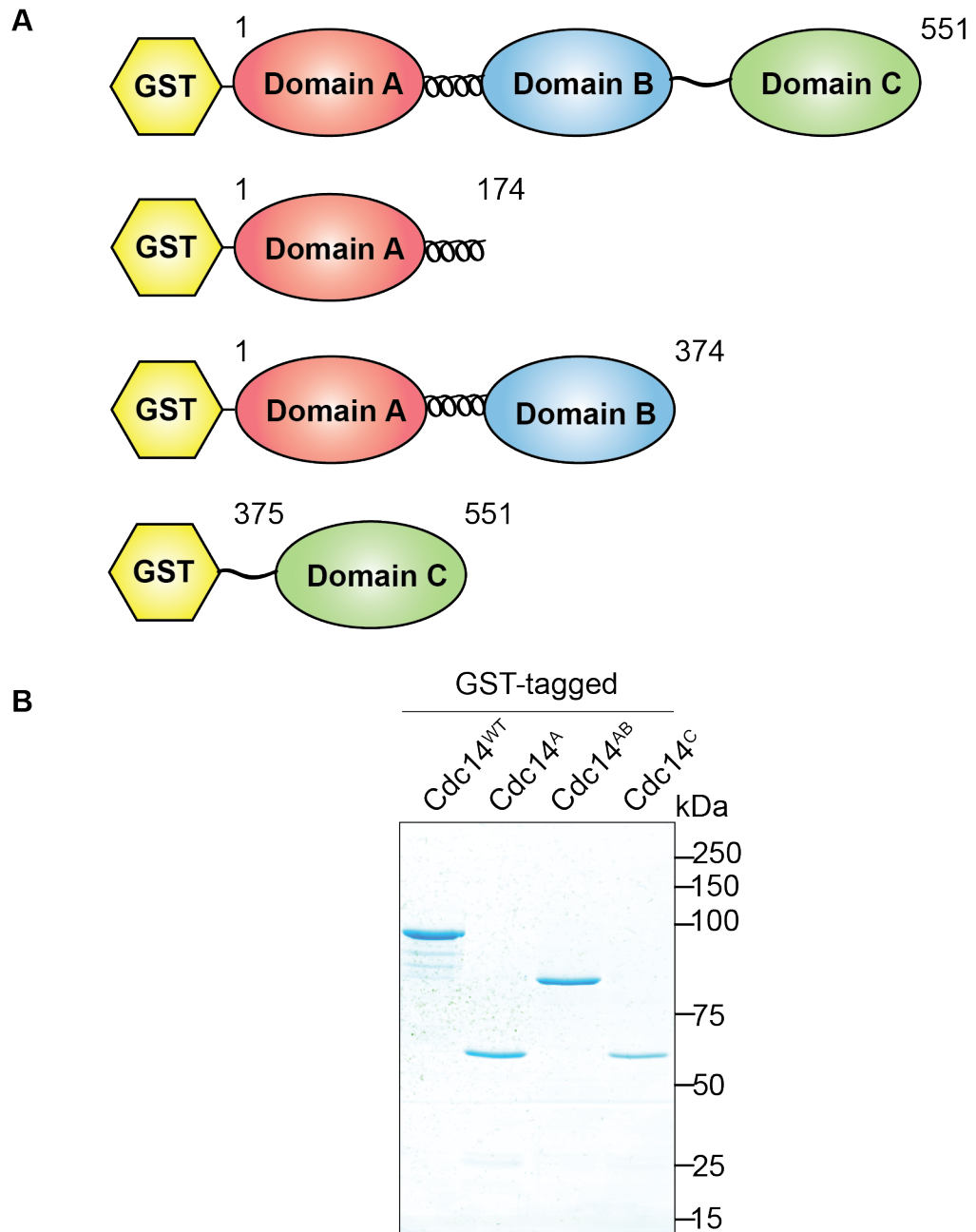


Figure 3.4 - Domains of Cdc14

A. Schematic of GST-tagged domains of Cdc14. **B.** SDS-PAGE gel depicting the purified proteins.

Next, I asked whether these domains are capable of interacting with Cdc14 substrates. The full-length protein and Cdc14^{AB} could bind to both the early substrate Fin1, and the intermediate substrate Sli15 (Fig. 3.5). Surprisingly, the non-catalytic Cdc14^A, too, bound these substrates. Although possessing little in the way of sequence identity, domains A and B form two structurally equivalent domains, with an r.m.s.d. of 2.6 Å.

Whilst domain A contains the WPD loop comprising the invariant general acid/base aspartic acid, it crucially lacks the signature PTP motif of domain B (Gray et al., 2003). Thus, it is possible that this domain is engaging in a ‘pseudo-domain B’ interaction with substrates. Alternatively, domain A might be important for substrate recognition. Cdc14^C, however, did not interact with either of the substrates, indicating that it is inessential for substrate interaction *per se*.

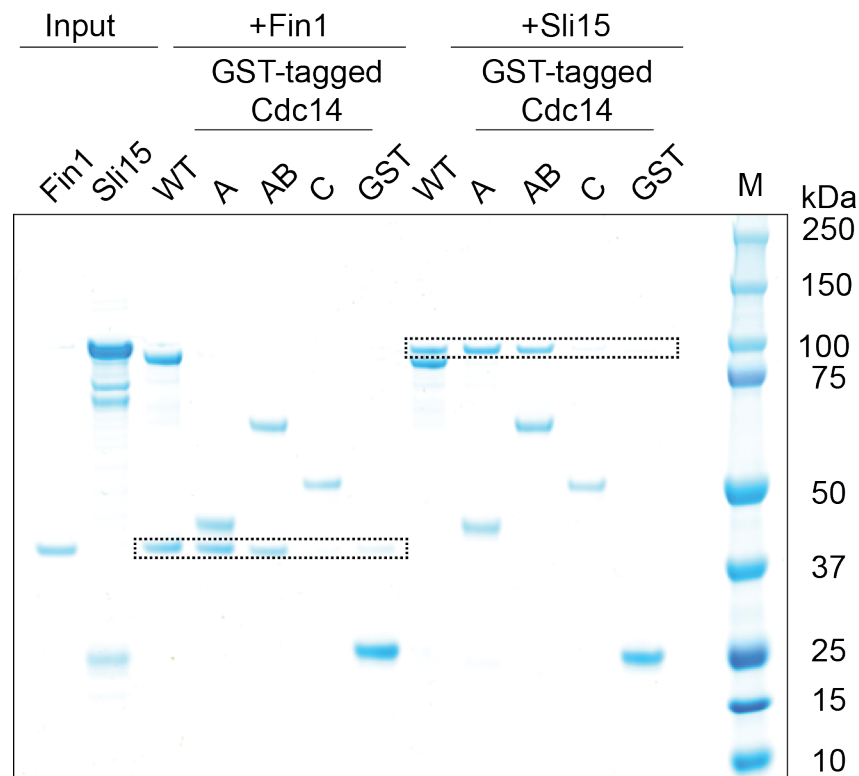


Figure 3.5 – Cdc14 domain interactions with the substrates Fin1 and Sli15. Bead immobilized Cdc14^{WT}, Cdc14^A and Cdc14^{AB} efficiently pull down both added Fin1 and Sli15, whilst immobilized Cdc14^C and the control protein GST do not. Pulled down proteins have been indicated by a dotted box.

3.2.2 Cdc14^{AB} is a hypomorphic Cdc14 allele, whilst the C-terminal domain is dispensable for Cdc14 function *in vivo*

As Cdc14^C does not contain residues required for phosphatase catalysis, dimerization and interaction with substrates, I wanted to understand its importance *in vivo*. This domain has been implicated in a number of regulatory functions: firstly, it houses numerous residues that are extensively phosphorylated *in vivo* in anaphase by Cdc5,

with contribution from Cdk1 (Holt et al., 2009). Their phosphorylation is thought to weaken its binding to its stoichiometric inhibitor, Net1 (Shou et al., 2002; Stegmeier and Amon, 2004). Secondly, the very C-terminus of the protein functions as a nuclear localization signal (Mohl et al., 2009). Consistent with this hypothesis, a Cdc14 C-terminus-derived peptide was recently crystallized with the karyopherin Kap121. MEN-activated Dbf2-Mob1 is thought to abrogate this NLS by its phosphorylation in late anaphase, leading to translocation of the protein into the cytoplasm (Mohl et al., 2009).

Before performing an *in vivo* comparison, I first wanted to determine if Cdc14^{WT} and the C-terminal truncated Cdc14^{AB} possessed equivalent phosphatase activities. Using purified proteins, the basal phosphatase activities of each were measured by employing the colorimetric *p*-nitrophenyl phosphate (*p*-NPP) phosphatase assay. Cdc14^{AB} exhibited a defect in velocity of substrate hydrolysis (Fig. 3.6). Thus, Cdc14's activity is compromised in the absence of domain C, possibly due to small defects in protein folding.

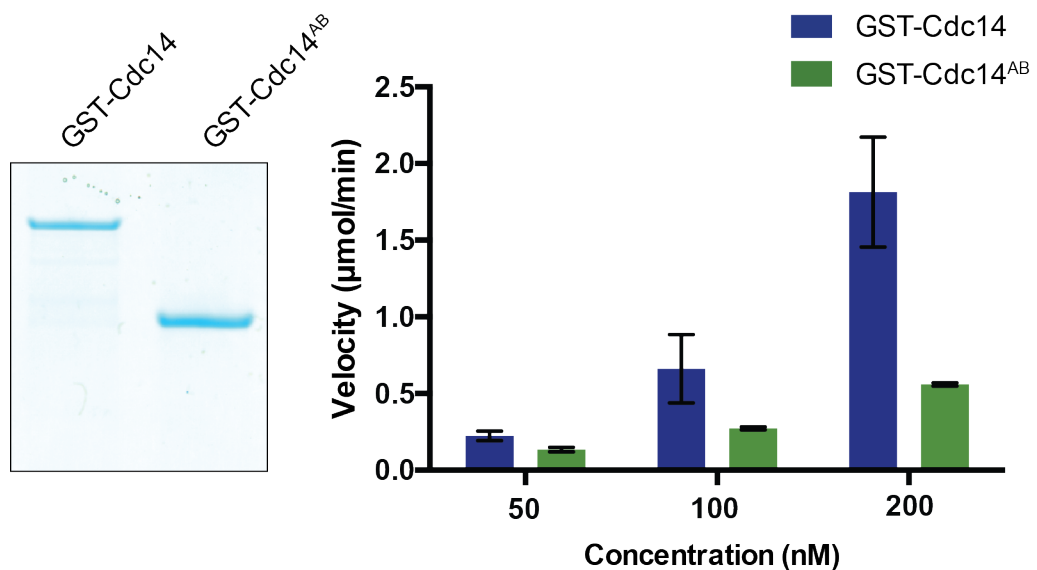


Figure 3.6 – Comparison of phosphatase activities of wild type and truncated GST-tagged Cdc14 proteins.

The velocity of hydrolysis (right) of 20 mM *p*-NPP by various concentrations of the two purified proteins (left), GST-Cdc14 and GST-Cdc14^{AB}, is depicted. The error bars indicate standard deviation from the mean. The experiment was independently repeated three times.

Next, a yeast strain was constructed which had its endogenous *Cdc14* gene replaced with *Cdc14^{AB}*, under the control of its own promoter. The strain was not only viable, but also exhibited growth indistinguishable from the wild type control (Fig. 3.7).

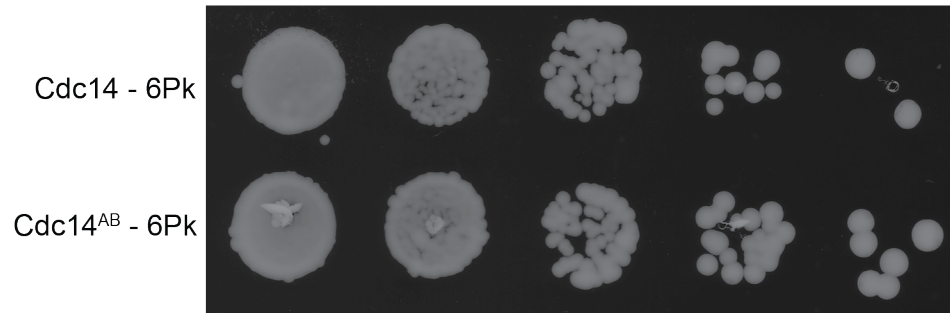


Figure 3.7 – *Cdc14^{AB}* does not exhibit a growth defect.

Serial dilutions of strains harbouring the wild type and truncated *Cdc14* alleles were spotted on to a YPD plate, which was grown at room temperature for 2 days. Representative images are shown.

Next, I sought to test whether the lack of domain C has any bearing on the order and extent of dephosphorylation of proteins during exit from mitosis, when *Cdc14* function is essential. After synchronising *Cdc14^{WT}* and *Cdc14^{AB}* cells in the G1 phase using the pheromone α -factor, I released them to progress through a synchronous cell cycle, taking protein samples at the indicated time points (Fig. 3.8). The cells were re-arrested in the subsequent G1 by re-addition of α -factor towards the end of the experiment.

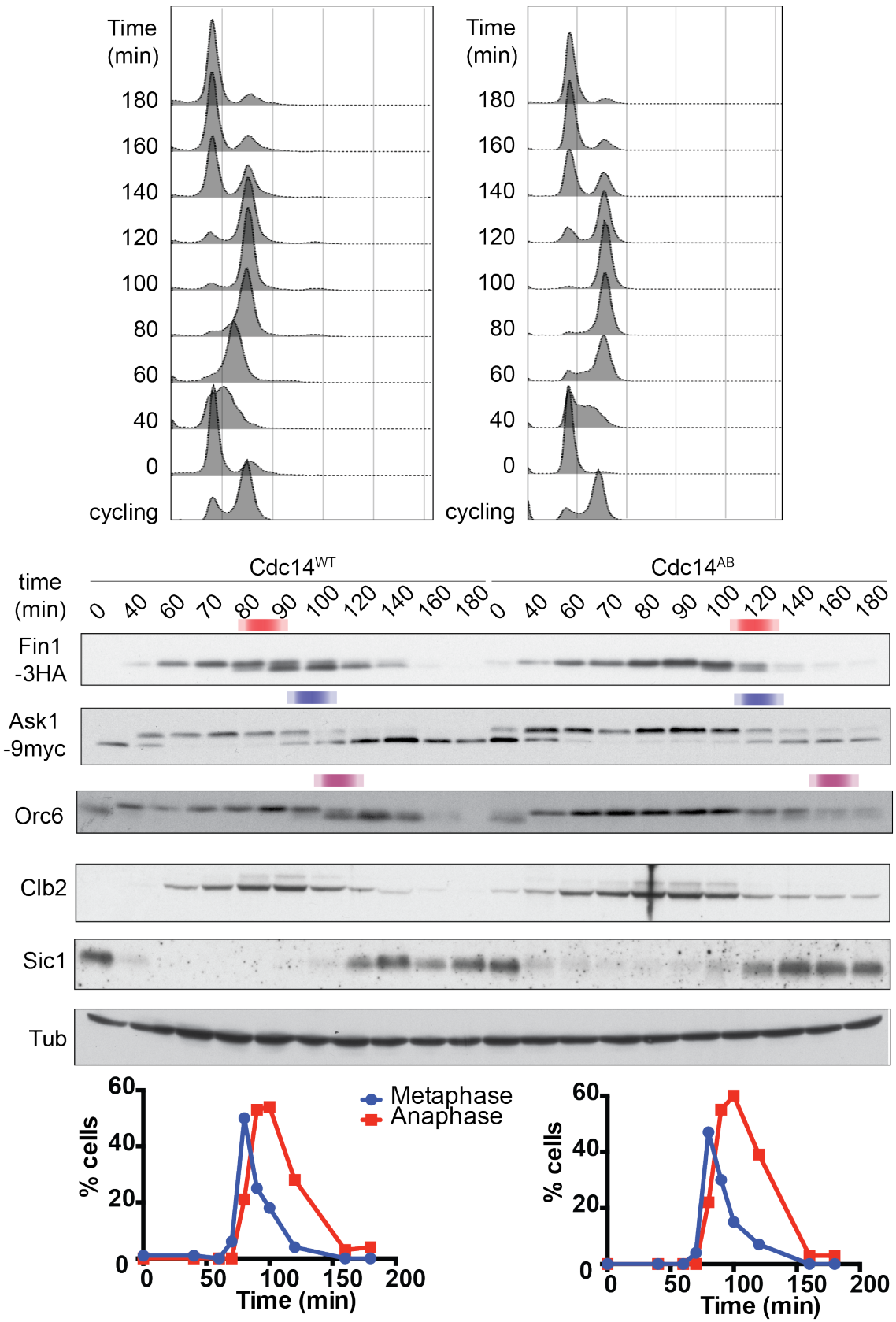
I compared the dephosphorylation timings of known *Cdc14* targets, namely *Fin1*, *Ask1* and *Orc6* in the two strains. The dephosphorylation of the three proteins was delayed by up to 20 minutes in *Cdc14^{AB}* cells (Fig. 3.8). Difference in timings of entry into anaphase was not a reason for these observations, as both strains entered anaphase at the same time. This was adjudged by counting spindles corresponding to metaphase (short) and anaphase lengths (medium or long), a commonly used cell cycle marker in budding yeast (Fig. 3.8). Even though a considerable delay in substrate dephosphorylation was observed, the dephosphorylation order was preserved, indicating that the cells must await the release of higher amounts of active *Cdc14*, perhaps due to the hypomorphic nature of this allele.

Nonetheless, Clb2 degradation and Sic1 accumulation occurred on the clock, demonstrating that the APC function was not adversely affected.

Overall, the FACS profiles of the two strains were nearly identical, indicating that, firstly, the cells can survive with reduced phosphatase activity, and secondly, there are other, redundant, mechanisms that ensure timely decline of kinase activity, such as cyclin degradation.

Figure 3.8 – Dephosphorylation of substrates is delayed in Cdc14^{AB}.

FACS and western blot profiles of Fin1, Ask1, Orc6, Clb2 and Sic1 at the indicated time points in Cdc14^{WT} (left) and Cdc14^{AB} (right) from a representative experiment are shown. Tubulin (tub) serves as the loading control. Red, blue and magenta shaded boxes indicate the mid-point of protein dephosphorylation, when 50% of the indicated protein is in a dephosphorylated state. Percentages of cells containing metaphase and anaphase spindles were also determined at each time point for the two strains. Four repeats of the experiment were performed.



Next, I examined the profiles of the two Cdc14 proteins during the cell cycle. Whilst Cdc14^{WT} was phosphorylated at a time coinciding with anaphase and dephosphorylated as the cells underwent cytokinesis and re-arrested in the following G1, no phosphorylation of Cdc14^{AB} was apparent, confirming that the C-terminal domain is the hub of most Cdc14 phosphorylation events (Fig. 3.9A).

As the C-terminal domain also harbours the NLS (Bembenek et al., 2014), it is possible that Cdc14^{AB} could have been mislocalized. To test this possibility, I also examined the localization of the proteins during G1 phase of the cell cycle by indirect immunofluorescence, when Cdc14 is supposed to be sequestered in the nucleolus by its inhibitor Net1, to assess whether this sequestration is perturbed. The two proteins appeared to be fully sequestered, showing only a nucleolar density (Fig. 3.9B), denoting that Cdc14^{AB} was not mislocalized. This was surprising, as the very end of domain AB contains the NES, which would be expected to predominate in the absence of the NLS.

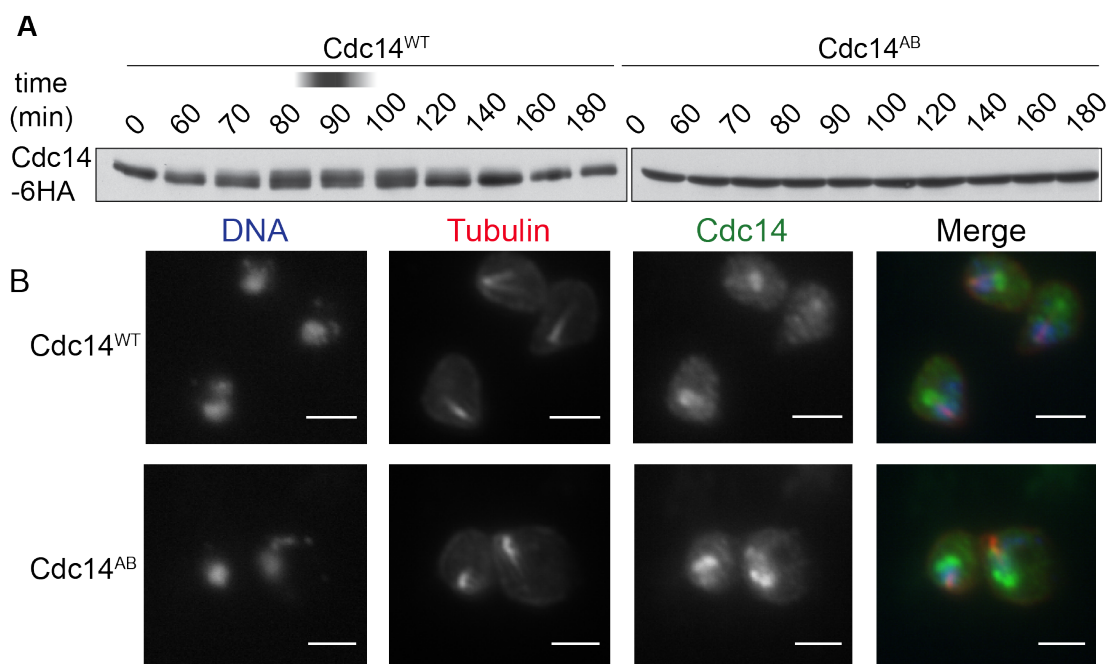


Figure 3.9 – Cdc14^{AB} is not mislocalized in the G1 phase.

A. Western blot profiles of Cdc14^{WT} (left) and Cdc14^{AB} (right) proteins are shown at the indicated time points over the course of the cell cycle. **B.** Indirect immunofluorescence of the two Cdc14 proteins (green) at time point 0 minutes, with tubulin (red) and DNA (blue) marked for reference. The scale bar represents a length of 5 μ m.

Thus, the C-terminal domain is required for full catalytic activity of Cdc14 *in vitro* and *in vivo*. However, cell cycle progression and, in particular, the overall timing of exit from mitosis and cytokinesis appear to be unaffected. Thus, it is possible that phosphatases other than Cdc14 are active during mitotic exit, and are able to compensate for the lack of its full activity, thereby ensuring timely exit from the mitotic program.

Chapter 4. Phosphosite-specific features of efficient Cdc14 substrates

Thus far, little is known about substrate specificity of Cdc14 phosphatases other than the facts that they are Cdk1-opposing, and that they preferentially target pSP-x-(K/R)-containing peptides (Bremmer et al., 2012; Eissler et al., 2014). Given the large range of dephosphorylation timings of substrates *in vivo*, I theorized that it is possible that there are differences within the phosphosite features of substrates that are dephosphorylated with an ‘early’ timing, and those that are dephosphorylated ‘late’ in anaphase. For instance, it has been suggested that a close match to a pSP-x-KKK motif would constitute a particularly good Cdc14 substrate (Eissler et al., 2014).

4.1 Phosphosite composition of Cdc14 substrates dephosphorylated ‘early’ and ‘late’ into anaphase is similar

To systematically examine whether phosphosite features distinguish early from late dephosphorylated Cdc14 substrates in an unbiased way, I took advantage of a mass spectrometry-based screen performed by T. Kuilman in the lab (Kuilman et al., 2015). Briefly, the cells were arrested in metaphase by depleting the APC regulator Cdc20, and Cdc14 was then overexpressed. Protein samples were taken at specific time points. These were then subjected to mass spectrometric analysis to ascertain phosphosubstrate abundance at different time points upon Cdc14 induction – a measure for dephosphorylation. Whilst this does not represent an unperturbed exit from mitosis, previous work has shown that a series of candidate substrates tested maintain the correct order of dephosphorylation following Cdc14 overexpression as compared to a natural mitotic exit program (Bouchoux and Uhlmann, 2011).

Thus, I first selected phosphopeptides that disappeared with ‘early’ dephosphorylation timing, i.e. reached their minimum value no more than 20 minutes after Cdc14 induction. The list was further reduced to remove proteins that had fewer than 30% of

peptides in the ‘early’ category. This step was included to ensure that the final list contained high confidence early phosphosubstrates, as mass spectrometry based assignments can contain errors. This led to 40 unique peptides (listed in section 7.2). A dataset containing ‘late’ dephosphorylated phosphopeptides (containing 72 unique peptides) was used for comparison (Kuilman et al., 2015).

Next, using MotifX and WebLogo, a sequence logo for both early and late dephosphorylated Cdc14 substrate peptides was made (Fig. 4.1A). These logos depict the probability of occurrence of a particular amino acid at each position relative to the phosphosite of both early and late phosphopeptides. The sequence logos are centred on the phosphorylated Ser or Thr residue, which is followed by a proline – the minimal Cdk consensus. Using a list of Cdk-phosphorylated peptides (547 unique peptides in total) identified in another mass spectrometry-based study (Holt et al., 2009), I also made a sequence logo to represent all ‘Cdk phosphopeptides’ for comparison (Fig 4.1B). The three sequence logos were analysed for enriched residues at each position with the help of Probir Chakraborty from The Francis Crick Institute’s Bioinformatics and Biostatistics facility.

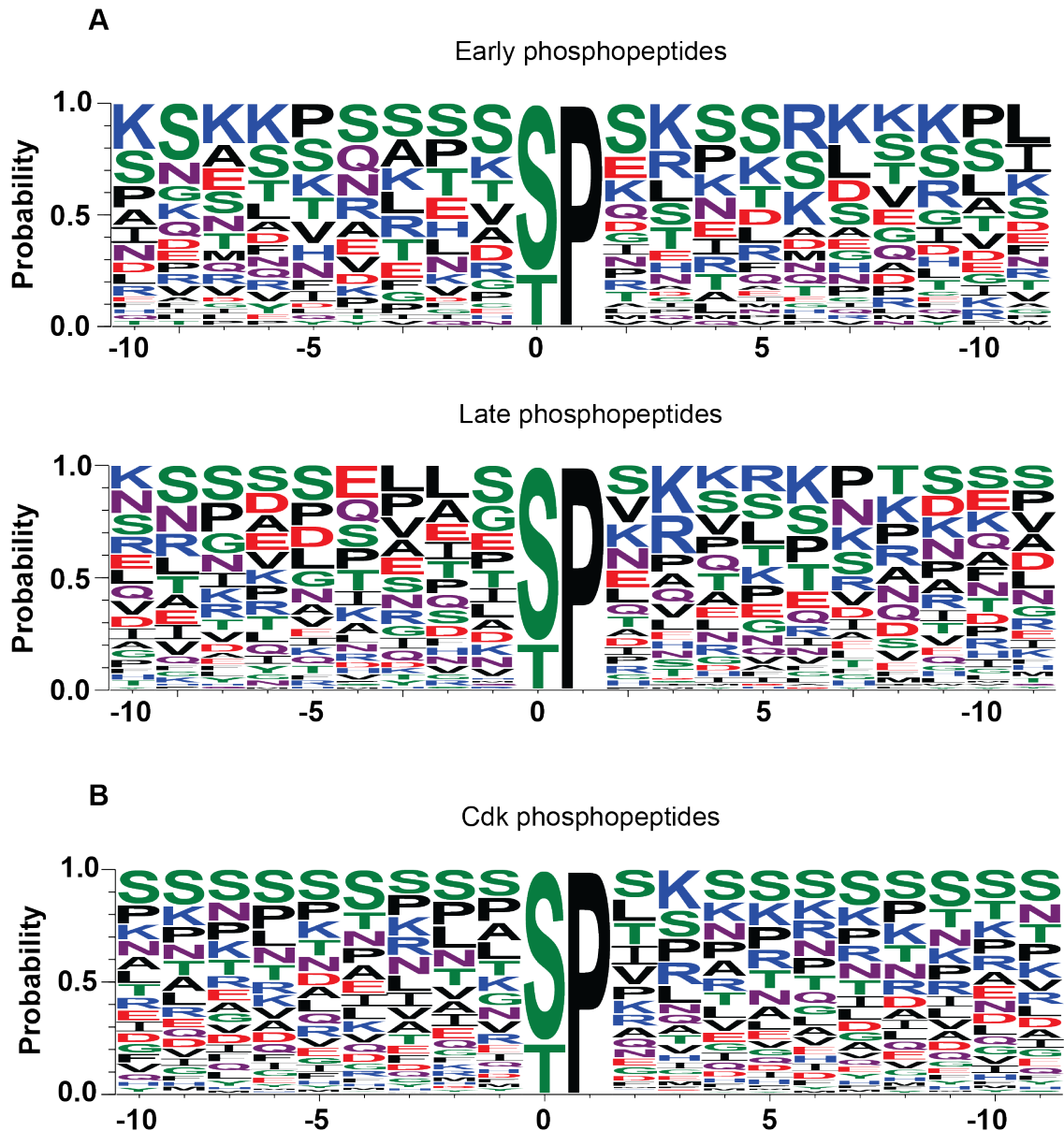


Figure 4.1 – Comparison of sequence logos derived from ‘early’, ‘late’ and ‘Cdk’ phosphopeptides.

The X-axis indicates the position relative to the phosphosite identified in the mass spectrometric screens, which has been denoted ‘0’. The Y-axis denotes probabilities. The height of each amino acid within the sequence logo is indicative of the probability with which it occurs within each dataset.

First, it is apparent that there is an overwhelming predominance of Ser over Thr at position 0 in all three datasets. Cdk’s preference for phosphorylating serines has been previously exhibited *in vitro* (Suzuki et al., 2015). Also, whilst the frequency of SP and TP occurrence in the *S. cerevisiae* genome is similar (with the SP/TP ratio being 1.2, as

calculated by Probir Chakraborty), the ratio of SP/TP in this aforementioned Cdk substrate list is 3.4. Thus, at least a part of this SP enrichment might be driven by Cdk's substrate preferences.

Next, an overabundance of positively charged residues is also apparent particularly at the +3 position in both the early and late datasets, much more so than the enrichment within the Cdk dataset. This proteome-wide trend agrees well with previously published data (Eissler et al., 2014), wherein a few Cdc14 targets were examined *in vitro*.

There also appears to be a slight enrichment of non-polar, aliphatic residues at the -3 position, particularly in the 'late' list.

Overall, however, there is not a strict consensus within the 'early' list outside of the pSP-x-(K/R) preference that is also shared by late dephosphorylated Cdc14 targets; whilst the pattern of amino acid enrichment differs between the two lists, there is no clear preference for residue(s) belonging to a particular physicochemical class. This analysis indicates that there are no obvious phosphosite-specific features that are solely responsible for defining an early substrate.

4.2 Phosphosite mutants of Fin1 reveal Cdc14 substrate specificity *in vivo*

Although comparison of early and late dephosphorylated phosphopeptides yielded little differences between the two, an overall striking feature of this proteomic analysis revealed that phosphoserines, followed by positively charged residues at the +3 position are features that are generally preferred by Cdc14. These observations are in accordance with previously published data (Bremmer et al., 2012; Eissler et al., 2014) as has been discussed in section 1.8.3.

In order to further verify these Cdc14 substrate preferences, I wanted to ascertain if abrogation of these features has any effect on the dephosphorylation timings of otherwise efficient Cdc14 targets *in vivo*. I chose Fin1 for this analysis, as the phosphatase possesses high catalytic efficiency towards it and the protein is one of the earliest Cdc14 targets known. Further, Fin1 is also rich in SP-x-(K/R) sites, making it an ideal tool for such an analysis. Thus, I sought to examine Cdc14's predicted preference for serines over threonines *in vivo*, using Fin1 as a tool.

Table 4.1 outlines the phosphosite composition of wild type Fin1, along with the mutants tested in the next few sections.

	SP-x-(K/R)	SP	TP-x-(K/R)	TP
Fin1 ^{WT}	4	1	1	0
Fin1 ^{6TP}	0	0	5	1
Fin1 ^{6TPxA}	0	0	0	6
Fin1 ^{+3A}	0	5	0	1

Table 4.1 – Phosphosite composition of Fin1 alleles

The table provides a breakdown of phosphosites in the wild type protein, along with those of all the Fin1 mutants tested *in vivo* or *in vitro* in the following sections.

4.2.1 Dephosphorylation of Fin1^{6TP} is markedly delayed *in vivo*

Fin1 is a serine-rich substrate, with five out of the six Cdk-phosphosites being serines (refer to table 4.1). Each of these serine residues was replaced with threonines, creating a *Fin1*^{6TP} allele. I then substituted the endogenous allele with this construct. Next, I performed a time course analysis by arresting the cells in G1 and releasing them synchronously into the next cell cycle, and examined the dephosphorylation timings of the two Fin1 proteins (Fig 4.2). A high time resolution around the expected time of anaphase was achieved by taking protein samples at intervals of 5 minutes, to look for subtle differences in protein dephosphorylation, if any.

Although Fin1 contains six phosphosites, the phosphoshift visualized on an SDS-PAGE gel arises primarily due to phosphorylation of Ser148 (data not shown). Mass spectrometric analysis showed that phosphosites within this protein are dephosphorylated with similar timings and kinetics (Kuilman et al., 2015). Furthermore, emergence of faster migrating species of Fin1 was found to correlate with reduced overall phosphorylation of the protein *in vivo* (Bouchoux and Uhlmann, 2011). Thus, in the following experiments, Fin1 phosphoshift has been used as a reporter for bulk protein dephosphorylation.

In a wild type strain, Fin1 begins to be dephosphorylated in early anaphase, and the protein quickly shifts to a majority-dephosphorylated species. During mid-to-late anaphase, the protein also starts to be degraded by APC^{Cdh1} action.

As expected, Fin1^{WT} was dephosphorylated early, with the mid-point of dephosphorylation being 90 minutes. In contrast, Fin1^{6TP}'s dephosphorylation was markedly delayed, with the dephosphorylated species only becoming apparent as late as cytokinesis and after most of the protein had been degraded – well after the function of Fin1 is usually thought to be required. Thus, it is possible that a substrate preference of Cdc14 for serines translates *in vivo* as well as *in vitro*, with the phosphatase only being able to target Fin1^{6TP} very late into the cell cycle, when the activity of the phosphatase is at its maximum and Cdk activity has fully declined.

The abundance of Fin1^{6TP} was reduced in comparison to its wild type counterpart. This could be due to Cdk1 not fully phosphorylating this all-threonine allele (Suzuki et al., 2015), which is known to be required for 14-3-3 binding to this protein (Hall et al., 2008) during interphase. This might target the protein for inappropriate degradation.

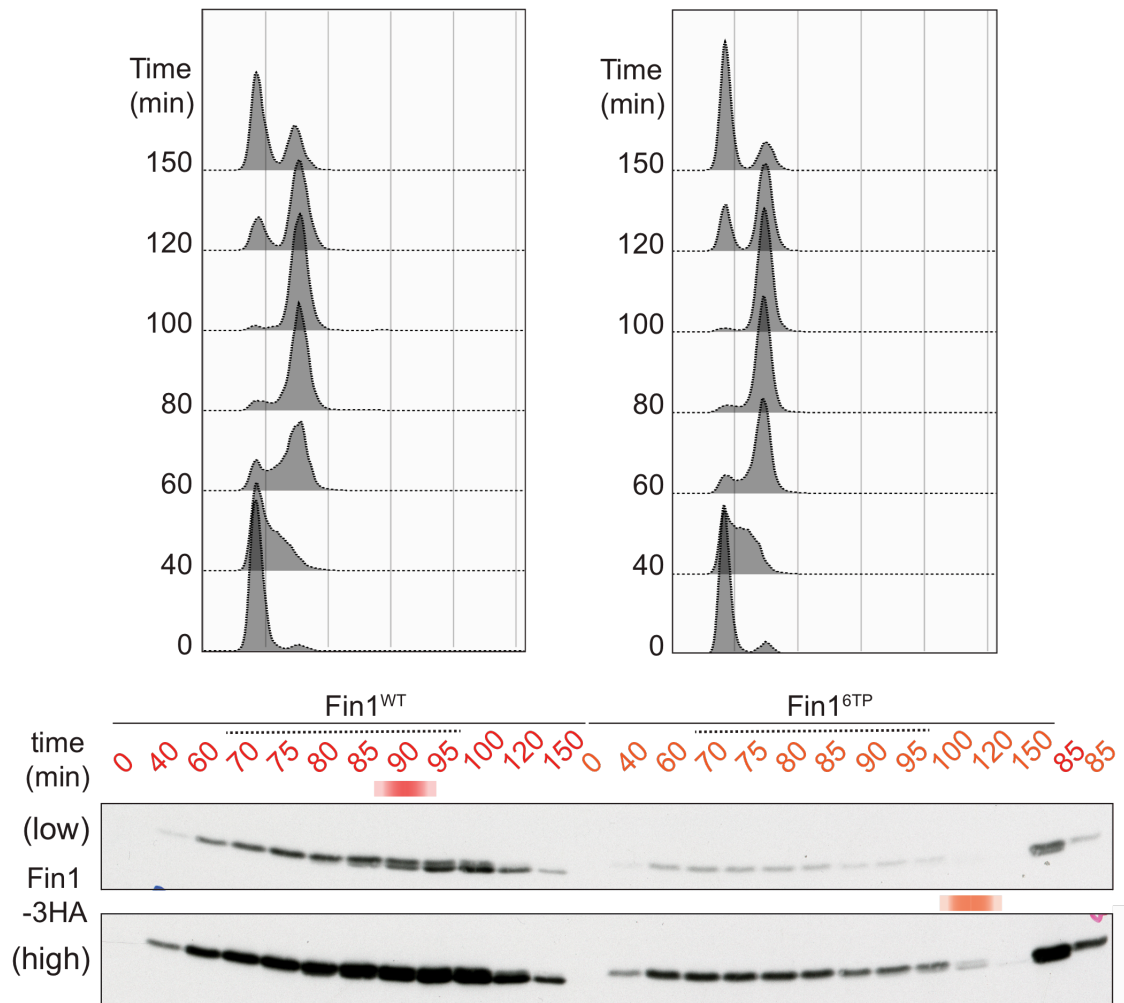


Figure 4.2 - Comparison of *in vivo* dephosphorylation timings of Fin1^{WT} and Fin1^{6TP}.

Representative FACS and western blot profiles showing the progression from G1 to the subsequent G1 and phosphorylation profiles of the two Fin1 protein variants, respectively. Comparison of proteins from the 85th minute time point shows that the band observed in Fin1^{6TP} is the higher, phosphorylated form of the protein. Red and orange shaded boxes show dephosphorylation mid-points of proteins.

4.2.2 Fin1^{6TPxA} is dephosphorylated very early into anaphase

Since the early Cdc14 substrate Fin1 can be converted into an inefficient substrate by replacing its phosphosites with threonines, I wanted to further examine the phosphosite specificity of the phosphatase, by combining this allele with mutations of the +3 positively charged residues within Fin1. Five out of the six Fin1 phosphosites contain a lysine or an arginine at the +3 position. As before, I replaced all serines with

threonines, and all lysines/arginines with alanines. I then replaced *Fin1*^{WT} with the *Fin1*^{6TPxA} mutant allele *in vivo*. As before, the two strains were arrested in G1 and released to progress synchronously through the next cell cycle. As release from α -factor can vary between strains, dephosphorylation of Ask1, an unrelated Cdc14 target that gets dephosphorylated shortly after Fin1, was used as a biochemical marker of anaphase and served as a tool for independent comparison of experiments.

Relative to the wild type protein, the behaviour of *Fin1*^{6TPxA} was surprising: firstly, *Fin1*^{TPxA} never gets fully phosphorylated during interphase. Secondly, when compared to dephosphorylation timings of Ask1 within the two strains, *Fin1*^{6TPxA} dephosphorylation was found to precede even the wild type protein (Fig. 4.3). Whilst the mid-point of *Fin1*^{WT} dephosphorylation was five minutes before that of Ask1, mid-point of *Fin1*^{6TPxA} occurred 10 minutes prior to Ask1 dephosphorylation.

As was the case for *Fin1*^{6TP}, the abundance of *Fin1*^{6TPxA} was reduced even further, with there being a correlation between reduced phosphorylation and diminished stability of the latter protein variant.

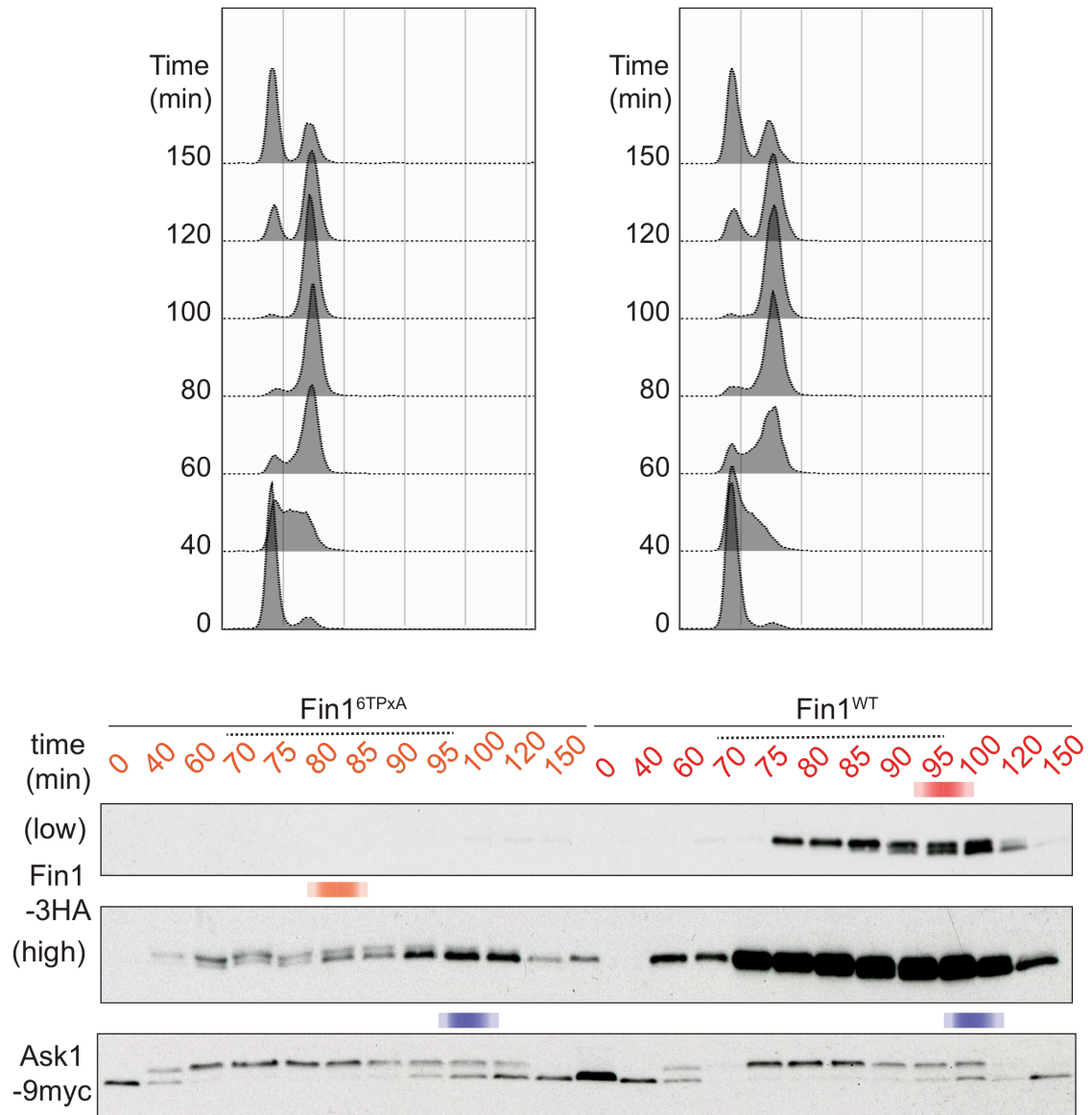


Figure 4.3 – $Fin1^{TPxA}$ is dephosphorylated very early in anaphase.

FACS and western blot profiles of progression of G1 to the next G1 of $Fin1^{WT}$ and $Fin1^{6TPxA}$ strains. Ask1, another early protein, has been used as an independent biochemical marker of entry into anaphase. Red, orange and blue shaded boxes indicate mid-points of dephosphorylation of proteins. The trend was observed in three independent repeats of the experiment.

For comparison, I also monitored the dephosphorylation timings of the wild type protein and a mutant variant which only had the positively charged residue at the +3 position replaced with alanines, $Fin1^{+3A}$. Figure 4.4 shows that when compared to wild type protein dephosphorylation, $Fin1^{+3A}$ does not exhibit any considerable differences.

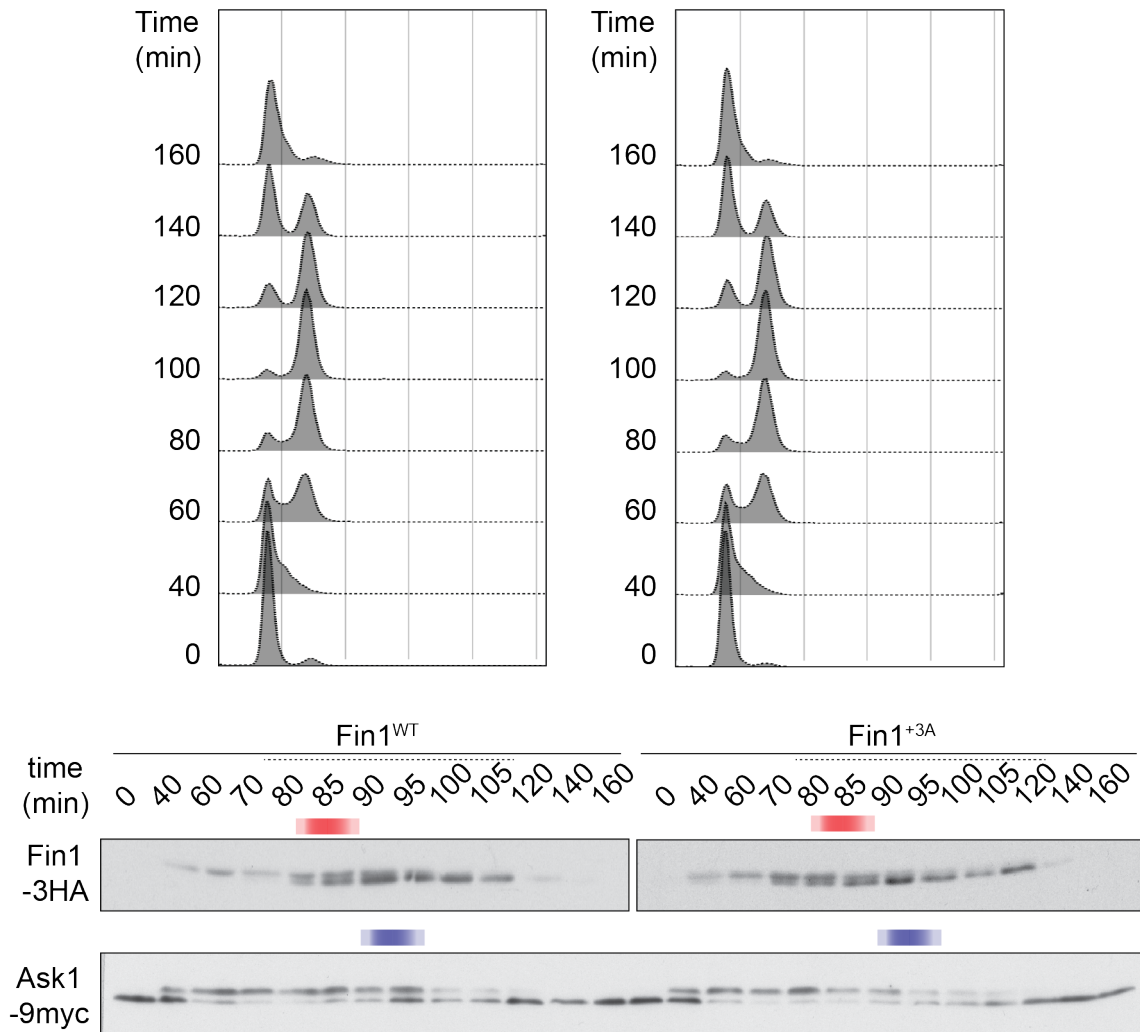


Figure 4.4 – Dephosphorylation timing of Fin1^{+3A} is unaffected. Representative FACS and western blot profiles of progression from G1 to subsequent G1 of Fin1^{WT} and Fin1^{+3A} strains. Ask1, another early protein, has been used as an independent biochemical marker of entry into anaphase. Red and blue shaded boxes indicate mid-points of protein dephosphorylation.

What explains the results of experiments discussed herein? Whilst replacement of serine phosphosites to threonines delays Fin1 dephosphorylation timing, the impact of the additional +3 K/R mutations is less clear. It is possible that that these dephosphorylation timings can be explained when one accounts for both the kinase and the phosphatase reactions: the kinase-to-phosphatase activity ratio experienced by the wild type and phosphosite mutant proteins.

4.2.3 The ratio of kinase to phosphatase activities explains the dephosphorylation timings of Fin1^{WT}, Fin1^{6TP}, and Fin1^{6TPxA}

To get a clear understanding of the behaviour of Fin1^{WT}, Fin1^{6TP} and Fin1^{6TPxA} *in vivo*, and I sought purify them and study their behaviour, along with the kinase and phosphatase reactions *in vitro*.

Purification of Fin1^{WT}, Fin1^{6TP}, and Fin1^{6TPxA} yielded the same molar concentrations of the proteins. Furthermore, they also exhibited identical gel filtration profiles, indicating that the mutants are well folded, and gross mis-folding cannot explain their phosphorylation and/or dephosphorylation differences.

Next, their ability to interact with Cdc14 *in vitro* was examined, as previous studies have reported that Cdc14 loses binding to phosphosite mutants of substrates such as Acm1 and Yen1 (Bremmer et al., 2012; Eissler et al., 2014). In contrast to previously published observations for other substrates, the phosphosite mutants of Fin1 were pulled down as efficiently as the wild type counterpart by glutathione-immobilized GST-Cdc14^{C283S}, a substrate-trap allele described previously which is thought to bind substrates with high affinity (Bloom et al., 2011) (Fig. 4.5). Under the same conditions, Ask1, an inefficient substrate and a poor interactor, was not pulled down by the phosphatase. This implies that firstly, *in vitro*, the mutants are well folded, and secondly, Fin1 displays phosphosite-independent interactions with Cdc14. Further, this observation bolsters the argument that the *in vivo* phosphorylation and/or dephosphorylation profiles of Fin1^{6TP} and Fin1^{6TPxA} are not due to overall protein folding, but due to catalytic defects exhibited by Cdc14 and/or Cdk towards them.

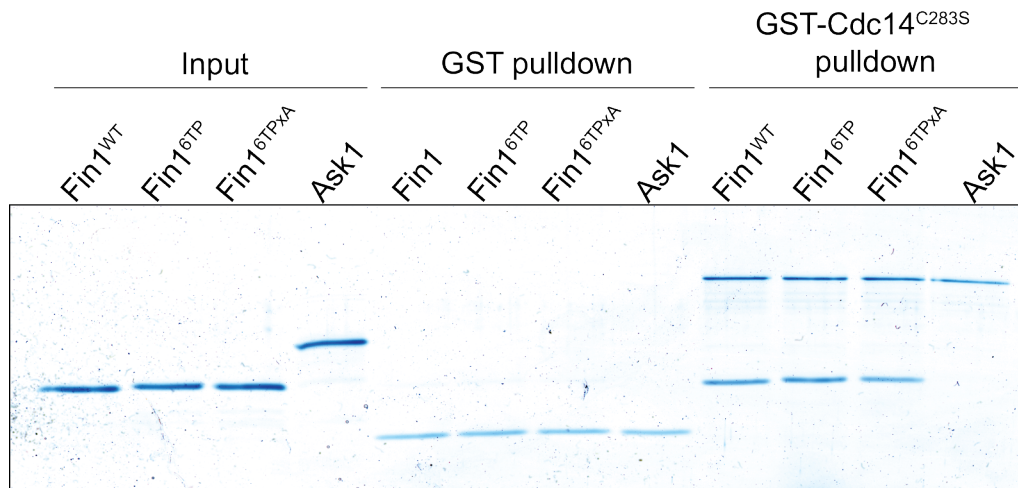


Figure 4.5 – Fin1 phosphosite mutants interact efficiently with the immobilized phosphatase.

Either GST alone, or GST-Cdc14^{C283S} was immobilized on glutathione beads. Next, the three Fin1 variants and Ask1 were added to the reaction. After binding and washing, the beads were boiled in sample buffer, and the proteins were separated by SDS-PAGE and stained with InstantBlue. The experiment was repeated twice.

4.2.3.1 Clb2-Cdc28 exhibits a defect in phosphorylation of Fin1^{6TP_{XA}} *in vitro*

In order to gain a fuller understanding of *in vivo* dephosphorylation timings of Fin1^{WT}, Fin1^{6TP}, and Fin1^{6TP_{XA}}, I first tested the ability of the kinase to phosphorylate these proteins *in vitro*. It is possible that Cdk is able to discriminate between them.

As Clb5 is degraded very early upon APC activation (Lu et al., 2014), Clb2 as the major cyclin present during anaphase. Thus, I performed the following analyses with purified Clb2-Cdc28. The ability of the kinase to phosphorylate the three Fin1 protein variants was tested.

Full phosphorylation of Fin1 causes the emergence of slower migrating species of the protein (Bouchoux and Uhlmann, 2011). The ability of increasing amounts of Clb2-Cdc28 to phosphorylate the three proteins was examined. If EDTA, a magnesium chelator, was added to the reactions before incubation with the substrates, no band-

shift was observed, indicating that Clb2-Cdc28 was the sole provider of kinase activity in these reactions.

Fin1^{WT} and Fin1^{6TP} both exhibited full phosphorylation and a quantitative band-shift within 30 minutes of 33 nM Clb2-Cdc28 addition. If there are small differences within the phosphorylation efficiencies of the kinase towards these two variants, I suspect that one would need a more quantitative way of examining them. Fin1^{6TPxA}, however, was found to be only partially phosphorylated, even long after incubations with high kinase amounts (Fig 4.6).

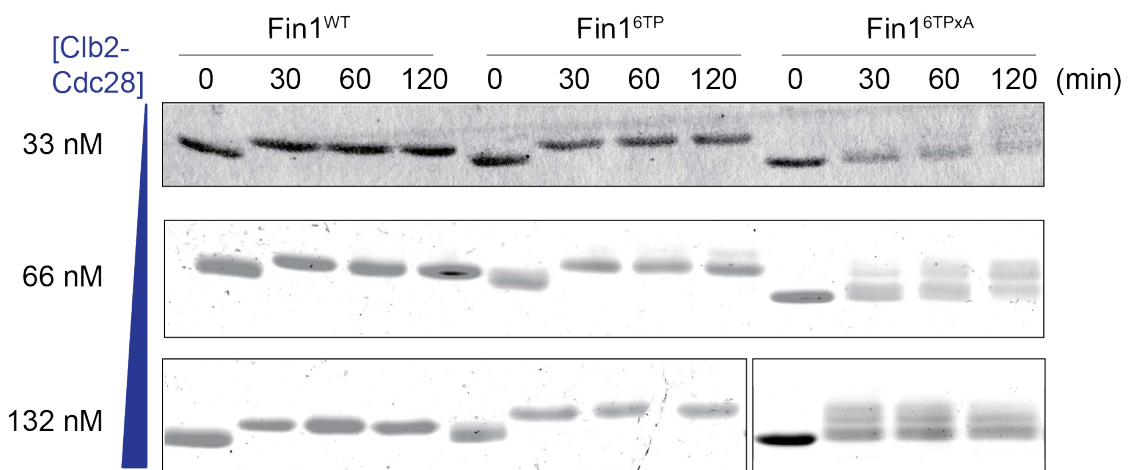


Figure 4.6 – Clb2-Cdc28 differs in its abilities to phosphorylate Fin1^{WT}, Fin1^{6TP}, and Fin1^{6TPxA}.

Kinase reactions were performed using 1.66 μ M of each substrate and indicated amounts of the purified kinase in the kinase buffer (see materials and methods). 10 picomoles of reaction aliquots were removed at the indicated time points, resolved using SDS-PAGE and stained with InstantBlue. Fin1^{WT} and Fin1^{6TP} are well phosphorylated in all reactions, whilst Fin1^{6TPxA} is only partially phosphorylated. All reactions were independently repeated thrice.

This observation corroborates the inability of the kinase to fully phosphorylate Fin1^{6TPxA} *in vivo*. As such, this handicap of Cdk1 has previously also been noted in the vertebrate protein *in vitro* (Suzuki et al., 2015).

4.2.3.2 *Cdc14 displays a strong preference for SP-x-(K/R) in vitro*

Next, I performed similar analyses with purified Cdc14 and phosphorylated Fin1 proteins. First, the three Fin1 protein variants were phosphorylated with 300 nM Clb2-Cdc28, which still did not lead to complete Fin1^{6TPxA} phosphorylation. Next, increasing amounts of the phosphatase were added, and reaction aliquots removed at indicated time points (Fig. 4.7).

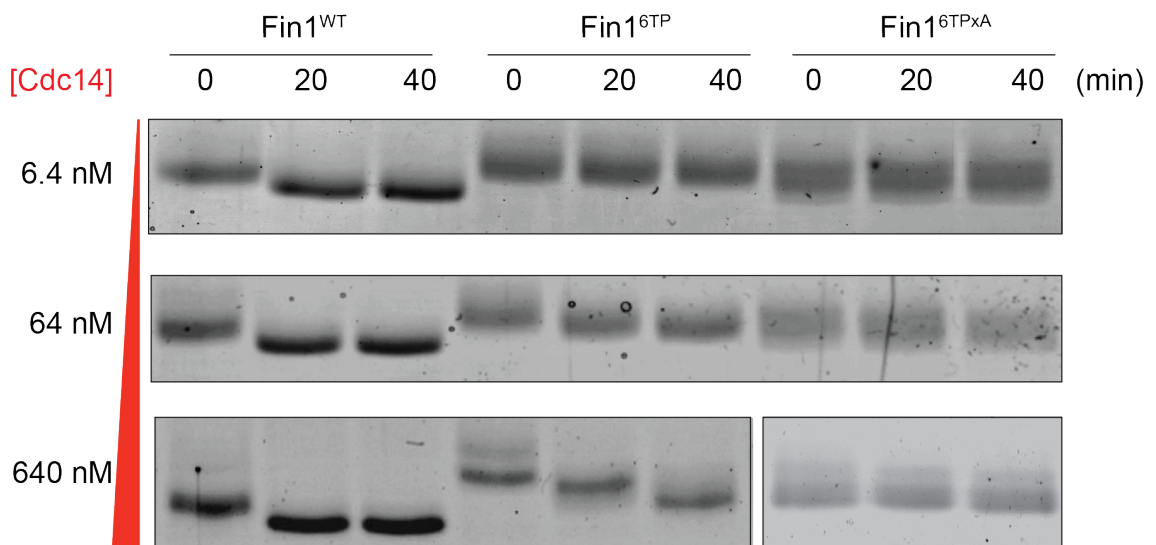


Figure 4.7 – Cdc14 differs in its abilities to dephosphorylate Fin1^{WT}, Fin1^{6TP}, and Fin1^{6TPxA}.

Kinase reactions were performed as described previously. Varying amounts of Cdc14 were added to 640 nM of each substrate, and aliquots (10 picomoles) removed at the indicated time points. These were resolved using SDS-PAGE and stained with InstantBlue. Whilst Fin1^{WT} is easily dephosphorylated at low Cdc14 concentrations, Fin1^{6TP} and Fin1^{6TPxA} are not. All dephosphorylation reactions were independently repeated thrice.

As expected, Fin1^{WT} was efficiently dephosphorylated within 20 minutes of 6.4 nM phosphatase addition. However, dephosphorylation of Fin1^{6TP} only became apparent upon addition of 640 nM, i.e. equimolar amounts of Cdc14. This behaviour is reminiscent of Fin1^{6TP} only being dephosphorylated very late into anaphase, when Cdc14 is fully released from its sequestration. In fact, considering that the wild type protein is almost completely dephosphorylated in just over a minute upon addition of 6.4 nM phosphatase (see section 5.6.2), the dephosphorylation defect in Fin1^{6TP} is striking by comparison. As Fin1^{6TPxA} is still not fully phosphorylated, its

dephosphorylation pattern is harder to examine. Nonetheless, qualitatively, $\text{Fin1}^{6\text{TPxA}}$ dephosphorylation was not apparent. This is at odds with the expectation from the *in vivo* experimental result, wherein this mutant protein could be dephosphorylated very early into anaphase. It is possible that subtle dephosphorylation of the protein is not apparent by the relatively insensitive Coomassie staining used in the experiment and is complicated by the phosphorylation pattern. Further, it is also possible that a different phosphatase targets $\text{Fin1}^{6\text{TPxA}}$ *in vivo*.

4.2.3.3 *The kinase-to-phosphatase activity ratio could explain in vivo dephosphorylation timings of Fin1 variants*

As the kinase and phosphatase reactions do not exist in isolation within the cells, one must consider the two together (Table 4.2). With the readout being substrate dephosphorylation, it appears that phosphosite composition has a profound impact on the ability of both Cdc14 and Cdc28 to act on this otherwise highly efficient substrate.

	Cln2 phosphorylation	Cdc14 dephosphorylation	Dephosphorylation timing
Fin1^{WT}	Wild type	Wild type	Early
$\text{Fin1}^{6\text{TP}}$	Wild type	Impaired	Late
$\text{Fin1}^{6\text{TPxA}}$	Strongly impaired	Strongly impaired	Early

Table 4.2 – A summary of the abilities of Cln2 and Cdc14 to target the three Fin1 variants.

Integrating kinase and phosphatase activities towards the three Fin1 variants could provide an explanation for the dephosphorylation timing exhibited by each *in vivo*.

Differing phosphosite sensitivities of the two regulators, however, lead to differences in dephosphorylation timings. At least in the context of Fin1, Cdc28's activity is not drastically hampered towards $\text{Fin1}^{6\text{TP}}$, which contains TP-x-(K/R) residues, whereas Cdc14 is severely debilitated. However, additional removal of the +3 positively charged residue changes the fate of the protein entirely, with both Cdc28 and Cdc14 being now challenged.

Chapter 5. Phosphosite-independent features that contribute to dephosphorylation of the early substrate, Fin1

5.1 Early degradation of Clb5 in part enables early dephosphorylation of the Clb5-specific substrate, Fin1

As outlined in Chapter 1, budding yeast exhibits a unique pattern of cyclin proteolysis during mitotic exit. The S-phase cyclin Clb5 is degraded early on by the APC (Lu et al., 2014), but Clb2 exhibits a biphasic pattern of destruction, with 50% of its activity persisting until Cdh1-mediated destruction later in anaphase.

Thus, it has been postulated that early Clb5 degradation might bring about early substrate dephosphorylation: perhaps Cdc14 would be able to better target these Clb5-specific substrates, as they no longer receive any input from their favoured kinase (Jin et al., 2008; Jin, Richmond and Wang, 2014).

Whilst a systematic analysis remains to be performed, anecdotally, however, this does not hold up to scrutiny as a general ordering principle. Amongst substrates with known dephosphorylation timings, the RxL-containing Orc6, Cdh1 and Sic1, are also late substrates of Cdc14, even though they would be expected to be dephosphorylated earlier due to Clb5 degradation.

5.1.1 Mutation of the RxL motif within Fin1 does not hasten its dephosphorylation *in vivo*

Though it is unlikely to be a general principle governing ordered substrate dephosphorylation, I still wanted to examine whether Clb5's specificity for certain targets could contribute to dephosphorylation of a known early substrate.

As before, I turned to our model early substrate Fin1, which is also a Clb5-specific substrate. As a first step, I replaced the endogenous Fin1 gene with an allele that had its Clb5-binding motif (KxL, residues 194-196) (Loog and Morgan, 2005) abrogated. A time course analysis from G1 into the subsequent G1 did not reveal a defect in the protein's phosphorylation during S-phase, even on higher exposures of the western blots, as had been previously reported (Loog and Morgan, 2005) (Fig. 5.1). Furthermore, the protein's dephosphorylation timing was not altered, as adjudged by comparing its dephosphorylation timing to that of the independent biochemical marker Ask1 which is dephosphorylated shortly after Fin1.

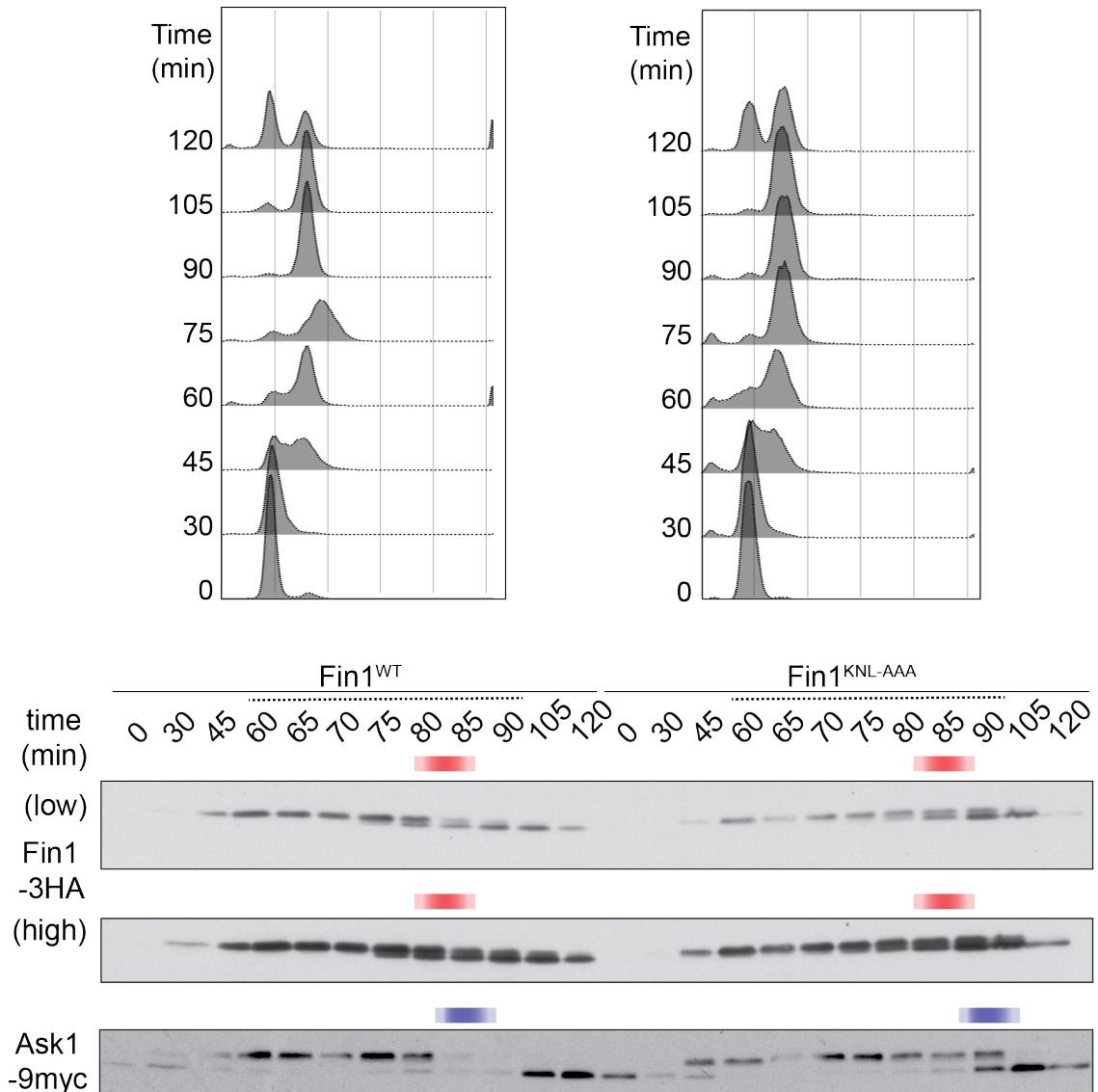


Figure 5.1 – Comparison of *in vivo* dephosphorylation of Fin1^{WT} and Fin1^{KNL-AAA}.

FACS and western blots showing the progression from G1 to the next G1 and phosphorylation profiles of Fin1^{WT} and Fin1^{KNL-AAA}, respectively, with a high and low exposure. Fin1^{KNL-AAA} does not show either a phosphorylation defect, or earlier dephosphorylation. The red and blue shaded boxes show dephosphorylation mid-points of proteins. Representative images from three independent experiments are shown.

5.1.2 Stabilization of Clb5 throughout the cell cycle leads to impaired Fin1 dephosphorylation

The removal of the RxL motif within Fin1 might have led to its earlier dephosphorylation, but given the fact that its dephosphorylation is already very early, it

might have been difficult to observe a further advance in dephosphorylation kinetics of Fin1. As an alternative approach, I sought to stabilize Clb5. This would provide a direct way of testing whether Clb5 degradation in early anaphase contributes towards early Fin1 dephosphorylation. The endogenous Clb5 gene was replaced by one that lacks a Cdc20-dependent destruction box (Clb5^{Δdb}) which leads to partial stabilization of the protein (Wäsch and Cross, 2002). As before, cell cycle profiles of a wild type (Clb5^{WT}) and the mutant strain (Clb5^{Δdb}) were compared in a G1-to-G1 experiment (Fig. 5.2). Stabilization of the cyclin led to a reproducibly earlier release from the α -factor arrest, as is apparent by the FACS profiles - an effect that perhaps can be explained by the cells reaching the activity threshold required for S-phase more quickly in the context of Clb5^{Δdb}. Further, examination of Fin1's cell cycle profile revealed that although the protein started being dephosphorylated early in anaphase, it only reached a partially dephosphorylated state, even at later points during the cell cycle. Comparison with the mid-point of Ask1 dephosphorylation in the Clb5^{Δdb} strain revealed that Fin1's dephosphorylation exhibited a small, but highly reproducible delay of five minutes, even though both Ask1 and Fin1 experience the same kinase activities at each point in the cell cycle.

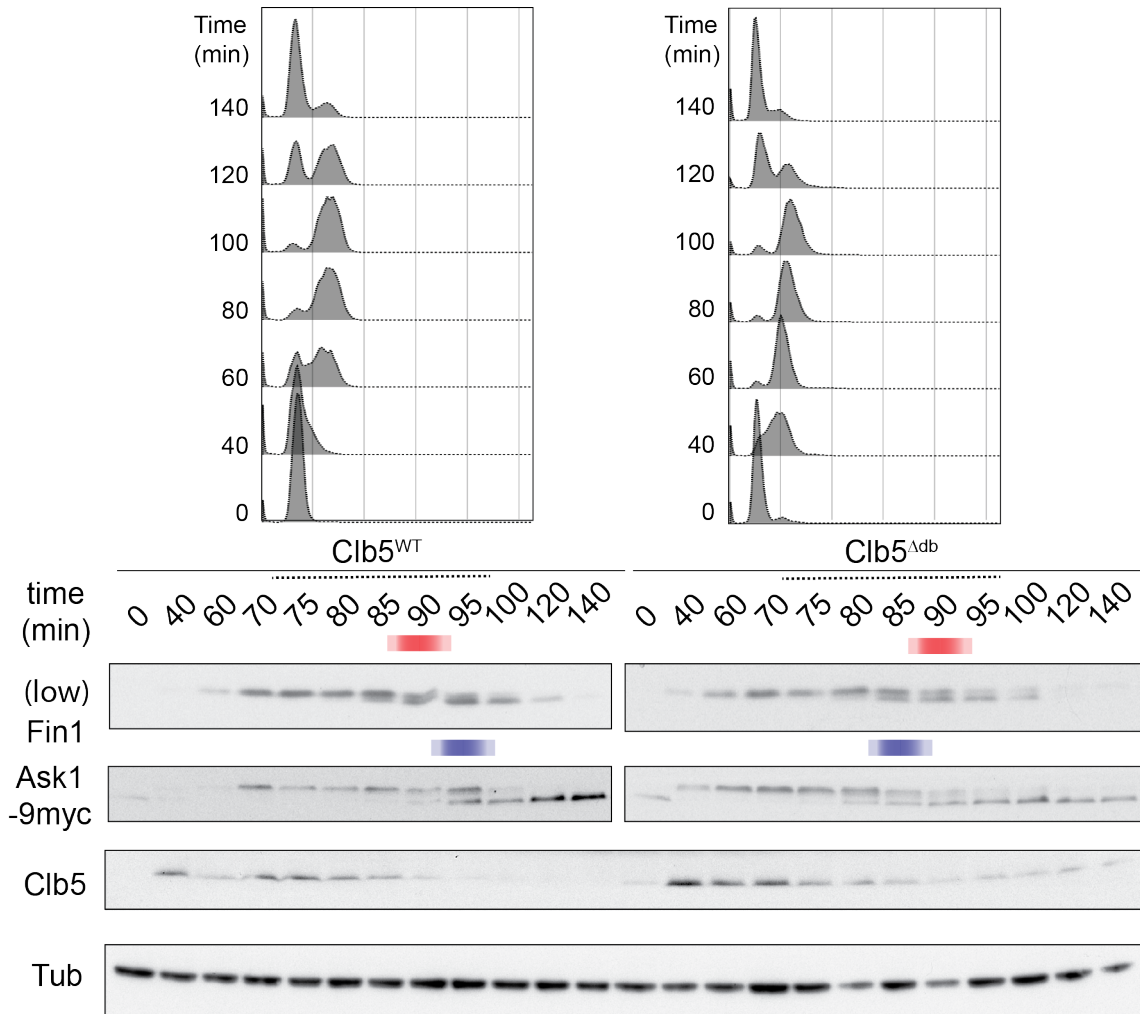


Figure 5.2 – Comparison of Fin1 dephosphorylation in Clb5^{WT} and Clb5^{Δdb} strains.

FACS and western blots showing the progression through G1 to the next G1 and phosphorylation profiles of Fin1 and Ask1 in Clb5^{WT} and Clb5^{Δdb} strain backgrounds. Red and blue shaded boxes indicate dephosphorylation mid-points of proteins. In the Clb5^{Δdb} strain, mid-point of Fin1 dephosphorylation is 90 minutes post-release, whilst that of Ask1 is 85 minutes. Representative images from four independent experiments are shown.

5.1.3 Disruption of the RxL motif of Fin1 restores its dephosphorylation timing in the Clb5^{Δdb} background

Since stabilization of Clb5 during mitotic exit prevents complete dephosphorylation of Fin1, I next tested whether this effect is contingent on Fin1's RxL motif. I reasoned that preventing docking interactions between Fin1 and Clb5^{Δdb} should render the former protein 'blind' to the stabilized cyclin during mitotic exit, perhaps leading to a

restoration of its dephosphorylation timing. This hypothesis was tested in a G1-to-G1 experiment, wherein the dephosphorylation timing of Fin1^{WT} was compared to Fin1^{RxL-AAA} mutant in a Clb5^{Δdb} background (Fig. 5.3). Indeed, disruption of the RxL motif within Fin1 not only hastened its dephosphorylation, but also enabled complete catalysis of the protein, with its dephosphorylation profile being indistinguishable to that of the wild type protein.

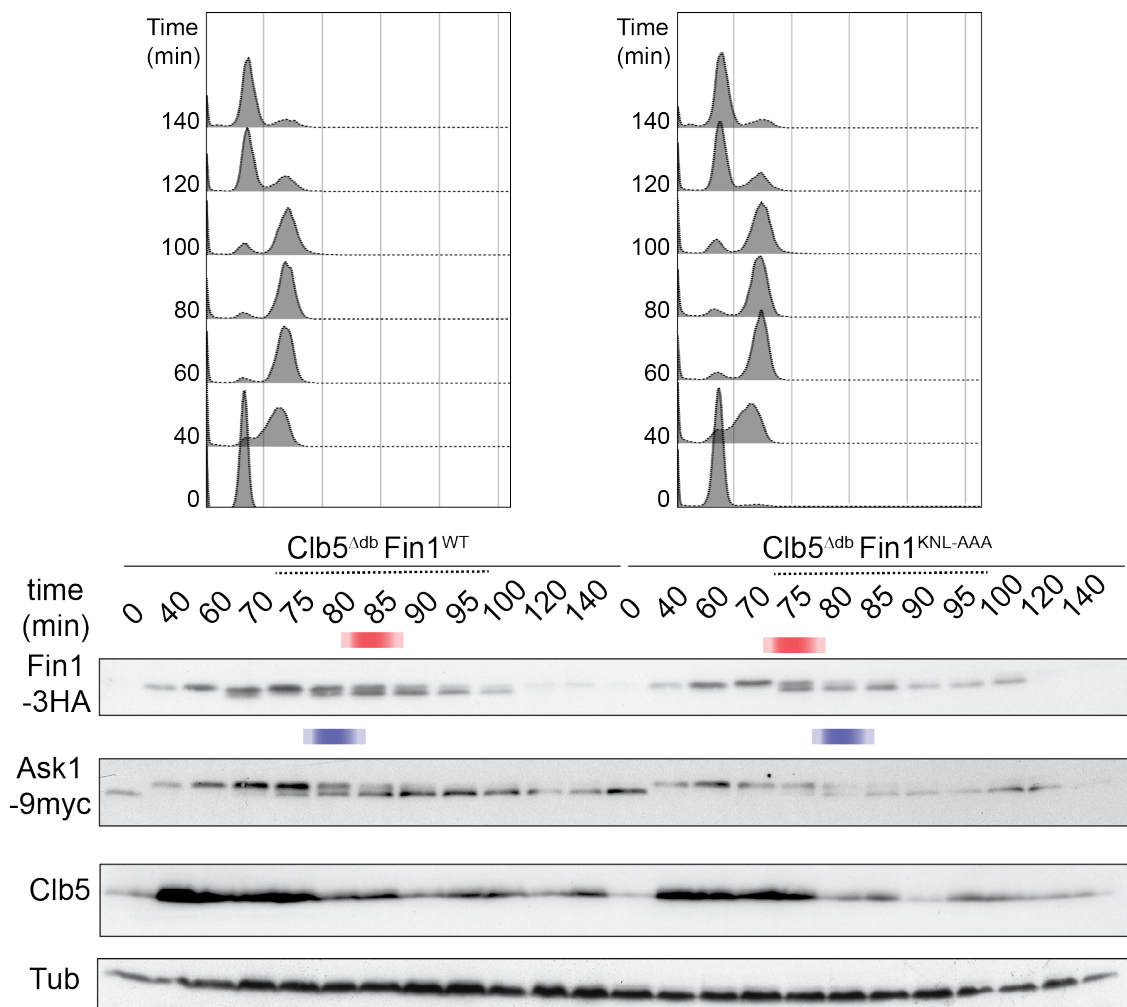


Figure 5.3 – Comparison of Fin1^{WT} and Fin1^{KNL-AAA} dephosphorylation in a Clb5^{Δdb} background.

FACS and western blots showing the progression through G1 to the next G1 and phosphorylation profiles of Fin1 and Ask1 in Clb5^{WT} and Clb5^{Δdb} strain backgrounds. Red and blue shaded boxes indicate dephosphorylation mid-points of proteins. In the Clb5^{Δdb} strain, mid-point of Fin1 dephosphorylation is 90 minutes post-release, whilst that of Ask1 is 85 minutes. Representative images from four independent experiments are shown.

These experiments support the conclusion that early degradation of Clb5 at least partially contributes to early dephosphorylation of Fin1 in a wild type setting. Nonetheless, this explains only part of the equation; Cdc14 is also able to discriminate this protein amongst others, and contribute to its efficient catalysis.

5.2 Fin1 causes a modest stimulation of Cdc14's phosphatase activity

In order to explain the high catalytic activity of Cdc14 towards Fin1, I examined the hypothesis discussed herein. Early in anaphase, a small amount of active Cdc14 is able to target Fin1 and bring about its dephosphorylation. One explanation of this behaviour could be that Fin1 is able to stimulate the phosphatase activity of Cdc14, in turn leading to its own dephosphorylation in an efficient manner. This is known to be the case for the dual-specificity phosphatase MAP kinase phosphatase-3 (MKP-3) and its substrate phospho-ERK2. Binding of phospho-ERK2 leads to an allosteric change in MKP-3, which causes its activation loop to close, making it catalysis-competent (Camps et al., 1998).

To test this hypothesis, I made use of purified Cdc14 and Fin1 in a *p*-NPP phosphatase assay. As described in section 2.4.3, *p*-NPP activity assays were performed with reactions containing 100 nM Cdc14 and varying amounts of (unphosphorylated) Fin1 added into the reaction mixture. Next, accumulation of the product due to substrate hydrolysis was measured after an incubation period (Fig. 5.4A). As a control, purified GST, which is a similarly-sized protein to Fin1, was added to separate reactions. Surprisingly, addition of small amounts of Fin1 led to greater phosphate hydrolysis by Cdc14, whereas addition of the same amounts of GST had no effect. Increasing the final concentration of Fin1 to high amounts did not cause further stimulation of the phosphatase in this end point assay.

To further study this effect, I used a continuous assay to determine the velocity of substrate hydrolysis by Cdc14 over time. Addition of Fin1 to these reactions caused a

dose-dependent increase in the velocity of product accumulation. As before, no further phosphatase stimulation was seen upon addition of Fin1 at a final concentration higher than 200 nM (Fig. 5.4B). Finally, addition of 800 nM of Fin1 alone exhibited no detectible substrate dephosphorylation, confirming that a contaminant phosphatase activity was not responsible for the effect.

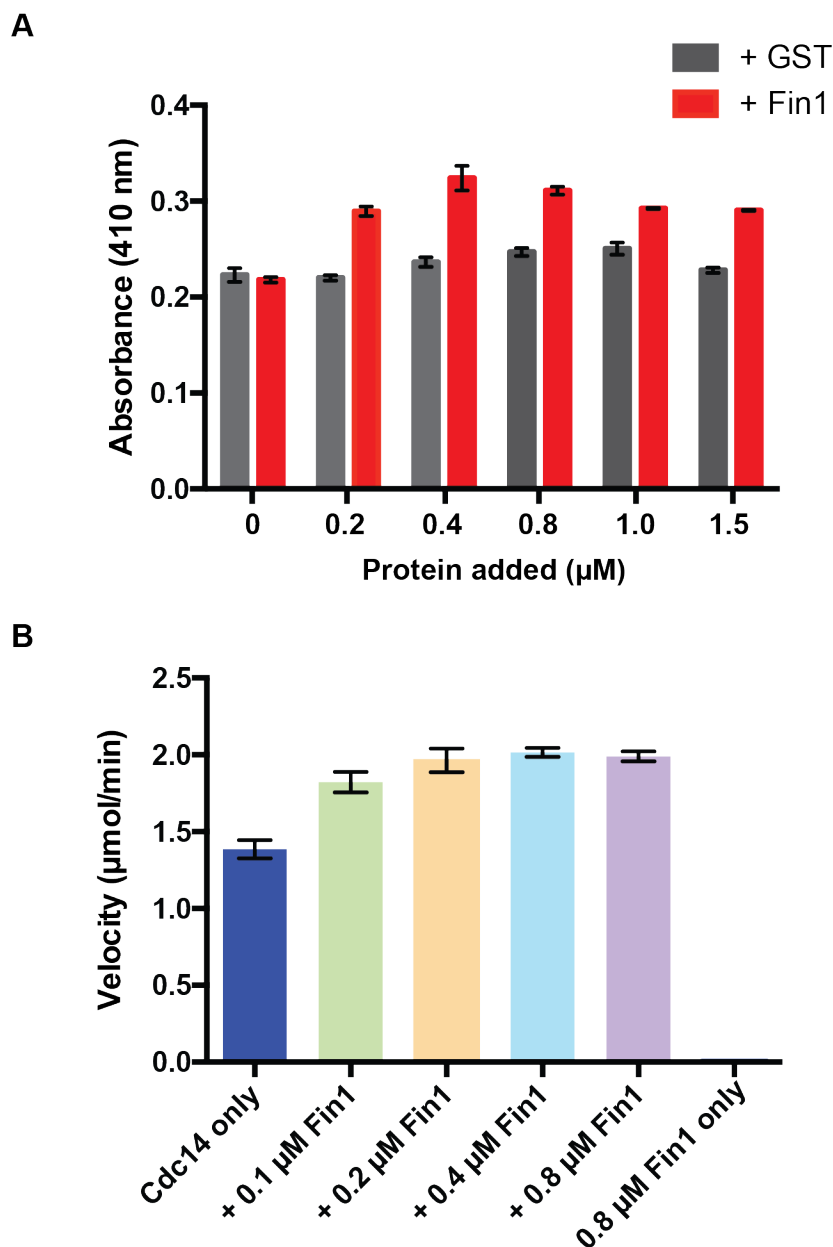


Figure 5.4 – Fin1 causes a moderate stimulation of the phosphatase activity of Cdc14 *in vitro*.

A. Addition of increasing amounts of Fin1 (0 – 1.5 μM) to *p*-NPP reactions containing 100 nM Cdc14. The reactions were incubated at 37 °C for 40 minutes after which they were stopped by addition of sodium hydroxide, and their absorbance was measured at 410 nm. **B.** Continuous spectrophotometric

(figure 5.4 continued) reactions containing 100 nM Cdc14 and increasing concentrations (0 – 0.8 μ M) of Fin1 were set up, and the absorbance at 410 nm monitored for an hour. All reactions were performed in triplicate, with the error bars indicating standard deviation from the mean.

From the experiments outlined above, one can conclude that whilst Fin1 stimulates the Cdc14 phosphatase activity, the effect is modest in comparison to the 30-fold stimulation of MKP-3 exhibited upon ERK2 binding. The crystal structure of hCdc14B revealed that Cdc14 is dephosphorylation competent even when not bound to a phosphosubstrate, unlike other dual-specificity phosphatases. Thus, Fin1 binding likely causes a small allosteric change within the enzyme leading to a small degree of enzyme activation.

5.3 Fin1 is a high affinity Cdc14 substrate

This part of project has been based on the observation that Cdc14's ability to pull-down its substrates positively correlates with its catalytic efficiency towards them, and that efficient pull-down of Fin1 by Cdc14 might explain the phosphatase's high catalytic efficiency towards it. This could be achieved by a possible docking site-mediated interaction increasing the local concentration of the phosphatase with respect to the substrate within the cell, overcoming competition by other substrates and lowering the K_m of the dephosphorylation reaction.

Previous observations that Fin1 interacts with the non-catalytic domain A of the protein, and that phosphosite mutants of Fin1, too, bind the protein with wild type efficiency pointed to the existence of phosphosite-independent interactions.

Qualitatively, interactions between Fin1 and Cdc14 are well defined. Next, we sought to assess them in a quantitative manner by determining the equilibrium dissociation constant (K_d) of the binding reaction between the two proteins.

Microscale thermophoresis (MST) is a technique that enables K_d measurements between two proteins in solution. Briefly, it tracks the changes in the hydration shell of a fluorescently labelled protein, and changes it incurs upon binding of a partner (Wienken et al., 2010). To a fixed amount of the fluorescently labelled protein, varying concentrations of the binding partner are added. Binding then causes changes in the hydration shell of the former. Next, a temperature gradient is applied, which leads to an increase in Brownian motion and movement of the fluorescent protein along this gradient. This movement varies depending on the hydration shell, and therefore, binding of the partnering protein, and can be measured by tracking the fluorescence.

As labelling Cdc14 with a fluorescent dye compromised its folding and stability, I constructed a plasmid containing full-length Cdc14 tagged with superfolder GFP. Comparison of phosphatase activities of purified GFP-Cdc14 and His₆-Cdc14 showed that the tag does not affect catalysis (Fig. 5.5A).

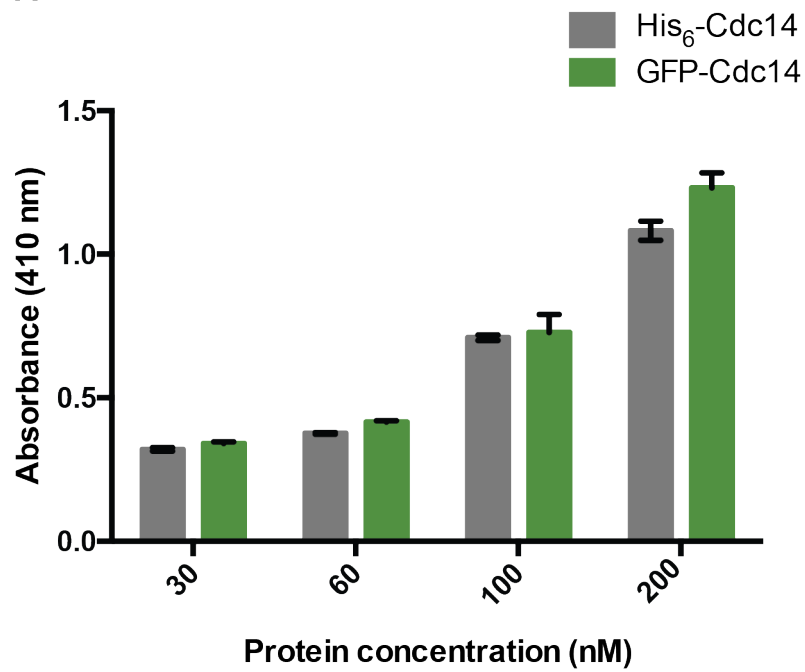
Binding of this fluorescent protein to a dilution series of purified Fin1 was then assessed using MST, yielding a K_d of about 700 nM (Fig. 5.5B). In contrast, purified Ask1, a poor Cdc14 substrate, exhibited a considerably higher K_d of at least 4.3 μ M. This value could not be accurately determined as binding could not be saturated even at high concentrations of Ask1. Neither Fin1 nor Ask1 exhibited detectible interactions with GFP alone.

Thus, in line with previous observations, Fin1 exhibits strong interactions to Cdc14.

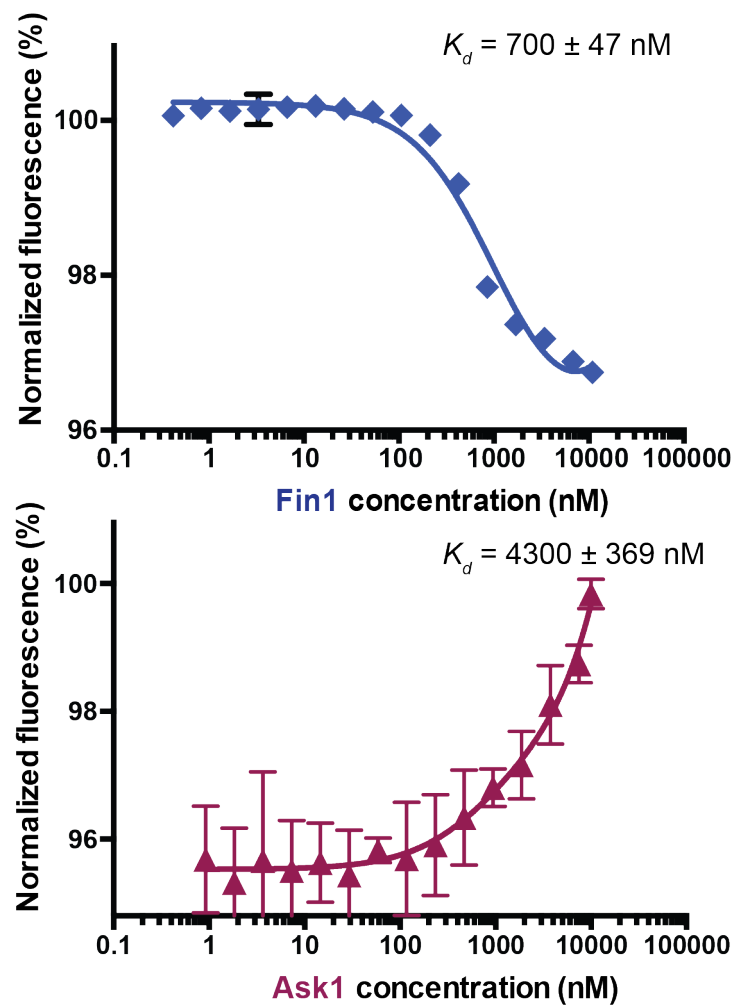
Figure 5.5 - Fin1 shows increased affinity to Cdc14 compared to Ask1.

A. Activities of hexahistidine- and GFP-tagged Cdc14 were compared in triplicate using varying amounts of the proteins in a *p*-NPP activity assay, which showed that the latter was equally competent at catalysis. Error bars indicate standard deviation from the mean. **B.** Interactions of Fin1 (blue) and Ask1 (magenta) with GFP-Cdc14 were analysed in triplicate with three independent protein preparations, with the error bars depicting standard deviation from the mean. The X-axis shows the fluorescence (expressed as a percentage of the maximum) in response to a temperature gradient in each reaction mixture.

A



B



5.4 Crosslinking and mass spectrometry identify extensive interactions between Cdc14 and Fin1

To further delineate the interactions between Fin1 and Cdc14, in search of a possible docking site, I decided to crosslink bound Fin1 and Cdc14 and identify the interaction sites via mass spectrometry. This methodology has been used extensively for a number of protein complexes (Chen et al., 2010). Further, it allows one to precisely identify interacting residues within natively folded proteins in solution.

The experiment relies on the ability of a primary amine-reactive crosslinker to covalently crosslink residues containing this functional group - lysines - that are in close proximity to each other. Subsequent protein digestion and identification by mass spectrometry detects the intra- or inter-molecular sites where they have been crosslinked.

Before performing the analysis, an optimal concentration of the hydrophilic crosslinker BS3 (Bissulfosuccinimidyl suberate) had to be determined. I purified Fin1 and Cdc14 in an appropriate buffer (using a buffering agent that lacks primary amines), and incubated them together with increasing amounts of the crosslinker. After quenching, the products were visualised on a protein gel (Fig. 5.6A). The proteins were also incubated separately so as to identify bands corresponding to self-crosslinks. A concentration of 0.25 mM BS3 was deemed appropriate for further analysis, as this led to appearance of visible inter-protein crosslinks, without the generation of highly complex, slower migrating species due to over-crosslinking.

Next, products from this reaction were subjected to mass spectrometric analysis. Figure 5.6B shows a visual representation of crosslinks detected with high confidence.

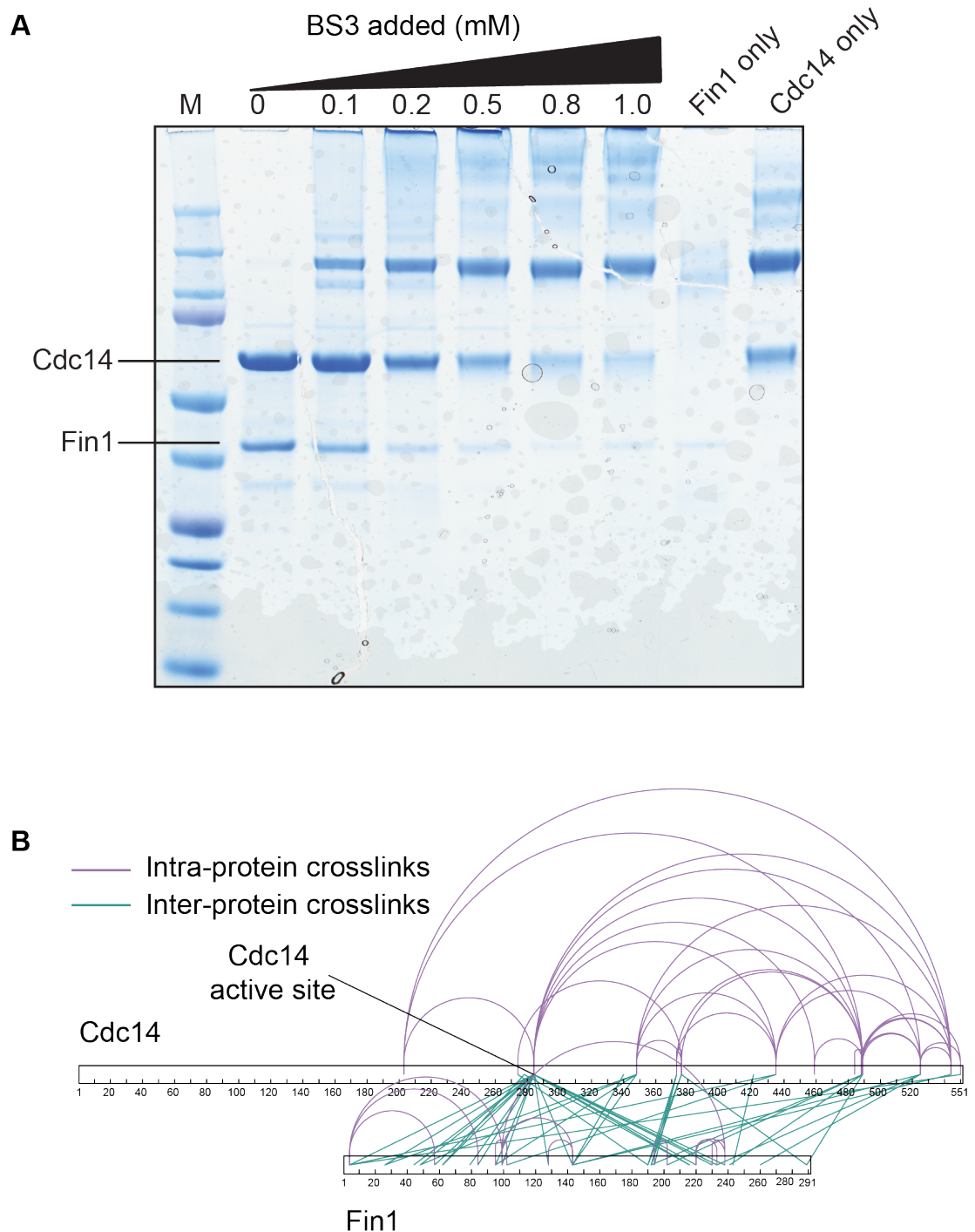


Figure 5.6 – Crosslinking and mass spectrometric analysis of Fin1 and Cdc14.

A. Cdc14, Fin1, and the indicated amount of BS3 were mixed together for 45 minutes in the dark at room temperature. After quenching with ammonium bicarbonate, the mixtures were subjected to SDS-PAGE and visualized by staining with InstantBlue. Fin1- and Cdc14-only reactions contained 0.5 mM BS3. **B.** A visual representation of all the inter- and intra-molecular crosslinks identified along the primary sequences of Fin1 and Cdc14. Cdc14 active site has been identified for reference.

Extensive crosslinking, both within each protein and with the partner is apparent; however, there is no enrichment of crosslinks within a particular motif in Fin1. This could be due to the fact that Fin1 has 32 lysines (>10% of the protein) all of which are equally distributed along the protein. If it interacts with Cdc14 in multiple conformations in a dynamic manner (a likely scenario considering Cdc14 must dephosphorylate six separate phosphosites distributed equally within the N-terminus of the protein), this would lead to a high number of crosslinks. Further, Fin1 is predicted to have few strongly structured parts; this flexibility in solution could also contribute to both self- and Cdc14 crosslinks.

Within Cdc14, the active site lysine, which is a part of the Cdc14 dual-specificity phosphatase consensus, by far exhibited the largest number of crosslinks with Fin1, indicating the solvent-exposed, flexible nature of this motif, as well as confirming that the active site contacts Fin1.

The C-terminal domain of Cdc14 also showed a number of self-crosslinks, and crosslinks to Fin1. However, considering that the purified Cdc14 domain C does not show detectable physical interactions with Fin1 in a pull-down assay, these are likely to be artefacts that have arisen due to the flexibility and lysine-richness of this domain. Domain A of Cdc14, however, did not exhibit any crosslinks to Fin1, despite its strong interaction with the latter protein in pull-down assays. As this domain is highly acidic, and contains almost no lysines, this observation is perhaps not surprising. Accordingly, similar crosslinking analysis performed with purified GST-tagged domain A and Fin1 did not lead to reliable identification of any inter-protein crosslinks, indicating that crosslinking and mass spectrometry is undemocratic.

Overall, whilst the two proteins crosslink efficiently, I was not able to gather any further insights into the molecular details of their interaction, especially of the strong biochemically observed interaction between the Cdc14 domain A and Fin1.

5.5 Cdc14 binds to a number of Fin1 peptides *in vitro*

5.5.1 Cdc14 interacts with preferred Cdk consensus sites within Fin1 in addition to other sequence features *in vitro*

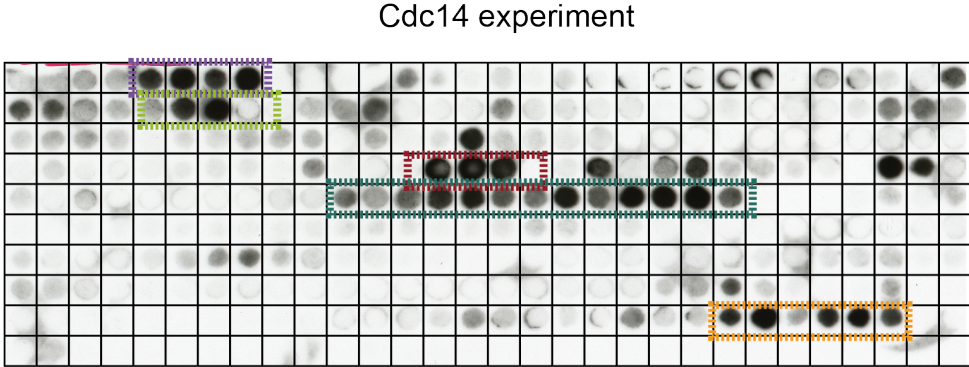
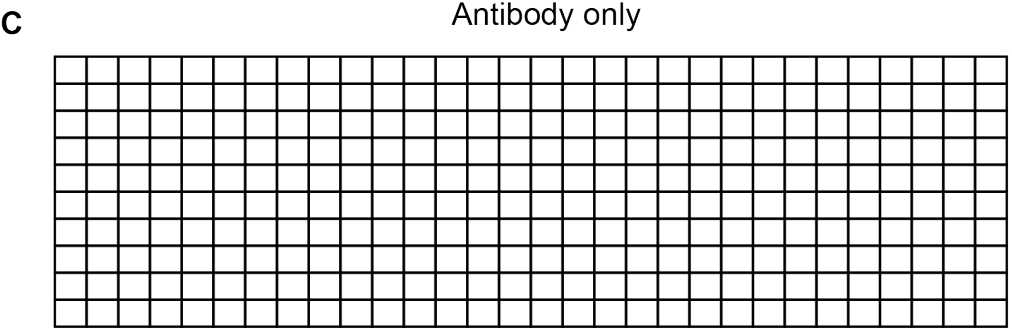
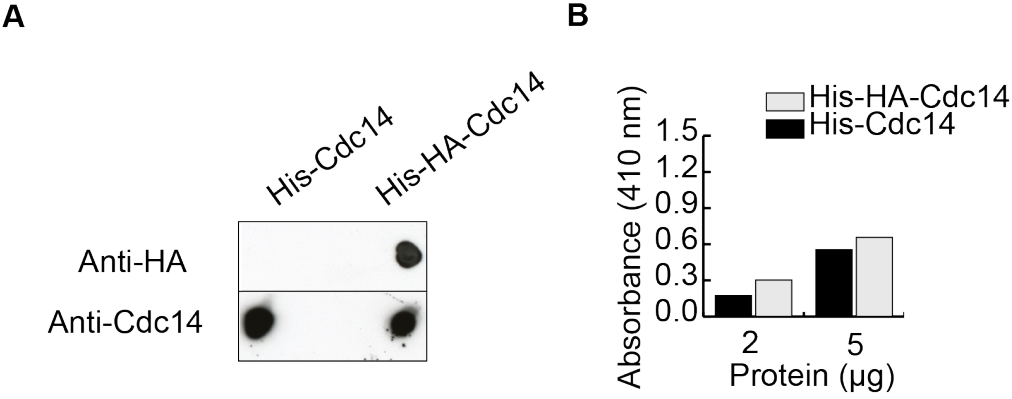
As an alternative approach, I sought to define the interaction sites of Cdc14 within Fin1 on a sequence level using a peptide array. Briefly, the technique can be thought of as a far-western blot, where a protein of interest is used to probe arrayed peptides derived from its binding partner. Binding is then detected using an antibody against the bound protein.

The peptide array consisted of 20-mer peptides derived from Fin1, with a successive shift of one amino acid, synthesized on a membrane support. For instance, if peptide 1 contains residues 1-20 from the N-terminus of Fin1, peptide 2 is composed of residues 2-21 and so on. This setup enables one to “walk” through the entire protein.

Purified His₆-HA-tagged Cdc14 was chosen to probe the array due to high background obtained from a histidine-specific antibody against His₆-Cdc14. The anti-HA antibody was specific for the HA tag (Fig. 5.7A). Further, presence of the tag did not interfere with the activity of the protein (Fig. 5.7B). The array was probed with either the anti-HA antibody alone as a control (Fig. 5.7C), or His-HA-Cdc14 first followed by the antibody to detect the bound protein. A number of peptide hits were detected upon latter analysis.

Figure 5.7 – Peptide array analysis reveals Cdc14-binding peptides within Fin1.

A. Dot blots showing that the anti-HA body is highly specific, detecting only His-HA-Cdc14. **B.** *p*-NPP assays showing that the two constructs have similar phosphatase activities. **C.** The peptide array was probed with the anti-HA antibody alone (top), or His-HA-Cdc14 first, followed by the antibody to detect the bound protein (bottom). Colour-coded sequences of Cdc14-interacting peptides within Fin1 are shown. Cdk consensus sites detected herein are shown in bold and have been underlined.



MSNKSMPRRSLRDIGNTIGRNNIPSDKDNV FVRLSM **SPLR**TTTSQKEFLKPPMR
ISPNKTDGMKHSIQVTPRRIMSPECLKGYVSKETQSLDRPQFKNSNKNVKIQ
NSDHTNIIFPT**SPT**KLTFSENKIGGDGSLTRIRARFKNGLM**SPER**IQQQQQ
HILP**S**DAKSNTDLCNTELDKAPFENDLPRAKLKGKNLLVELKKEEEDVNGI
ESLTKSNTKLNMLANEGKIHKASFQKSVKFKLPDNI VTEETVELKEIKDLLLQ
MLRRQREIESRLSNIELQLTE**PKHK***

Surprisingly, Cdc14 bound to four out of the six Cdk consensus sites within Fin1-derived peptides. All of these contained the 'full' Cdk consensus, SP-x-(K/R). The remaining two Cdk sites that Cdc14 did not bind to contained the minimal SP or a TP-x-R motif, which are expected to be poorer targets. Thus, *in vitro*, Cdc14 preferentially binds to its favoured motifs, even though they were not phosphorylated. This shows that the phosphatase shows distinct affinities for potential phosphosites.

In addition to the phosphosite, Cdc14 also bound to a number of other unique features within Fin1. To test their importance, the experiment was repeated by probing an array composed of these hits (Fig. 5.7C), where each residue had been sequentially mutated to a residue of different physico-chemical classes. However, no clear trend in binding requirements could be detected (data not shown).

5.5.2 Fin1 dephosphorylation timing *in vivo* is remarkably resilient to mutagenesis

To test the importance of these putative Fin1 binding sites in an *in vivo* setting, a mutational screen was set up. The mutations described herein were made in the context of the full-length protein. Five sequential amino acids were mutated at a time, walking through all the regions highlighted by the peptide arrays as possible interactors. The rationale behind this strategy was that if any of these hits contains sequence features that are important for the high affinity binding of Cdc14 to Fin1, it is possible that disrupting this interaction would lead to a considerable delay in the *in vivo* dephosphorylation timing of the mutant protein. This is analogous to the observations of Loog and Morgan (2005), where disruption of Fin1's RxL motif caused a defect in the overall phosphorylation of the protein during interphase, although this effect was not observed in my hands (Fig. 5.1).

Each peptide hit was divided into groups consisting of five residues each, which were then mutated into the following sequence within the full-length protein: G-A-G-N-G. This sequence of internal substitutions was chosen so as to ensure that the mutated part of the protein would be flexible, lack a specific physico-chemical character, and is less

likely to interfere with the folding of the rest of the protein. If the peptide hit consisted of residues at the very N- or C-terminus of Fin1, a terminal deletion of the residues was made. Overall, this strategy was chosen to avoid disrupting the structure (and function) of Fin1 with large internal mutations or deletions.

Next, following mutagenesis, each of these 22 Fin1 alleles was integrated into the genome, where it replaced the endogenous allele. A time course was conducted for each strain by arresting it in G1 using the pheromone α -factor, and releasing the cells to undergo the cell cycle synchronously. As before, the phosphorylation profile of Fin1 mutants was monitored by western blotting. Further, Ask1 was again chosen as an independent biochemical marker for anaphase, as it exhibits no known genetic interactions with Fin1, and its dephosphorylation timing is expected to be unaffected by perturbations in Fin1 abundance or dephosphorylation (as has also been shown in section 4.2). Table 5.1 summarizes all of the 22 mutants tested in this *in vivo* mutagenesis screen. Figure 5.8 shows a few examples of these G1-to-G1 experiments. A delay in Fin1 dephosphorylation should be visible as the mutant being dephosphorylated with kinetics similar to or later than those that of Ask1.

Number	Alias	Mutated residues	Residue position	Mutation
1	Mut A	Δ N27	1-27	Deletion
2	Mut B	KSVKF	238-242	GAGNG
3	Mut C	GGDGS	130-134	GAGNG
4	Mut D	LTRIR	135-139	GAGNG
5	Mut E	ARFKN	140-144	GAGNG
6	Mut F	GLMSP	145-149	GAGNG
7	Mut G	QQQQQ	153-158	GAGNG
8	Mut H	ERIQQ	150-154	GAGNG
9	Mut I	QHILP	155-159	GAGNG
10	Mut J	TPRRI	168-172	GAGNG
11	Mut K	QNSDH	104-108	GAGNG
12	Mut L	ITNII	109-113	GAGNG
13	Mut M	FPTSP	114-118	GAGNG
14	Mut N	TKLTF	119-124	GAGNG
15	Mut O	LTFSN	121-125	GAGNG
16	Mut P	SPLRT	36-40	GAGNG
17	Mut Q	TSQKE	41-45	GAGNG
18	Mut R	FLKPP	46-50	GAGNG
19	Mut S	MRISPN	51-55	GAGNG
20	Mut T	KEFLK	44-48	GAGNG
21	Mut U	SLDRP	88-92	GAGNG
22	Mut V	Δ C	263-291	Deletion

Table 5.1 - List of all Fin1 mutants tested for changes in *in vivo* dephosphorylation timing.

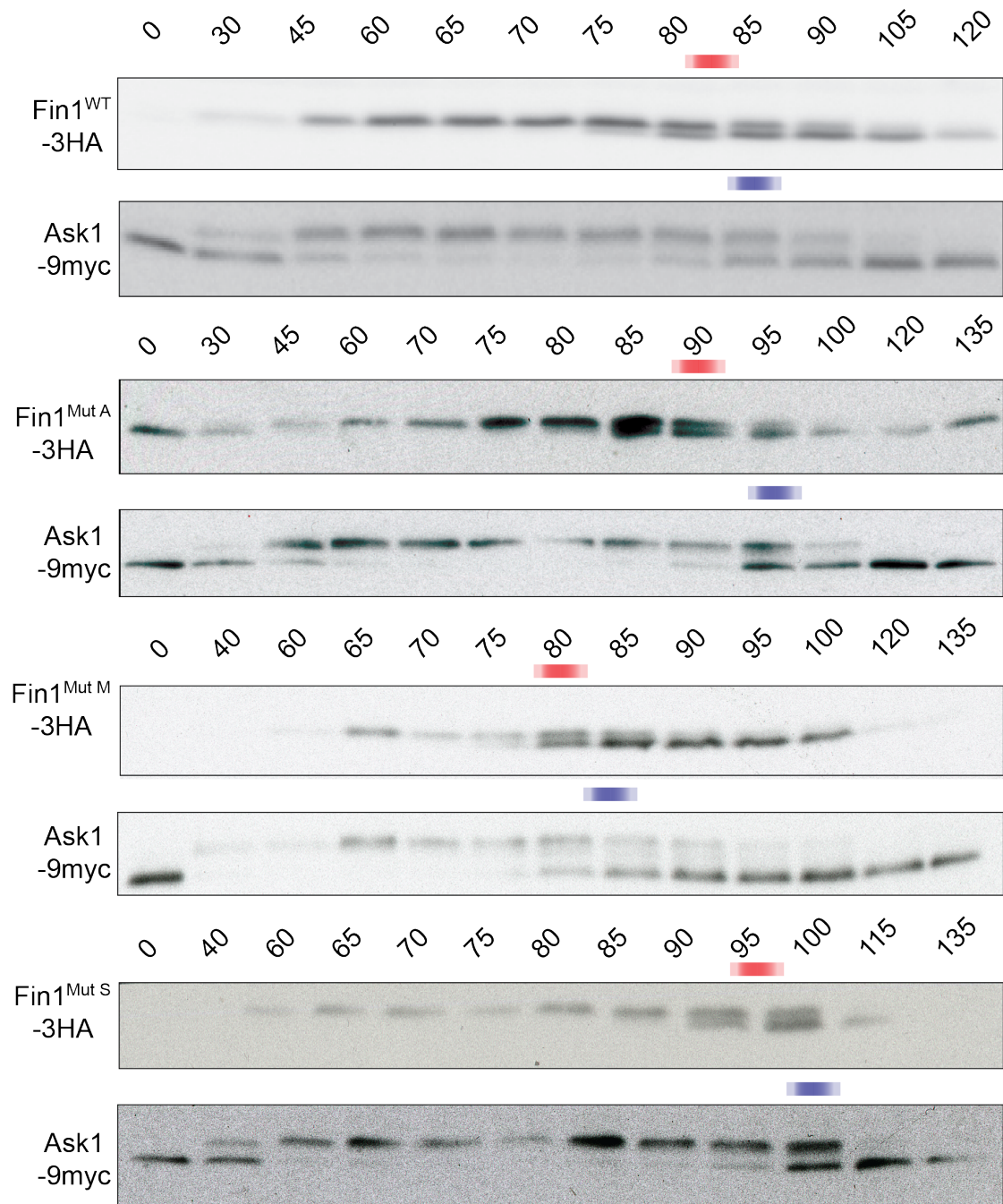


Figure 5.8 – Examples of time courses from the mutagenesis screen for Fin1 mutants with altered dephosphorylation timings.

Western blot profiles tracking phosphorylation and dephosphorylation of Fin1^{WT} and the indicated Fin1 mutants as the cells progress from G1 to the subsequent G1. Ask1 profiles have been used as independent biochemical markers for anaphase in each of the experiments. Red and blue shaded boxes show mid-points of dephosphorylation of protein.

Overall, barring a few changes in phosphorylation efficacy (data not shown), none of the mutations tested caused a defect in timing and extent of dephosphorylation of the protein compared to those of wild type. For instance, Fin1^{Mut A}, which contains an N-terminal deletion encompassing the D-box of the protein, led to its stabilisation. But, the mid-point of dephosphorylation upon anaphase entry was still earlier than that of Ask1.

One can conclude that firstly, Fin1 dephosphorylation is remarkably robust, and mutations over the entire protein do not cause a significant change in dephosphorylation. Secondly, it is possible that Fin1 and Cdc14 interactions are not coded in the primary sequence; instead, they might rely on the tertiary/quaternary structure of the natively folded protein which were not sufficiently disrupted by these mutations.

5.6 Binding of Fin1 to Cdc14 exerts a small effect on its efficient catalysis

The experiments so far indicate that whilst Fin1 and Cdc14 interact strongly and independently of the phosphosites of the former, the determinants of this interaction might not be encoded in the primary, peptide-level sequence of the protein. Alternatively, it is also possible that I was not able to identify the determinant if it exists.

Thus, I next wanted to examine the possibility that a larger part of the protein is important for efficient Cdc14 binding, and by extension, dephosphorylation.

5.6.1 Truncation analysis of Fin1

To directly test this hypothesis and narrow down Cdc14 interaction determinants within Fin1, I decided to perform a systematic truncation analysis of Fin1 in search of mutants that do not bind Cdc14. As a starting point, I divided the protein into three equal parts, and cloned and purified a truncation mutant of Fin1, called Fin1^{M1}, that

lacked the latter third of the protein, but possessed all potential phosphosites (Fig. 5.8). Fin1^{M1} failed to interact with glutathione-immobilized GST-Cdc14.

To further narrow down the interaction determinants, a series of truncation mutants was additionally cloned, Fin1^{M2} - Fin1^{M9} (Fig. 5.9), spanning the C-terminal domain of the protein that contains the two predicted coiled-coils thought to be important for self-association (Woodbury and Morgan, 2007). I then purified these nine proteins to homogeneity and tested their ability to interact with GST-Cdc14 as before. As expected, Fin1^{WT} interacted efficiently, though a number of mutants (including Fin1^{M1}) lost this interaction (Fig. 5.10). The ability to interact with Cdc14 followed a trend: if a large portion of the protein had been removed, it would not interact with Cdc14. If the same portion, however, was removed in smaller internal deletions, the protein showed robust Cdc14-binding ability. Furthermore, I observed another correlation: mutants that were dimeric like the wild type protein efficiently bound Cdc14, whilst those that were monomeric did not (as adjudged by elution volumes of purified proteins from a gel filtration column). This observation opens the possibility that dimerization of Fin1 is required to generate a strong interaction surface with Cdc14.

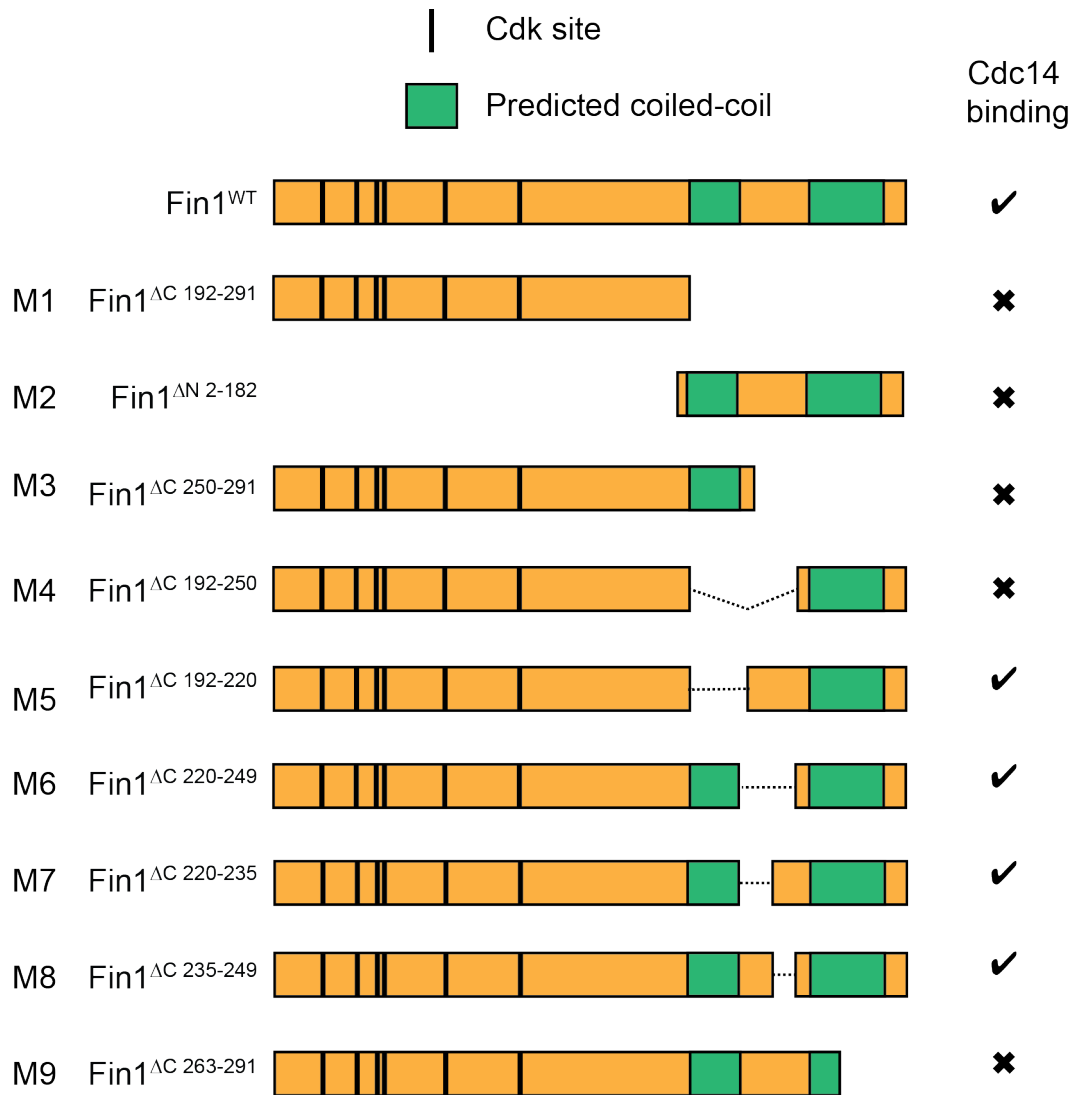


Figure 5.9 – Schematic depicting truncation mutants of Fin1.

Positions of Cdk consensus sites and coiled-coils, along with their Cdc14-binding abilities are indicated in all Fin1 mutants (M1 – M9).

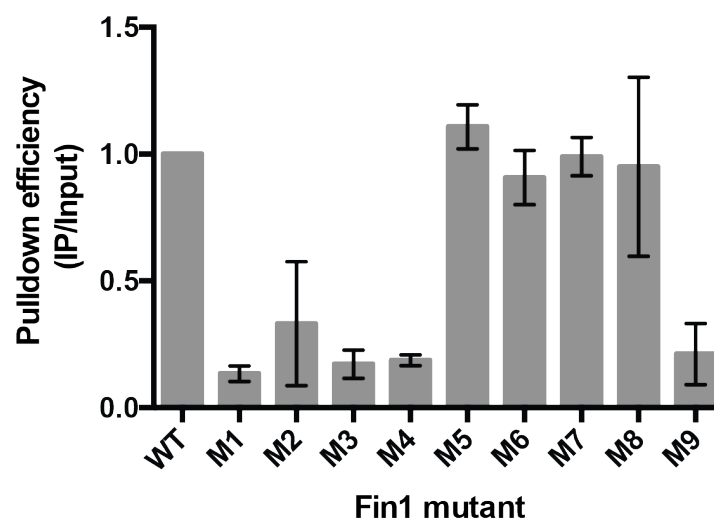
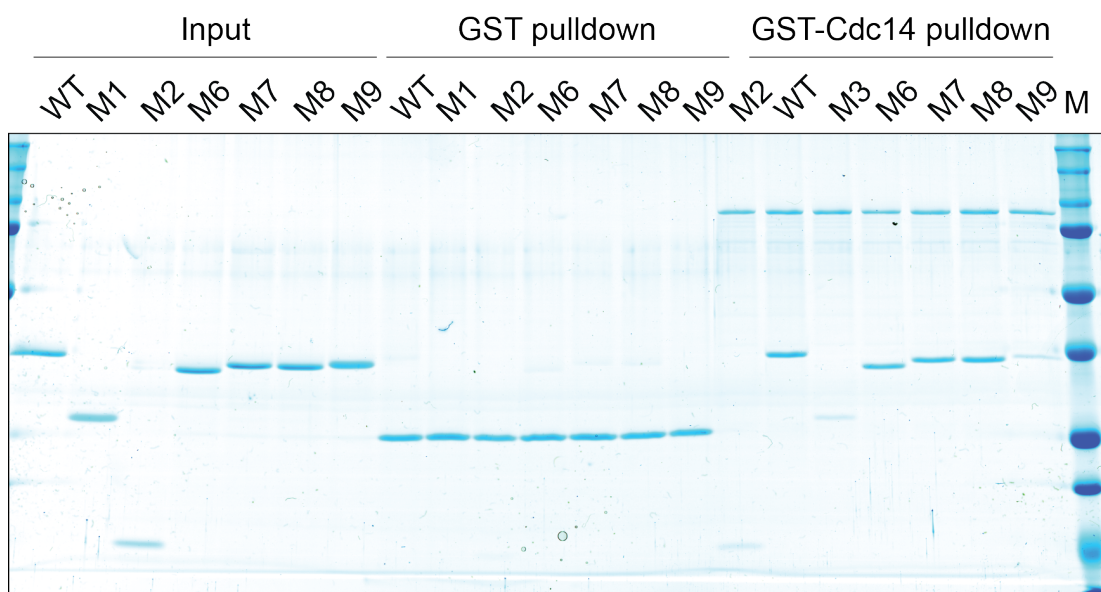
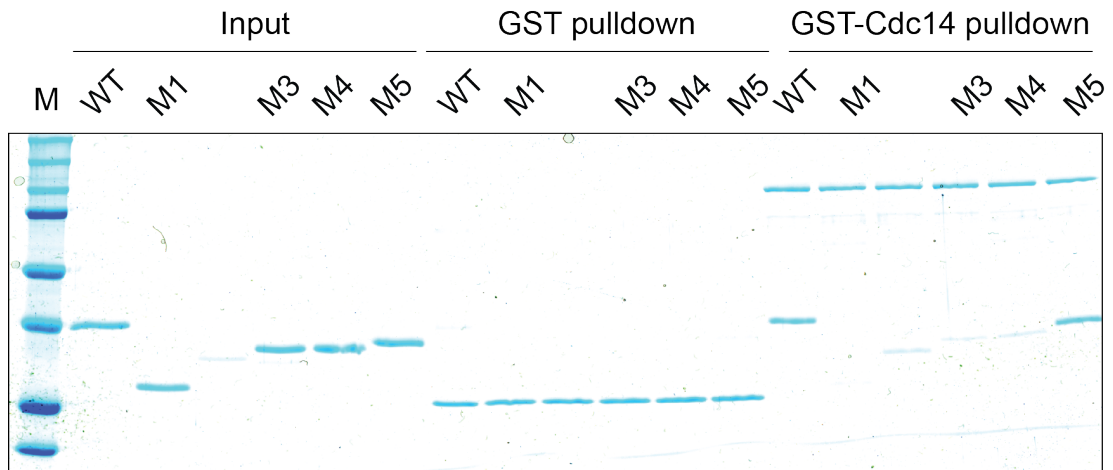


Figure 5.10 – Pull-down of Fin1 truncation mutants by immobilized GST-Cdc14

(Fig. 5.10 continued) The two representative SDS-PAGE gels (top) show the abilities of either GST alone, or GST-Cdc14 to interact with the purified Fin1 truncation mutants. The efficiency of pull-down (pull-down/input) was also quantified (bottom), with the error bars depicting standard deviation from the mean calculated from three independent experiments. The values were normalized to that of the wild type protein.

Whilst there are a number of possibilities that could explain this result, I favour the following: firstly, it is possible that the strong Cdc14 binding determinant is present not in the primary sequence of the C-terminal region of Fin1, but within the tertiary/quaternary, folded structure of the protein, as has also been indicated by previous experiments. It is also possible that efficient Cdc14 binding of Fin1, at least in the context of the pull-down experiments performed, requires dimerization of the protein, as is the case for Eph receptor tyrosine kinases and ephrins (Pabbisetty et al., 2007). The fact that Cdc14 itself is a dimer could mean that a dimeric substrate offers better recognition. It would be interesting to examine if other early, efficient Cdc14 substrates are also dimeric.

5.6.2 Cdc14 targets Fin1^{ΔC250} with reduced efficiency

Truncation analysis of Fin1 enabled me to answer the next question: if Fin1 loses its wild type binding efficiency to Cdc14, does it also experience a reduced catalytic efficiency? I chose the Cdc14 non-binder M3, Fin1^{ΔC250} for further *in vitro* analysis. Purified Fin1^{WT} or Fin1^{ΔC250} were first fully phosphorylated with 33 nM Clb2-Cdc28. A quantitative band-shift was observed for the two proteins upon phosphorylation, indicating complete phosphorylation.

The proteins were then incubated with catalytic amounts of Cdc14 (6.4 nM), with reaction aliquots taken every 15 seconds, to observe the dephosphorylation reaction. Quantifying the band intensities obtained with a phospho-specific antibody gave a measure of substrate dephosphorylation over time (for a full description, see section 2.4.2). The data obtained for the two proteins were fitted to an integrated form of the

Michaelis-Menten equation (Bouchoux and Uhlmann, 2011), yielding the catalytic efficiencies of Cdc14 towards the two proteins (Fig. 5.11).

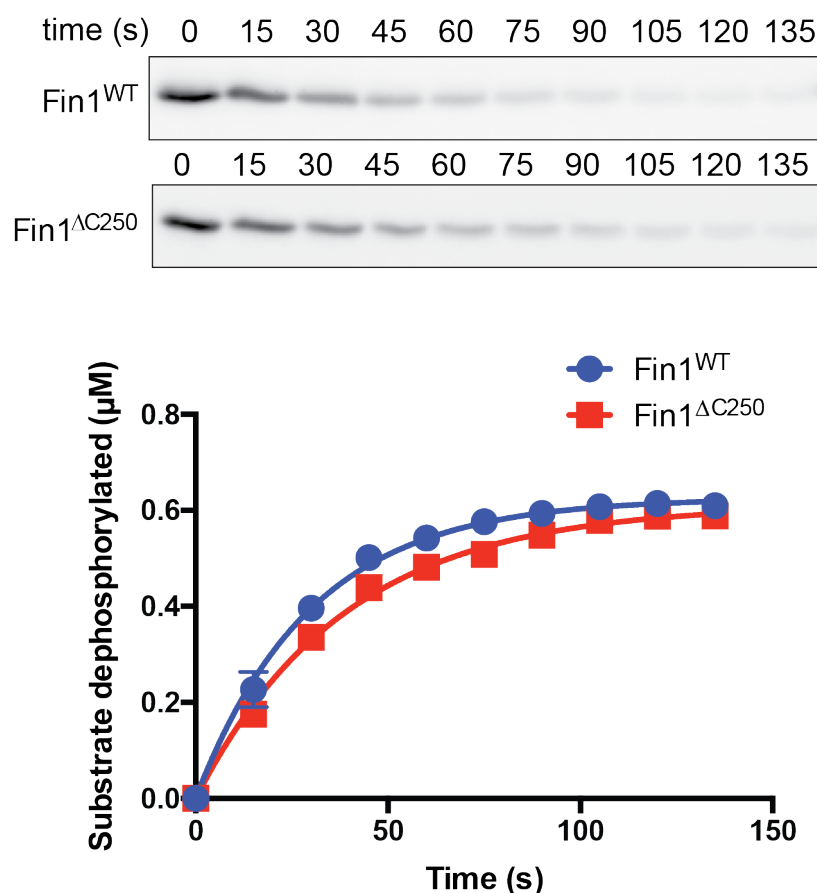


Figure 5.11 – Comparison of catalytic efficiencies of Cdc14 towards Fin1^{WT} and Fin1^{ΔC250}.

Fully phosphorylated proteins were incubated with 6.4 nM Cdc14 and reaction aliquots were taken at the indicated times (top panel). These were resolved using SDS-PAGE. Remaining phosphorylation was quantified at each point, and the data fitted to an integrated form of the Michaelis-Menten equation (bottom panel). The experiment was performed in duplicate, with the error bars indicating standard deviation from the mean.

Whilst Fin1 exhibited a catalytic efficiency of $5.21 (\pm 0.19) \times 10^6 \text{ M}^{-1} \text{ s}^{-1}$ (in close agreement with the previously calculated value of $5.39 (\pm 0.30) \times 10^6 \text{ M}^{-1} \text{ s}^{-1}$ (Bouchoux and Uhlmann, 2011), the value for Fin1^{ΔC250} was $4.03 (\pm 0.13) \times 10^6 \text{ M}^{-1} \text{ s}^{-1}$. Thus, there was a small dephosphorylation defect upon Fin1's loss of binding to Cdc14, but the value is not as low as that observed for other substrates such as Sli15 ($1.8 \pm 0.46 \times 10^6 \text{ M}^{-1} \text{ s}^{-1}$), which is dephosphorylated slightly later than Fin1 (Bouchoux and Uhlmann, 2011).

Thus, inability to bind Cdc14 causes a measurable dephosphorylation defect in Fin1. The magnitude of the defect however, is smaller than what would be expected if substrate interaction were the major determinant of catalytic efficiency.

5.6.3 Dephosphorylation timing of Fin1^{ΔC250} is same as that of the wild type protein

Following the *in vitro* analyses outlined above, I next wanted to ascertain the effect of Fin1^{ΔC250} mutation *in vivo*. As before, the endogenous allele was replaced with *Fin1*^{ΔC250}. Firstly, I wanted to establish whether Fin1^{ΔC250} loses interaction with Cdc14 *in vivo* too. To this end, Cdc14 was immunoprecipitated from asynchronous cells (Fig. 5.12). Whilst Fin1^{WT} was efficiently co-immunoprecipitated with Cdc14, Fin1^{ΔC250} remained undetectable, indicating that the loss of interaction observed *in vitro* could be recapitulated *in vivo* as well.

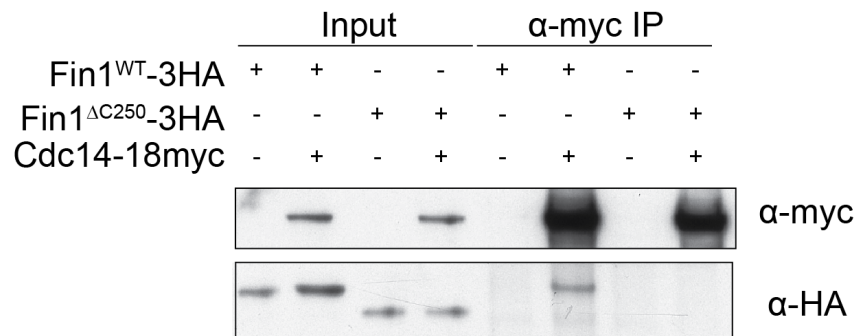


Figure 5.12 – Coimmunoprecipitation of Fin1^{WT} and Fin1^{ΔC250} with Cdc14. Endogenous Cdc14-18myc was immunoprecipitated from asynchronously growing cells containing HA-tagged Fin1^{WT} or Fin1^{ΔC250}.

Next, I sought to ascertain the dephosphorylation timing of Fin1^{ΔC250}. As the dephosphorylation defect one would expect is small, I chose to synchronize the cells in metaphase, by using a galactose-inducible Cdc20 background strain. Growing the cells in raffinose as the sole carbohydrate source turns off the galactose promoter and causes depletion of Cdc20, leading to metaphase accumulation of cells. They are then released synchronously into anaphase by addition of galactose. This method leads to excellent synchrony of cells during anaphase, making small differences easier to visualize.

Release from metaphase showed that both Fin1^{WT} and Fin1^{ΔC250} were completely dephosphorylated early within anaphase, with the mid-point of dephosphorylation being 15 minutes after release. In this instance, Orc6 was used as an independent marker of anaphase (Fig. 5.13). Degradation of Fin1^{ΔC250} appeared to be hastened during mitotic exit. However, a G1-to-G1 analysis did not show reduced stability of the protein during interphase (data not shown), perhaps indicating enhanced action of the APC on this protein during mitotic exit.

Nonetheless, the inability of Fin1 to bind to Cdc14 does not show a measurable dephosphorylation defect *in vivo*. This result is not entirely unexpected given the small dephosphorylation defect shown by the mutant *in vitro*. As temporal resolution in this experiment only extends to five-minute time points, should the defect be smaller than this window, it would not be observable. For instance, abrogation of the Cdc20-binding ABBA motif within Clb5 causes the cyclin's destruction to be delayed by 2 minutes *in vivo* (Lu et al., 2014). Overall, one can conclude that Cdc14 binding is not a major determinant of efficient Fin1 dephosphorylation.

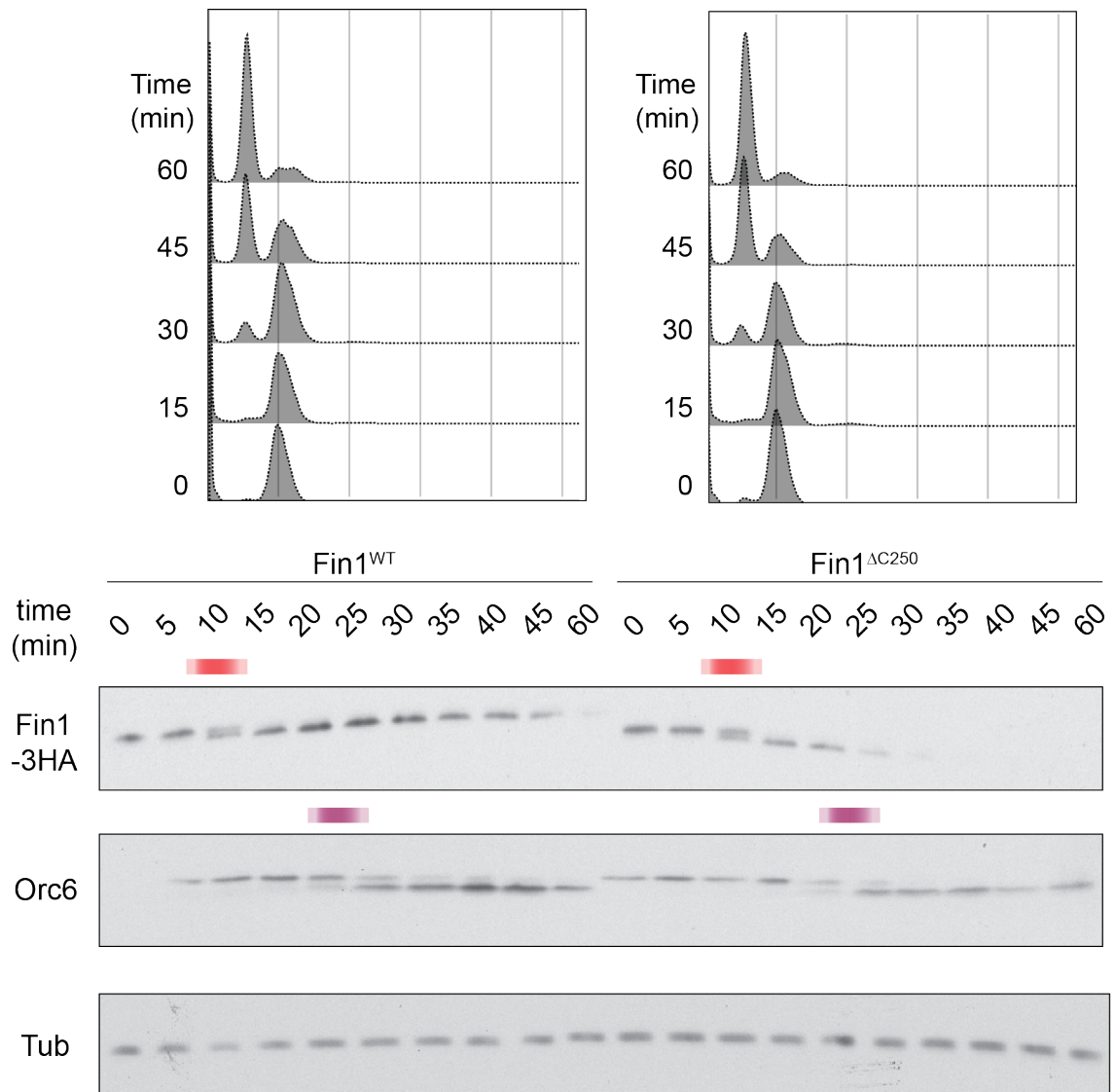


Figure 5.13 – Comparison of *in vivo* dephosphorylation of Fin1^{WT} and Fin1^{ΔC250}.

FACS and western blot profiles showing the progression through metaphase to the subsequent G1 of the two strains. Phosphorylation profiles of Fin1^{WT} and Fin1^{ΔC250}, along with Orc6 in both strains are depicted with the red and magenta shaded boxes showing mid-points of dephosphorylation of the two proteins, respectively. Tubulin (tub) has been used as a loading control. Representative blots from three independent experiments have been shown.

5.7 Probing Cdc14 - Fin1 interactions using Net1 as a tool

Although Fin1's binding to Cdc14 does not strongly impact its dephosphorylation, I next wondered if I could learn qualitative aspects of this enzyme-substrate interaction using Cdc14-Net1 interactions as a tool.

Net1 is a stoichiometric inhibitor of Cdc14, and is thought to not only tether Cdc14 in the nucleolus (Visintin, Hwang and Amon, 1999), but also restrict its phosphatase activity by a mode of competitive inhibition (Traverso et al., 2001b), until it is phosphorylated by various mitotic kinases.

Net1 is thought to occlude the Cdc14 active site (Traverso et al., 2001b); it also exhibits crucial interactions with the non-catalytic domain A of the phosphatase, as a dominant active point mutation (P116L) within the *CDC14*^{TAB-6} allele reduces its ability to bind to and be inhibited by Net1 (Shou et al., 2001).

Random mutagenesis of Cdc14 conducted by the Charbonneau group yielded additional point mutants, close to P116, that cluster within a single face of domain A (Fig. 5.14), away from the catalytic centre, and reduce its affinity for Net1 (Bremmer, 2009). These mutants lie at the 'back' of the phosphatase, on the opposite face as that occupied by the active site.

Thus, using Net1-Cdc14 interaction as a tool, I next wanted to examine the commonalities between the binding of Fin1 and Net1 to Cdc14. Is Net1 engaging in 'substrate-like' interactions with Cdc14?

All experiments discussed henceforth were repeated at least twice.

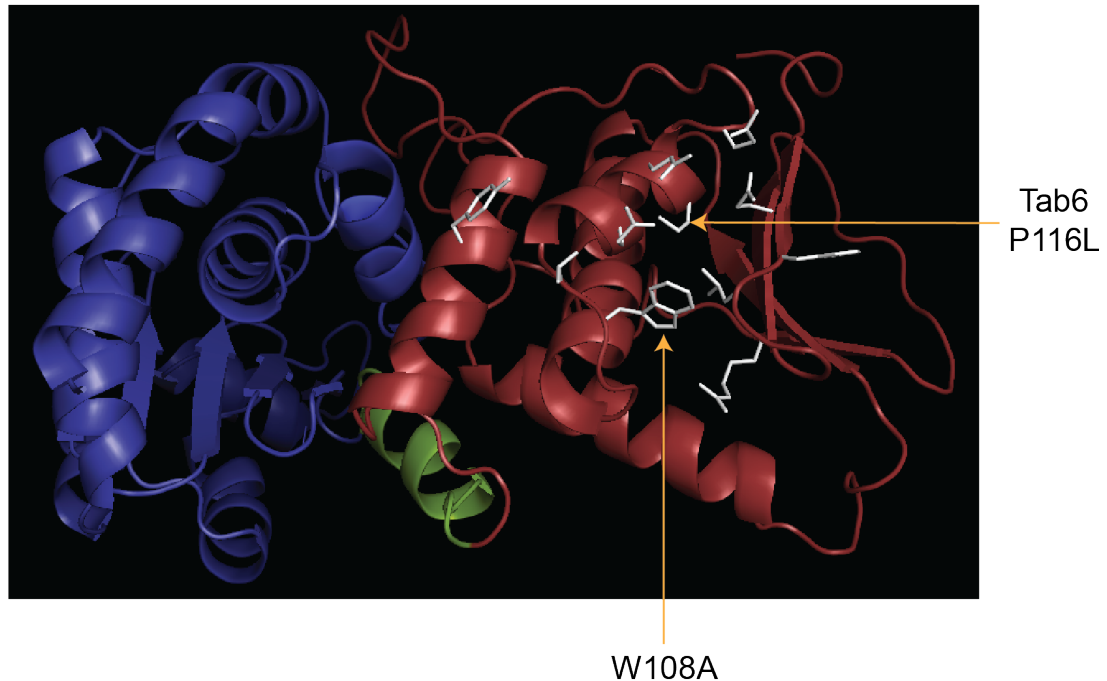


Figure 5.14 – Cdc14 point mutations that disrupt Net1 interaction.

A homology model of Cdc14 is depicted with domain A in red, the linker alpha helix in green, and domain B in blue. In stick representations are the point mutants identified by the Charbonneau group that greatly reduce binding to and inhibition by Net1 (Bremmer, 2009). Positions of Tab6 and W108A mutants are indicated.

5.7.1 Net1 and Fin1 can outcompete each other for binding to Cdc14

As Net1 is a large, 128 kDa protein which is challenging to purify, I decided to work with a smaller truncation, Net1¹⁻⁶⁰⁰, that has been shown to be necessary and sufficient for Cdc14 binding and inhibition (Traverso et al., 2001b).

Would Fin1 be able to compete with Net1 for binding to Cdc14? To answer this question, I immobilized GST-Cdc14 on glutathione beads, and bound Net1¹⁻⁶⁰⁰ to it. After washing, I incubated the pre-bound proteins with increasing amounts of either His₆-Fin1, or the similarly sized His₆-GFP, employed here as a control protein (Fig. 5.15A). Only Fin1 was able to efficiently evict Net1 from GST-Cdc14.

Further, could this competition work both ways – can Net1 also compete with Fin1 for Cdc14 binding? Increasing amounts of one protein were added in the presence of fixed

amounts of the other, in concentrations as indicated (Fig. 5.15B). This revealed that either protein could efficiently compete with the other for Cdc14 binding.

The fact that complete binding of one protein to Cdc14 precludes the binding of the other indicates that they possess overlapping binding sites, or that binding of one induces a conformational change within the phosphatase such that the other cannot bind.

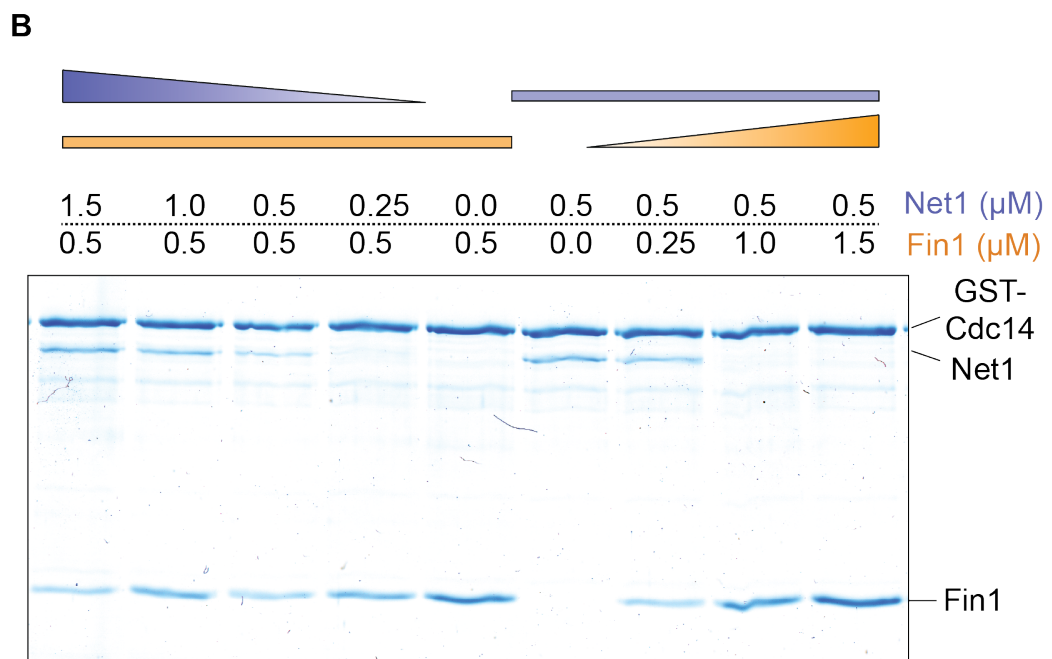
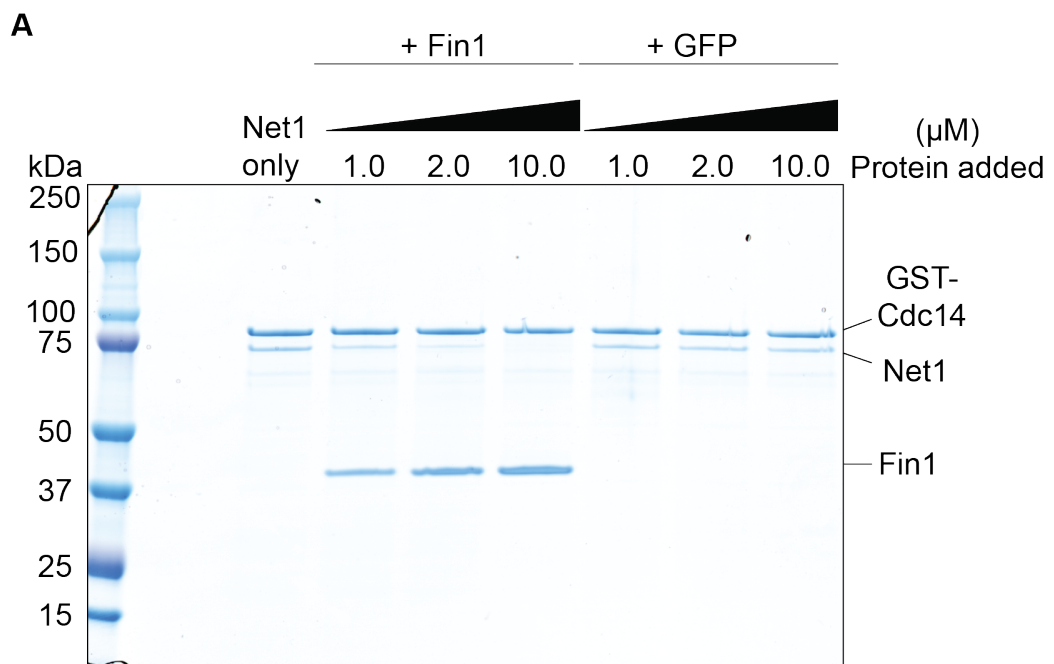
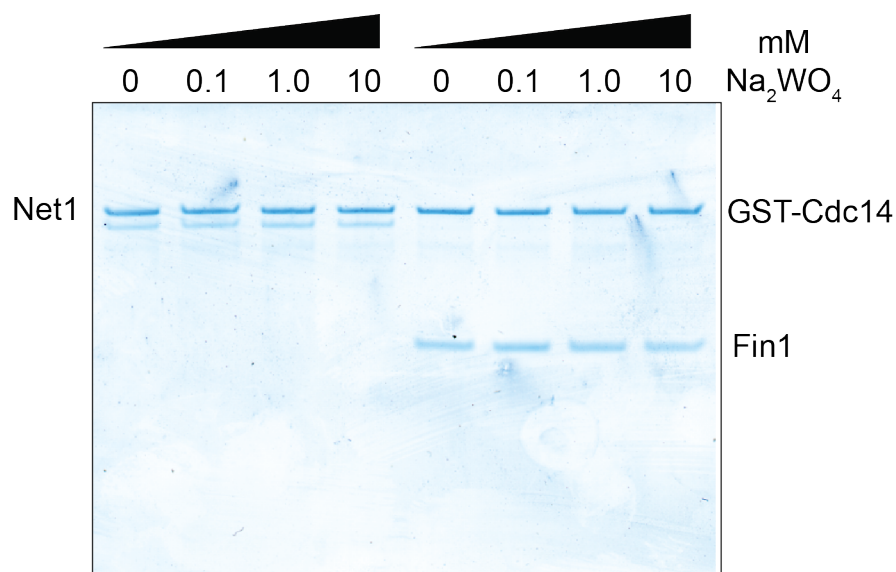


Figure 5.15 – Fin1 and Net1 can compete for binding to Cdc14.

A. To GST-Cdc14 – Net1¹⁻⁶⁰⁰ complex bound to glutathione beads, 1-10 μ M of Fin1 or GFP were added. After binding and washing, the beads were boiled in sample buffer, and the proteins visualized by SDS-PAGE and InstantBlue staining. **B.** As in A. GST-Cdc14 was immobilized on beads, and the indicated concentrations of Net1 and Fin1 were added together.

It is possible that the two proteins are competing for the active site of Cdc14. To address this question, I made use of the observation that tungstate (WO_4^{2-}), a phosphate mimic, can displace Net1¹⁻⁶⁰⁰ bound to Cdc14, presumably by competing with it for the active site (Traverso et al., 2001b). Increasing amounts of sodium tungstate were added to reactions containing fixed amounts of either Net1 or Fin1 (Fig 5.16). However, contrary to the published observations, Net1 displacement was not observed. Fin1, too, stayed put on Cdc14. Therefore, I cannot rule out this additional possibility of competition for the active site.

**Figure 5.16 – Tungstate ions do not compete with Net1 or Fin1 for binding to Cdc14.**

To glutathione beads-immobilized GST-Cdc14, 1 μ M of Net1 or Fin1 was added in the presence of 0-10 mM sodium tungstate ($\text{Na}_2\text{WO}_4^{2-}$). Even at high concentrations, tungstate ions could not prevent the proteins from binding to Cdc14.

5.7.2 Net1 and Fin1 share distinct, but overlapping binding sites within Cdc14

To further narrow down nature of interactions between these proteins, I asked if Net1, like Fin1, binds to the N-terminal domain A of Cdc14. This is a possibility as a number of Net1-disrupting mutations cluster within this domain of Cdc14 (Fig. 5.14). Pull-downs with GST-tagged Cdc14^{WT}, or its constituent domains revealed that only the wild type protein or Cdc14^{AB} were able to interact with Net1¹⁻⁶⁰⁰ (Fig. 5.17A). This implies that firstly, the C-terminal domain of Cdc14 is dispensable for Net1 interaction, and secondly, unlike for substrate Fin1 binding, domain A is not sufficient for efficient interaction with Net1. There might be further interaction sites on domain B that are necessary.

As mentioned earlier, the Cdc14^{Tab-6} mutation abrogates its binding to Net1. Is this the case for Fin1 as well? In addition to this point mutant, I chose Cdc14^{W108A} (Fig. 5.14) a mutant identified by the Charbonneau lab, that shows poor binding to and inhibition of Cdc14 (Bremmer, 2009).

Pull-downs with nickel-immobilized hexahistidine-tagged GFP (used as a control), Net1¹⁻⁶⁰⁰ or Fin1 revealed that whilst Net1 indeed does not bind to these mutant Cdc14 proteins, Fin1-binding was unperturbed (Fig. 5.17B).

Taken together, the above analyses reveal that Net1 and Fin1 indeed have commonalities in their mode of Cdc14 binding. However, they likely possess distinct, but overlapping binding sites.

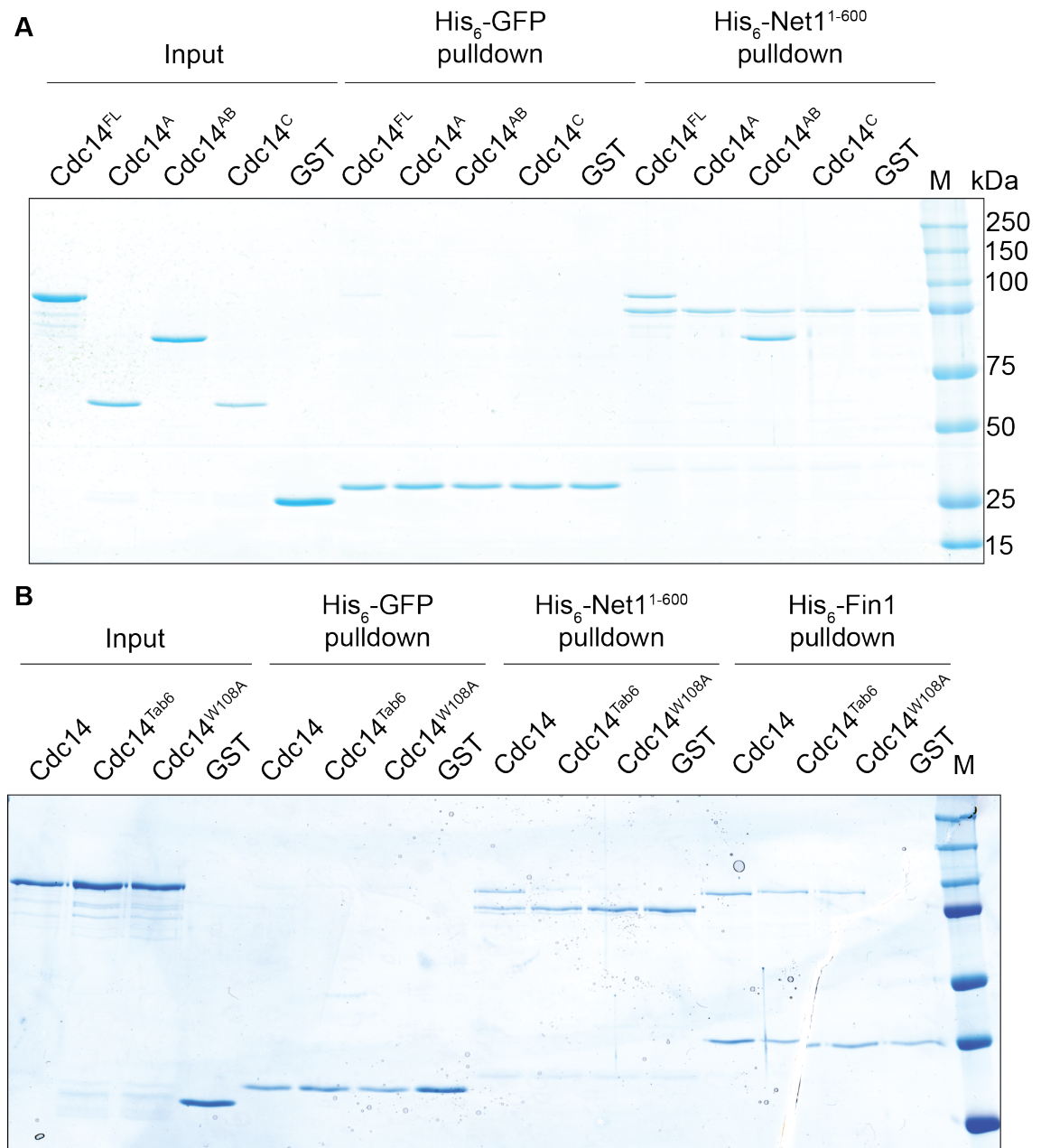


Figure 5.17 – Features of Fin1 and Net1 binding to Cdc14.

A. To nickel-immobilized Net1 or GFP, various Cdc14 constructs were added, and, following extensive washes, the bound proteins were visualized on stained SDS-PAGE gels. Only the full-length protein and domain AB interacted with Net1. **B.** As in A, GFP or Fin1 were first bound to nickel beads. The three Cdc14 constructs, or GST alone were added to the bound proteins. As before, binding was visualized on an SDS-PAGE gel. Fin1 was able to bind to all three Cdc14 alleles.

Chapter 6. Discussion and future perspectives

6.1 Biochemical properties of Cdc14

6.1.1 Cdc14 is a dimeric protein

Through a number of complementary techniques, I have established that Cdc14 exists as a dimer in solution. Further, the non-conserved domain C was found to be dispensable for dimerization. These measurements are unlikely to have arisen due to the *in vitro* nature of the analysis performed for the following reasons: glycerol gradient sedimentation and gel filtration were performed in a close-to-physiological ionic strength buffer, at a Cdc14 concentration in the low micromolar range - a setup reminiscent of the *in vivo* situation in the nucleus during anaphase (calculated from parameters in (Ghaemmaghami et al., 2003; Milo et al., 2009)). Thus, these *in vitro* conditions are unlikely to have driven spurious dimerization.

Crosslinking and mass spectrometric analysis also revealed a number of symmetric crosslinks between two Cdc14 molecules, supporting the hypothesis of Cdc14 dimerization in solution.

Further, both Cdc14^{WT} and Cdc14^{AB} could also dimerize in the presence of 500 mM NaCl. This could be due to the existence of strong electrostatic forces holding the dimerizing proteins together that are not disrupted by competition provided by ions high in the Hofmeister series. Alternatively, the dimers could also be held together by hydrophobic interactions that are enhanced due to the hydrophobic effect. The two possibilities are not mutually exclusive.

The fact that Cdc14 exists as a dimer is surprising considering that there is little functional requirement for dimerization. Extrapolating from the crystal structure of apo human Cdc14B, the catalytic Cys283 and general acid/base Asp253 are both primed for catalysis within the monomeric protein (Gray et al., 2003). Indeed, neither activation nor catalysis would need a dimeric Cdc14 protein. However, the observation

that the lethality of yeast *cdc14-1^{ts}* (a D323G substitution) can be rescued by introduction of a second protein – a catalytic site mutant of Cdc14 (C283S) (Taylor et al., 1997) suggests that perhaps swapping of some structural modules occurs upon dimerization of these two proteins. This dimerization in turn could lead to generation of a dephosphorylation-competent protein, although it is hard to envisage the mechanics structurally. This also begs the question: why did hCdc14B crystallized as a monomer? Whilst the contrary case of enforced multimerization within a crystal lattice (such as that of Cks1 (Bourne et al., 2000)) is more readily observed, it is possible that crystal contacts disrupt the dimer interface. Alternatively, it is also possible that dimerization of Cdc14 proteins has not been conserved in the evolutionary ladder between yeast and humans, as the proteins do exhibit some differences *in vitro*. For instance, the human protein does not exhibit Net1 binding (data not shown). Accordingly, no Net1 homolog has been found in humans.

6.1.2 Implications of Cdc14 dimerization

What could be the importance of Cdc14 dimerization? It is well understood that Cdc14 has a number of critical interactors throughout the cell cycle. Of them, Net1 is of chief importance, as it keeps its phosphatase activity in check via extensive physical interactions. It is possible that Cdc14 dimerization creates an interface that Net1 recognizes. Accordingly, truncation analyses of both Cdc14 (this thesis) and Net1 (Traverso et al., 2001b) have revealed that Net1 does not bind Cdc14 by a short, linear interaction motif, rather employing a web of extensive, structural interactions, of which dimerization could be a feature.

Further, I consider it highly likely that dimerization could serve to enhance dephosphorylation dynamics of substrates. This could occur as dimerization, in effect, increases the local concentration of the phosphatase with regards to a substrate. Even if one molecule is engaged with the target of catalysis, it obligatorily brings in a second. This is known to be the case for Hsp90, wherein N-terminal dimerization enhances ATP hydrolysis (Richter, Muschler, Hainzl and Buchner, 2001).

The true significance of these properties of Cdc14 will only be revealed by comparison of monomeric and dimeric forms of the phosphatase. To identify the molecular basis of dimerization of Cdc14, it would be useful to first establish if hCdc14B is also dimeric. Should this not be the case, one could scan for differences between the primary sequences of human and yeast proteins and test if insertions in the latter are involved in dimerization. Preliminary analysis based on gel filtration profile of purified hCdc14B indicates that it is monomeric (data not shown). Alternatively, one could also take an error-prone mutagenesis approach, scanning for Cdc14 mutations that effect the dimerization equilibrium without having a significant impact in a *p*-NPP assay, for instance.

Once a dimerization domain is identified, it would be interesting to directly compare activities of wild type Cdc14 and a monomerizing mutant. Additionally, titrating just the dimerization domain into an assay for catalysis of a substrate containing the wild type protein, and observing the effect on catalytic efficiency would be interesting. Titration of the inactive dimerization domain alone would, in effect, compete off wild type protein dimers, allowing one to observe impact of dimerization on catalytic parameters, or ascertain if it has subtler, allosteric effects on the enzyme.

6.2 What is the function of different Cdc14 domains?

Analysing the contribution of various Cdc14 domains towards substrate binding has further revealed that, like the full length protein, N-terminal domain A is competent in binding the substrates Fin1 and Sli15, but not the inhibitor Net1, which needs both domains A and B for efficient interactions.

As hypothesized previously in chapter 3, it is possible that domain A is engaging in ‘B-like’ interactions with substrates, as the two exhibit a similar overall structure. Alternatively, the nature of domain A-substrate interactions could be dissimilar to that of domain B-substrate interactions - it could also be recognizing features within substrate proteins independently of its similarity to domain B. Previous observations

that strongly binding substrates like Fin1 bind Cdc14 independently of their phosphorylation status, whilst the interaction of weak substrates is phosphorylation-dependent (Bouchoux and Uhlmann, 20011) make it possible that domain A interaction, unlike that of domain B, is phosphorylation independent. Consistent with this possibility, domain A lacks all the residues required for catalysis.

Mutations within domain A that disrupt its Fin1 interaction would be informative to understand its significance.

6.2.1 Binding of Net1 and Fin1 to Cdc14 is mutually exclusive

Pull-down experiments with Net1 have revealed a number of features of its interaction with Cdc14 and, that of Cdc14 and Fin1. First, as mentioned before, Net1 likely possesses an extensive web of interactions with Cdc14, encompassing both domains A and B. Truncating Cdc14 to a form that solely contains domain A perhaps increases the K_d of the interaction between Net1 and Fin1, leading to loss of binding between them at the concentrations used in the pull-down assay. Second, a number of Net1-disrupting interactions cluster in a single face of Cdc14, away from the latter's active site. This suggests that Net1 could act as an allosteric inhibitor of Cdc14, perhaps leading to subtle changes in the active site, although it is been suggested to be a competitive inhibitor previously (Traverso et al., 2001b). The mode of inhibition can be ascertained by the following. For instance, should full length Net1 binding lead to a change in the K_m of catalysis of a substrate (such as a peptide, *p*-NPP or DiFMUP), this would indicate a competitive mode of inhibition. Should the change be within both K_m and V_{max} , a non-competitive allosteric mode would be suggested. Does the protein directly occlude the active site of Cdc14? Competition experiments employing high concentrations of tungstate ions failed to show an effect on Net1 binding, as had been observed in other studies. Thus, I cannot rule out the possibility of Net1 occluding the active site of Cdc14, and that of a mixed mode of inhibition of the phosphatase by Net1.

The observation that Fin1 was able to displace Cdc14-bound Net1 indicates that the two share a considerable overlap within key Cdc14-binding features. This binding appears to be mutually exclusive as the inhibitor evicts bound substrate and vice versa.

The fact that Fin1 was found to stimulate Cdc14 activity, rather than inhibiting it like Net1, also suggests a distinct mode of binding. Intriguingly, this effect has also been observed upon Cdc14 binding of Tof2, a protein that is present in the same complex as Net1, and shows some sequence identity to the N-terminus of Net1. Instead of inhibiting Cdc14 activity, Tof2 stimulates it *in vitro* according to one report (Geil, Schwab and Seufert, 2008).

However, mutations in Cdc14 domain A, that appear to completely disrupt Cdc14-Net1 interactions have little appreciable effect on Fin1 binding to the phosphatase. Thus, this binding interface within domain A is not conserved between the two proteins.

6.2.2 Domain C is primarily a hub of regulatory input into Cdc14

Cdc14 domain C is highly variable between different species. Coupled with the fact that it exhibits little in the way of reliably predicted structural features, its function is likely to be mostly regulatory rather than catalytic. Consistent with this hypothesis, domain C harbours regulatory NLS and NES signals within a number of known orthologs of Cdc14 (Mocciaro and Schiebel, 2010).

Deletion of domain C caused a reduction in catalytic abilities of Cdc14 both *in vitro* and *in vivo*. In my interpretation, this could be due to altered protein folding. I suggest this due to the following reasons: first, domain C exhibits binding to none of the Cdc14 interactors tested so far. Second, the order of protein dephosphorylation is not altered when Cdc14^{AB} is the sole copy of the phosphatase within the cells. These observations indicate that qualitatively, domain C exerts little effect. The fact that substrate dephosphorylation occurs later within Cdc14^{AB} cells indicates that they must await an

increased amount of released Cdc14^{AB} for efficient substrate dephosphorylation, due to its reduced activity, reaffirming the quantitative model.

Two studies have shown that there is a NLS at the very C-terminus of domain C (Mohl et al., 2009; Kobayashi, Hirano and Matsuura, 2015). One would expect that, in its absence, the NES would predominate and lead to mislocalization of Cdc14. However, I observed no adverse effects of domain C deletion on Cdc14 localization. In the same vein, if the phosphatase were mislocalized and were within the cytoplasm inappropriately during interphase, as is the case in *net1Δ* cells, one might expect an increase in the length of interphase, as Cdc14 would directly oppose substrate phosphorylation by the kinase. However, this was not the case, as exhibited by nearly identical FACS profiles and appearance of cell cycle markers within the wild type and mutant strains. These observations indicate that there is probably another sequence acting as an NLS within Cdc14^{AB}. A prediction program predicted an NLS at the very C-terminus of Cdc14^{AB}, next to the NES (Kosugi, Hasebe, Tomita and Yanagawa, 2009), perhaps providing an explanation for these observations. Mohl et. al. (2009) only analysed NLS function by overexpressing the last 100 amino acids of Cdc14 fused to GFP. This construct does not include the NLS predicted within Cdc14^{AB}. Also, deletion of the last 100 residues only caused a minor effect in the localization of the wild type protein in this setup, with the majority of it going into the nucleolus.

6.3 Phosphosite composition of a substrate has a profound impact on phosphorylation/dephosphorylation equilibrium

6.3.1 Cdc14 is a serine-directed phosphatase

A number of *in vitro* and *in vivo* experiments have shown that phosphosite composition of substrates is, by far, the largest determinant of dephosphorylation efficiency by Cdc14, at least in the context of Fin1. Replacement of Fin1's phosphoserines to phosphothreonines led to a substantial defect in its dephosphorylation by Cdc14. However, at high concentrations, Cdc14 was able to

target this mutant variant. This suggests that whilst Cdc14 undoubtedly prefers to act on serine phosphorylations, phosphosite preferences are not all-or-none, but rather have some fluidity encoded in them. In a similar vein, even though conventional wisdom states that Cdk only targets Ser/Thr-Pro sites, there are reports of non-Ser/Thr-Pro phosphorylations as well (Suzuki et al., 2015).

In any case, a prediction of this phosphosite preference is that dephosphorylation events occurring early in anaphase (with little released Cdc14) would be enriched in serine dephosphorylations. However, phosphoproteomic analysis of substrates following Cdc14 overexpression revealed that some threonines are also dephosphorylated at this stage. Is there a ‘threonine-adaptor’ protein or a post-translational modification of Cdc14 can direct its activity towards phosphothreonines *in vivo*? Or, is it possible, that there is division of labour between Cdc14 and a second, threonine-specific phosphatase that is active during mitotic exit?

6.3.2 Which phosphatase dephosphorylates threonines *in vivo*?

Thus far, a tacit assumption in budding yeast mitotic exit has been that Cdc14 is the only phosphatase that brings about dephosphorylation of all Cdk substrates. In the light of previously mentioned observations, it is worth considering whether other phosphatases also collaborate with Cdc14, as there is a high occurrence of pTPs amongst dephosphorylated substrates. The fact that multiple phosphatases are active during mitotic exit is well appreciated in some higher eukaryotes.

Furthermore, Kuilman et. al. (2015) found that overall, disparate phosphosites within the same protein are co-ordinately dephosphorylated *in vivo*. Accordingly, the only TP site within Fin1, T68, is known to be dephosphorylated very early in anaphase (Kuilman et al., 2015), even though in an *in vitro* setting, Cdc14 targets it poorly (Bremmer et. al., 2012). It is possible that this second, threonine-specific phosphatase forms a complex with Cdc14 *in vivo*, targeting threonines and ensuring synchronized dephosphorylation of all phosphosites within a protein.

Within *S. cerevisiae*, PP2A-Cdc55 is a good candidate for a threonine-directed phosphatase. It exhibits specificity for threonine-containing peptides *in vitro* (Agostinis et al., 1990; 1992). My recent work with M. Godfrey in the lab indeed shows that a deletion of Cdc55 causes a marked increase in threonine phosphorylation during interphase. Mitotic exit, too, was found to be delayed in a *cdc55Δswe1Δ* strain compared to the *swe1Δ* control (Godfrey et al., in revision). In addition, another study found that phosphoproteins dephosphorylated early during an induced exit from mitosis in human cells are significantly enriched in threonine phosphosites. The phosphatase activity responsible for early threonine dephosphorylation was found to be sensitive to low concentrations of okadaic acid (McCloy et al., 2015), suggesting PP2A's hand in the process. Moreover, a recent proteomic study of induced mitotic exit in human cells found that PP2A-B55 dependent targets are significantly enriched in threonines (Cundell et al., 2016). The structural basis of vertebrate PP2A-B55 threonine specificity has been speculated about in a recent review (Rogers, McCloy, Watkins and Burgess, 2015). Thus, it would be interesting to investigate if PP2A-Cdc55 is indeed a threonine-specific phosphatase in budding yeast mitotic exit.

The activity of PP2A-Cdc55 is downregulated in a separase-dependent manner at the metaphase-to-anaphase transition due to a change in subcellular localization of Cdc55 (Queralt, Lehane, Novak and Uhlmann, 2006; Rossio and Yoshida, 2011). At some point later in mitotic exit, it is thought to be reactivated. Whilst the activity dynamics of Cdc14 are well known, our knowledge of PP2A-Cdc55 lags behind in this regard. Thus, a method of detecting active Cdc55 within the cells would be immensely useful as one could then start to further interrogate its requirement as to substrate dephosphorylation. A Cdk1-cyclin B-inspired biosensor (Gavet and Pines, 2010) for PP2A-Cdc55, based on a known PP2A- phosphosite (such as those within Net1) would be one possible approach, as it would lead to *in vivo* activity measurements. This would circumvent the problem of disruption of subcellular localization in cell lysis and immunoprecipitation-type activity assays that are routinely performed for other proteins.

6.3.3 Phosphosite preferences of Cdk can also influence substrate dephosphorylation

A recent study found that potential sites of phosphorylation within a peptide that contain SP motifs, followed by positive charges at the +3 position constitute some of the best Cdk substrates. Further, replacing the Ser with a Thr in this context caused a reduction in overall peptide phosphorylation. TP sites lacking any positive charges downstream, by far, constituted the worst Cdk sites (Suzuki et al., 2015).

Accordingly, my experiments with the Fin1^{6TPxA} mutant variant revealed that this protein was never fully phosphorylated by the kinase either *in vivo*, or within the conditions tested, *in vitro*. This experiment also exhibited the combinatorial effects of tinkering with kinase and phosphatase specificity, as although this mutant is poorly targeted by both the kinase and the phosphatase, it is dephosphorylated very early into anaphase, showing that there are many ways of achieving ‘earliness’ of dephosphorylation. This also indicates that, to an extent, kinase and phosphatase substrate specificities have co-evolved, as Cdc14 also disfavours TP sites that lack basic residues downstream. However, there are important differences between the two that can have a significant impact on phosphorylation dynamics of a substrate.

Taken together with related experiments, this also shows that whilst the kinase does not exhibit appreciable defects in targeting Fin1^{6TP}, further challenging it by mutating the +3 basic residues leads to severe impairment of catalysis. A larger scale analysis of whether TP sites in proteins tend to also contain a +3 K/R would be interesting. Additionally, expanding on previous discussion, it is known that the kinase phosphorylates thrice as many SP sites as TP sites within the proteome, even though the overall occurrence of both SPs and TPs is very similar. Whilst some of it is likely to come down to Cdk’s preferences, it is also possible that the extra methyl group of threonines makes them more hydrophobic and hence more likely to be buried in the interior of the protein, and hence inaccessible to the kinase. Thus, if possible, a survey

must also take into account whether a Cdk consensus peptide in question is indeed solvent accessible.

Finally, budding yeast contains the Cdk accessory subunit Cks1, which docks on to phosphorylated residues and makes further Cdk phosphorylation events highly processive (McGrath et al., 2013). Thus, it is also possible that a Cks1-mediated switch from distributive to processive phosphorylation could enable full phosphorylation of non-preferred sites *in vivo*.

6.3.4 Phosphosite-level knowledge of dephosphorylation reaction is needed

So far, dephosphorylation has primarily been described in the context of entire proteins, which often contain multiple phosphosites. The points discussed above have revealed that significant catalytic differences are likely to exist between phosphosites even within a protein. Thus, we need to move away from ‘population’-level approaches, to a more granular approach, taking into account the behaviour of each phosphosite. This would also help explain which phosphosites/structures within a protein regulate its behaviour.

Further, we know little about catalysis by phosphatases. Is it a processive reaction, such that dephosphorylation of one phosphosite makes dephosphorylation of others more likely? Or is it distributive, such that the phosphatase ‘sees’ each phosphosite separately? Whilst interpretations from mobility shifts upon protein dephosphorylation should be cautious, anaphase sees each substrate get dephosphorylated in a sharp time window *in vivo*, as opposed to a gradual, slow process, pointing to the former possibility. Furthermore, the fact that Cdc14 exists as a dimer could also contribute to processivity of dephosphorylation.

6.4 Phosphosite-independent factors in substrate dephosphorylation

6.4.1 The role of early degradation of Clb5 in substrate dephosphorylation

The theory behind early degradation of Clb5 enabling substrate dephosphorylation has been extensively discussed in sections 1.10.1 and 5.1. Although it had long been postulated, Clb5's role in defining early substrate dephosphorylation had not been examined directly and represented a gap in our knowledge. In this study, I took advantage of the fact that catalytic efficiencies of both Clb5 and Clb2 have been determined towards Fin1, and it was found to be a preferred Clb5 target. Thus, it was possible to tease out the contribution of Clb5 degradation to Fin1 dephosphorylation in anaphase by stabilizing the former protein. Stabilization of its preferred cyclin-Cdk flavour caused a defect in Fin1's *in vivo* dephosphorylation, an effect contingent upon the RxL motif found within the substrate. Taken together with the fact that the catalytic efficiency of Clb5-Cdk towards Fin1 is about 3.8 times that of Clb2-Cdk, the sum of these kinase activities perhaps overwhelms Cdc14 during early anaphase.

It is indeed likely that evolution has chosen early Clb5 degradation as yet another way of bringing about early substrate dephosphorylation – rather than tinkering with the phosphatase input, choosing to dampen efficient kinase input towards the same end. We still do not know how general this principle is, and how other early, Clb5-specific substrates respond to its stabilization. In this regard, dephosphorylation of Yen1 – another early Cdc14 substrate possessing one of the highest Clb5-specificity scores (Loog and Morgan, 2005) – would be interesting to observe.

However, concepts governing dephosphorylation timing appear to be very protein specific: even though Orc6, Sic1 and Cdh1 are highly Clb5-specific, they are dephosphorylated in late anaphase, perhaps due to the inability of the phosphatase to efficiently target them. Late dephosphorylation of Orc6, in particular, is important to

ensure that origin licensing only occurs later in mitosis, when the kinase activity has declined sufficiently so as to prevent inappropriate relicensing.

6.4.2 Role of Cdc14 docking site interactions in Fin1 dephosphorylation

Docking site interactions are a ubiquitous feature of cell cycle regulators and indeed, cellular regulation, with more such interactions being discovered each year. They enhance functional versatility within protein-protein interactions by bypassing the need for evolution of dedicated structural domains.

Their contribution in facilitating kinase-substrate interactions has been appreciated for decades; but we are only beginning to scratch the surface as to their role in phosphatase-mediated regulation. In this regard, two studies have recently discovered a short linear motif that mediates interactions of substrates with the B56 regulatory subunit of PP2A, and guides PP2A-B56 towards them (Hertz et al., 2016; Wang et al., 2016). This motif joins the rapidly growing repertoire already known for other phosphatases such as PP2B/calcineurin (Goldman et al., 2014).

In this thesis, we hypothesized that Cdc14, too, could function by interacting with at least a subset of its substrates using docking motifs. Fin1 was chosen as a candidate to investigate this premise for the following reasons: its dephosphorylation occurs very early into anaphase, the phosphatase displays high catalytic efficiency towards it, and it has the ability to proficiently interact with the phosphatase compared to other substrates.

In line with these observations, I found that Cdc14-Fin1 interaction was preserved even when the phosphatase is no longer catalytically proficient towards the protein due to phosphosite mutations within Fin1. Further, quantitative measurements of this interaction reveal that the phosphatase's affinity towards Fin1 is considerably higher than that of Ask1.

However, analysing truncation mutants of Fin1 revealed that, whilst certain features within the C-terminus of the protein are important for efficient interaction, abrogating the interaction has comparatively little impact on catalysis *in vitro* and on dephosphorylation timing *in vivo*. Further, all Cdc14 non-interactors were found to be monomeric. It is possible that this causes a reduction in binding to Cdc14 due to lack of self-association of Fin1, without directly playing a part in Cdc14 recognition. Should this be the case, binding motif(s) present elsewhere would still be able to play a part, albeit slightly less efficiently. I consider this possibility likely because deletion of the C-terminal coiled-coils of Fin1 reduce its ability to bind microtubules *in vitro*, even though the N-terminal domain is thought to encode microtubule-binding activity (Woodbury and Morgan, 2007). A similar principle is applicable to Fin1's binding to the 14-3-3 protein Bmh2 (Mayordomo and Sanz, 2002).

Similarly, peptide array analysis also indicated that the phosphatase interacts with a number of features within Fin1, in addition to a subset of its phosphosites. Again, sequentially mutating them *in vivo* did not change Fin1's dephosphorylation timing. It is possible that mutating five residues at a time did not sufficiently abrogate a potential docking site. Further, it is also conceivable that Fin1 contains multiple, degenerate docking motifs, and mutating one would not have a significant impact. Such multiple, composite binding motifs are thought to govern the interactions between PP1 and its regulators/substrates (Wakula et al., 2003).

Another possibility is that Fin1's interaction with Cdc14 is not a major determinant of its efficient catalysis, but plays another role within the cells. It could be a targeting interaction, serving to recruit Cdc14 to the spindle and spindle pole bodies at anaphase where the latter can dephosphorylate other substrates. Such a targeting mechanism would be a variation on a well-appreciated theme, wherein a protein serves as a recruitment platform for others, that are then able to act on its surrounding proteins in a timely manner: a case well documented for PCNA. PCNA drafts in number of proteins (such as the flap endonuclease Fen1) to the replication fork via their PCNA interaction protein (PIP) boxes (Mailand, Gibbs-Seymour and Bekker-Jensen, 2013).

On a more general note, my computational analysis of *in vivo* Cdc14 substrates shows that whilst phosphosite motifs that predict efficient dephosphorylation by Cdc14 (SP-x-K/R) are overrepresented amongst substrates, this enrichment is found in all classes of dephosphorylated proteins: from early to late. Thus, phosphosites alone would provide poor discrimination of distinct substrate classes, and perhaps cannot order substrate dephosphorylation by themselves. Thus, I still consider it likely that docking site interactions could play a part in defining the timing of Cdc14-mediated substrate dephosphorylation.

In this regard, crystal structures of the tight complex that Cdc14 forms with Net1 would be particularly informative, as the inhibitor does appear to share similarities with substrates. Thus, it is possible that binding site(s) within Net1 is of such high affinity that it converts it into an inhibitor.

6.5 From yeast to higher organisms

6.5.1 Substrate dephosphorylation in higher eukaryotes

Is there a temporal order of substrate dephosphorylation within higher eukaryotes too? Whilst few studies have examined this question in depth, a gradual, reproducible decrease in substrate dephosphorylation - examined biochemically - following mitotic exit induction has been noted by many. In agreement, a dose-dependent effect of cyclin B1 on human mitosis has also been observed, with constantly high cyclin B1 levels causing a metaphase arrest whilst constant low levels allowing progression to telophase, where the cells then arrest (Wolf et al., 2006). Furthermore, mitotic exit events too follow a reproducible order. Elongation of mitotic spindle, chromosome decondensation, nuclear envelope reformation and cytokinesis obey a seemingly predetermined, logical sequence and occur long after cyclins have been degraded. While regulation of mitotic ordering by sequential APC substrate degradation has received attention (Glutzer, Murray and Kirschner, 1991; Pflieger and Kirschner, 1992), the above mentioned observations strongly suggest that the quantitative model of

substrate dephosphorylation is likely also applicable in higher organisms. Recent evidence from human cells by Cundell and colleagues (2016) also bolsters this argument.

6.5.2 Role of phosphatases and future avenues

Relentless pace of progress in a number of model organisms has brought to light the importance of phosphatases in cell cycle regulation. A close partnership between kinases and phosphatases is indeed a defining feature of eukaryotic life. However, we have but scratched the surface of the input of phosphatases to cell cycle regulation and as such, their precise identities, activity dynamics, features and important targets still remain to be uncovered.

Recent studies have brought home the fact that, like their budding yeast counterpart, an exquisite level of control restrains phosphatase activity both spatially and temporally in the form of the conserved Greatwall - ENSA - PP2A pathway. Thus, our next frontier must constitute providing the crucial link between phosphatase activation, substrate dephosphorylation and cytological events. Overall, we must also integrate these observations into a systems-level view of cell cycle regulation.

Do PP2A phosphatases exhibit substrate preferences too? The evolutionarily conserved PP2A-B56 binding motifs and receptor sites (Hertz et al., 2016), and the threonine and +3 lysine/arginine preference of PP2A-B55 (McCloy et al., 2015; Cundell et al., 2016) do argue in favour of this hypothesis. Further delineating phosphatase docking sites and other phosphosite preferences will provide a deeper mechanistic understanding of their activity. These could also provide new vistas for targeting cancer cells, which must be equally, if not more, reliant on phosphatase action.

Finally, our description of the cell cycle has to shift from the realm of descriptive, qualitative events to a more quantitative understanding of the concepts involved, such as catalytic specificities and affinities of phosphatases towards their substrates, precise *in vivo* concentrations within different subcellular compartments of these proteins,

rates of changes in localization, etc., because it is the principles of chemistry and physics that ultimately control every aspect of cellular physiology.

Chapter 7. Appendix

7.1 Determination of stoichiometry and shape of Cdc14

7.1.1 Svedberg equation

Used in chapter 3, the following equation gives the Svedberg equation:

$$S = M(1 - v_2\rho)/Nof = M(1 - v_2\rho)/(No6\pi\eta R_s)$$

Here, M is the mass of the protein molecule in Dalton; N_o is Avogadro's number; v_2 is the partial specific volume of the protein (Erickson, 2009).

7.1.2 S_{max} formula

The S_{max} value for Cdc14 was calculated using the following formula:

$$S_{max} = 0.00361M_{2/3}$$

Here, M is the mass of the protein molecule in Dalton.

7.2 List of early phosphopeptides

Table 7.1 gives the list of phosphopeptides that disappears with 'early' timing (using data from (Kuilman et al., 2015)). The site of phosphorylation is followed by a lower-case 'p'

Systematic name	Phosphopeptide
YAR002W	GDSTPVQPDLSTpQK
YBL007C	NFTKSpSR
YFL007W	SpGRPSSSQGEIK
YHR182W	TSSTPTTpERPK

YJR083C	VTTpLKPK
YKR069W	LEDFETSSSpNKK
YLR190W	NAGSFQNLLNSpTK
YMR303C;YOL086C	GLVKSpIK
YOR051C	KSDEPSRESTpVR
YPL116W	SNASpEKELHENKPR
YAR002W	SNVVVAETSpEKK
YGL222C	KHSpPSSpSSTTTLGK
YAL035W	STPAATPAATPTpSSASPNNK
YBL103C	VRSpSSSFR
YBR007C	LFKSpR
YCR093W	RQTpLQSN
YDL164C	NKPTEGTPSpK
YDR130C	HSIQVTpR
YDR155C	KVESLGSpSGATK
YDR358W	VSLSSPKSpQENDTVVDILGDAHSK
YDR458C	MQIQEEKSpK
YDR466W	ASSEPSSpPPISR
YER059W	HESpSNESSLDK
YER093C	NITSSSpSTITNESSK
YER161C	KASpGATLR
YGL075C	YVYAHDTpSQNSR
YHR056C	SDSpDVPSMDQIR
YHR090C	SVTPVSpSIEK
YHR149C	SHGSpIHNNQLSR
YJL050W	NADTNVGDTPDHTQDKK
YJL065C	ETASAPLCSpK
YKL042W	VKPENNMSETFATPTpNNR
YKL062W	QATVSpNTR
YLR219W	TRSpELQDNLK
YML057W	TERPQSSTTPIDSK

YML093W	TAQSNNGNDDDEDASpQLK
YNR006W	ANSSpTTNIDHLK
YOL081W	NSDNVNSLNSSpK
YOR222W	GISSpMLMEAPK
YPR022C	ENDNDLSPNSSSSpAER

Table 7.1 – List of ‘early’ substrates used for the sequence logo in Fig. 4.1.

The table gives the systematic name of the protein along with the phosphopeptide sequence, with the phosphorylation site denoted with a lower-case p.

7.3 Michaelis-Menten equation

Kinetics of enzyme substrate catalysis discussed in the introduction are often best described by the Michaelis-Menten equation:

$$v = \frac{V_{max} [S]}{K_m + [S]}$$

Here, v refers to the velocity of substrate catalysis or product accumulation, V_{max} is the maximum velocity achieved by the system and K_m is the Michaelis constant, substrate concentration at which v is 50% of V_{max} .

Integrated form of the equation used in section 5.6.2 is:

$$[S^P](t) = [S^P]_0 \left(1 - e^{-\frac{k_{cat}}{K_m}[E_0]t}\right)$$

where, $[S^P]$ is the phosphosubstrate concentration at time t , $[S^P]_0$ is the phosphosubstrate concentration at time 0 (0.64 μ M), e is Euler’s number = 2.71828, E_0 is the enzyme concentration = 6.4 nM, and k_{cat}/K_m is the catalytic efficiency.

Reference List

- Adams, P.D., Sellers, W.R., Sharma, S.K., Wu, A.D., Nalin, C.M. and Kaelin, W.G., Jr, 1996. Identification of a cyclin-cdk2 recognition motif present in substrates and p21-like cyclin-dependent kinase inhibitors. *Molecular and Cellular Biology*, 16(12), pp.6623–6633.
- Agostinis, P., Derua, R., Sarno, S., Goris, J. and Merlevede, W., 1992. Specificity of the polycation-stimulated (type-2A) and ATP, Mg-dependent (type-1) protein phosphatases toward substrates phosphorylated by P34cdc2 kinase. *The FEBS Journal*, 205(1), pp.241–248.
- Agostinis, P., Goris, J., Pinna, L.A., Marchiori, F., Perich, J.W., Meyer, H.E. and Merlevede, W., 1990. Synthetic peptides as model substrates for the study of the specificity of the polycation-stimulated protein phosphatases. *The FEBS Journal*, 189(2), pp.235–241.
- Akiyoshi, B. and Biggins, S., 2010. Cdc14-Dependent Dephosphorylation of a Kinetochores Protein Prior to Anaphase in *Saccharomyces cerevisiae*. *Genetics*, 186(4), pp.1487–1491.
- Akiyoshi, B., Nelson, C.R., Ranish, J.A. and Biggins, S., 2009. Quantitative proteomic analysis of purified yeast kinetochores identifies a PP1 regulatory subunit. *Genes & Development*, 23(24), pp.2887–2899.
- Archambault, V., Chang, E.J., Drapkin, B.J., Cross, F.R., Chait, B.T. and Rout, M.P., 2004. Targeted Proteomic Study of the Cyclin-Cdk Module. *Molecular Cell*, 14(6), pp.699–711.
- Asakawa, K., Yoshida, S., Otake, F. and Toh-e, A., 2001. A Novel Functional Domain of Cdc15 Kinase Is Required for Its Interaction With Tem1 GTPase in *Saccharomyces cerevisiae*. *Genetics*, 157(4), pp.1437–1450.
- Azzam, R., 2004. Phosphorylation by Cyclin B-Cdk Underlies Release of Mitotic Exit Activator Cdc14 from the Nucleolus. *Science*, 305(5683), pp.516–519.
- Bardin, A.J., Boselli, M.G. and Amon, A., 2003. Mitotic Exit Regulation through Distinct Domains within the Protein Kinase Cdc15. *Molecular and Cellular Biology*, 23(14), pp.5018–5030.
- Bardin, A.J., Visintin, R. and Amon, A., 2000. A Mechanism for Coupling Exit from Mitosis to Partitioning of the Nucleus. *Cell*, 102(1), pp.21–31.
- Bardwell, A.J., Flatauer, L.J., Matsukuma, K., Thorner, J. and Bardwell, L., 2001. A Conserved Docking Site in MEKs Mediates High-affinity Binding to MAP Kinases and Cooperates with a Scaffold Protein to Enhance Signal Transmission. *Journal of*

Biological Chemistry, 276(13), pp.10374–10386.

Baro, B., Rodriguez-Rodriguez, J.-A., Calabria, I., Hernandez, M.L., Gil, C. and Queralt, E., 2013. Dual Regulation of the Mitotic Exit Network (MEN) by PP2A-Cdc55 Phosphatase. *PLoS Genetics*, 9(12), p.e1003966.

Barral, Y., Jentsch, S. and Mann, C., 1995. G1 cyclin turnover and nutrient uptake are controlled by a common pathway in yeast. *Genes & Development*, 9(4), pp.399–409.

Bembenek, J., Kang, J., Kurischko, C., Li, B., Raab, J.R., Belanger, K.D., Luca, F.C. and Yu, H., 2014. Crm1-Mediated Nuclear Export of Cdc14 is Required for the Completion of Cytokinesis in Budding Yeast. *Cell Cycle*, 4(7), pp.961–971.

Berdougo, E., Nachury, M.V., Jackson, P.K. and Jallepalli, P.V., 2014. The nucleolar phosphatase Cdc14Bis dispensable for chromosome segregation and mitotic exit in human cells. *Cell Cycle*, 7(9), pp.1184–1190.

Bernal, M., Zhurinsky, J., Iglesias-Romero, A.B., Sanchez-Romero, M.A., Flor-Parra, I., Tomas-Gallardo, L., Perez-Pulido, A.J., Jimenez, J. and Daga, R.R., 2014. Proteome-wide search for PP2A substrates in fission yeast. *PROTEOMICS*, 14(11), pp.1367–1380.

Bhaduri, S. and Pryciak, P.M., 2011. Cyclin-Specific Docking Motifs Promote Phosphorylation of Yeast Signaling Proteins by G1/S Cdk Complexes. *Current Biology*, 21(19), pp.1615–1623.

Bhaduri, S., Valk, E., Winters, M.J., Gruessner, B., Loog, M. and Pryciak, P.M., 2015. A Docking Interface in the Cyclin Cln2 Promotes Multi-site Phosphorylation of Substrates and Timely Cell-Cycle Entry. *Current Biology*, 25(3), pp.316–325.

Bloom, J. and Cross, F.R., 2007a. Multiple levels of cyclin specificity in cell-cycle control. *Nature Reviews Molecular Cell Biology*, 8(2), pp.149–160.

Bloom, J. and Cross, F.R., 2007b. Novel Role for Cdc14 Sequestration: Cdc14 Dephosphorylates Factors That Promote DNA Replication. *Molecular and Cellular Biology*, 27(3), pp.842–853.

Bloom, J., Cristea, I.M., Procko, A.L., Lubkov, V., Chait, B.T., Snyder, M. and Cross, F.R., 2011. Global Analysis of Cdc14 Phosphatase Reveals Diverse Roles in Mitotic Processes. *Journal of Biological Chemistry*, 286(7), pp.5434–5445.

Bokros, M., Gravenmier, C., Jin, F., Richmond, D. and Wang, Y., 2016. Fin1-PP1 Helps Clear Spindle Assembly Checkpoint Protein Bub1 from Kinetochores in Anaphase. *Cell Reports*, 0(0).

Bouchoux, C. and Uhlmann, F., 2011. A Quantitative Model for Ordered Cdk Substrate Dephosphorylation during Mitotic Exit. *Cell*, 147(4), pp.803–814.

Bourne, Y., Watson, M.H., Arvai, A.S., Bernstein, S.L., Reed, S.I. and Tainer, J.A., 2000.

- Crystal structure and mutational analysis of the *Saccharomyces cerevisiae* cell cycle regulatory protein Cks1: implications for domain swapping, anion binding and protein interactions. *Structure*, 8(8), pp.841–850.
- Boustany, L.M. and Cyert, M.S., 2002. Calcineurin-dependent regulation of Crz1p nuclear export requires Msn5p and a conserved calcineurin docking site. *Genes & Development*, 16(5), pp.608–619.
- Bremmer, S.C., 2009. Characterization of the Cdc14 phosphatase activity and regulation in budding yeast. PhD Thesis, Purdue University.
- Bremmer, S.C., Hall, H., Martinez, J.S., Eissler, C.L., Hinrichsen, T.H., Rossie, S., Parker, L.L., Hall, M.C. and Charbonneau, H., 2012. Cdc14 Phosphatases Preferentially Dephosphorylate a Subset of Cyclin-dependent kinase (Cdk) Sites Containing Phosphoserine. *Journal of Biological Chemistry*, 287(3), pp.1662–1669.
- Burgess, A., Vigneron, S., Brioude, E., Labbé, J.-C., Lorca, T. and Castro, A., 2010. Loss of human Greatwall results in G2 arrest and multiple mitotic defects due to deregulation of the cyclin B-Cdc2/PP2A balance. *Proceedings of the National Academy of Sciences*, 107(28), pp.12564–12569.
- Camps, M., Anthony, N., Corine, G., Bruno, A., Marco, M., Christian, C., Ursula, B. and Steve, A., 1998. Catalytic Activation of the Phosphatase MKP-3 by ERK2 Mitogen-Activated Protein Kinase. *Science*, 280(5367), pp.1262–1265.
- Celton-Morizur, S., Bordes, N., Fraissier, V., Tran, P.T. and Paoletti, A., 2004. C-Terminal Anchoring of mid1p to Membranes Stabilizes Cytokinetic Ring Position in Early Mitosis in Fission Yeast. *Molecular and Cellular Biology*, 24(24), pp.10621–10635.
- Chen, F., Archambault, V., Kar, A., Lio, P., D'Avino, P.P., Sinka, R., Lilley, K., Laue, E.D., Deak, P., Capalbo, L. and Glover, D.M., 2007. Multiple Protein Phosphatases Are Required for Mitosis in *Drosophila*. *Current Biology*, 17(4), pp.293–303.
- Chen, Z.A., Jawhari, A., Fischer, L., Buchen, C., Tahir, S., Kamenski, T., Rasmussen, M., Lariviere, L., Bukowski-Wills, J.-C., Nilges, M., Cramer, P. and Rappsilber, J., 2010. Architecture of the RNA polymerase II-TFIIF complex revealed by cross-linking and mass spectrometry. *The EMBO Journal*, 29(4), pp.717–726.
- Chou, M.F. and Schwartz, D., 2002. *Biological Sequence Motif Discovery Using motif-x*. onlinelibrary.wiley.com. Hoboken, NJ, USA: Current Protocols in Bioinformatics.
- Cori, G.T. and Cori, C.F., 1945. The enzymatic conversion of Phosphorylase a to b. *The Journal of Biological Chemistry*, 158, pp.321–322.
- Coudreuse, D. and Nurse, P., 2010. Driving the cell cycle with a minimal CDK control network. *Nature*, 468(7327), pp.1074–1079.
- Crooks, G.E., Hon, G., Chandonia, J.M. and Brenner, S.E., 2004. WebLogo: A Sequence

Logo Generator. *Genome Research*, 14(6), pp.1188–1190.

Cueille, N., Salimova, E., Esteban, V., Blanco, M., Moreno, S., Bueno, A. and Simanis, V., 2001. Flp1, a fission yeast orthologue of the *S. cerevisiae*

CDC14 gene, is not required for cyclin degradation or rum1p stabilisation and at the end of mitosis. *Journal of Cell Science*, 114(14), pp.2649–2664.

Culotti, J. and Hartwell, L.H., 1971. Genetic control of the cell division cycle in yeast. *Experimental Cell Research*, 67(2), pp.389–401.

Cundell, M.J., Bastos, R.N., Zhang, T., Holder, J., Gruneberg, U., Novak, B. and Barr, F.A., 2013. The BEG (PP2A-B55/ENSA/Greatwall) Pathway Ensures Cytokinesis follows Chromosome Separation. *Molecular Cell*, pp.1–13.

Cundell, M.J., Hutter, L.H., Bastos, R.N., Poser, E., Holder, J., Mohammed, S., Novak, B. and Barr, F.A., 2016. A PP2A-B55 recognition signal controls substrate dephosphorylation kinetics during mitotic exit. *The Journal of Cell Biology*, 214(5), pp.539–554.

D'Amours, D., Stegmeier, F. and Amon, A., 2004. Cdc14 and Condensin Control the Dissolution of Cohesin-Independent Chromosome Linkages at Repeated DNA. *Cell*, 117(4), pp.455–469.

Davey, N.E., Cyert, M.S. and Moses, A.M., 2015. Short linear motifs – ex nihilo evolution of protein regulation. *Cell Communication and Signaling*, 13(43).

Dephoure, N., Zhou, C., Villen, J., Beausoleil, S.A., Bakalarski, C.E., Elledge, S.J. and Gygi, S.P., 2008. A quantitative atlas of mitotic phosphorylation. *Proceedings of the National Academy of Sciences*, 105(31), pp.10762–10767.

Draetta, G., Luca, F., Westendorf, J., Brizuela, L., Ruderman, J. and Beach, D., 1989. cdc2 protein kinase is complexed with both cyclin A and B: Evidence for proteolytic inactivation of MPF. *Cell*, 56(5), pp.829–838.

Drapkin, B.J., Lu, Y., Procko, A.L., Timney, B.L. and Cross, F.R., 2009. Analysis of the mitotic exit control system using locked levels of stable mitotic cyclin. *Molecular Systems Biology*, 5.

Dryden, S.C., Nahhas, F.A., Nowak, J.E., Goustin, A.S. and Tainsky, M.A., 2003. Role for Human SIRT2 NAD-Dependent Deacetylase Activity in Control of Mitotic Exit in the Cell Cycle. *Molecular and Cellular Biology*, 23(9), pp.3173–3185.

Egloff, M.P., Johnson, D.F., Moorhead, G., Cohen, P.T.W., Cohen, P. and Bardford, D., 1997. Structural basis for the recognition of regulatory subunits by the catalytic subunit of protein phosphatase 1. *The EMBO Journal*, 16(8), pp.1876–1887.

- Eissler, C.L., Mazón, G., Powers, B.L., Savinov, S.N., Symington, L.S. and Hall, M.C., 2014. The Cdk/Cdc14 Module Controls Activation of the Yen1 Holliday Junction Resolvase to Promote Genome Stability. *Molecular Cell*, 54(1), pp.80–93.
- Elia, A.E.H., Cantley, L.C. and Yaffe, M.B., 2003. Proteomic Screen Finds pSer/pThr-Binding Domain Localizing Plk1 to Mitotic Substrates. *Science*, 299(5610), pp.1228–1231.
- Epstein, C.B. and Cross, F.R., 1992. CLB5: a novel B cyclin from budding yeast with a role in S phase. *Genes & Development*, 6(9), pp.1695–1706.
- Erickson, H.P., 2009. Size and Shape of Protein Molecules at the Nanometer Level Determined by Sedimentation, Gel Filtration, and Electron Microscopy. *Biological Procedures Online*, 11(1), pp.32–51.
- Errico, A., Deshmukh, K., Tanaka, Y., Pozniakovsky, A. and Hunt, T., 2010. Identification of substrates for cyclin dependent kinases. *Advances in Enzyme Regulation*, 50(1), pp.375–399.
- Fabrini, R., De Luca, A., Stella, L., Mei, G., Orioni, B., Ciccone, S., Federici, G., Bello, Lo, M. and Ricci, G., 2009. Monomer–Dimer Equilibrium in Glutathione Transferases: A Critical Re-Examination. *Biochemistry*, 48(43), pp.10473–10482.
- Ferguson, A.M., White, L.S., Donovan, P.J. and Piwnica-Worms, H., 2005. Normal Cell Cycle and Checkpoint Responses in Mice and Cells Lacking Cdc25B and Cdc25C Protein Phosphatases. *Molecular and Cellular Biology*, 25(7), pp.2853–2860.
- Ferrigno, P., Langan, T.A. and Cohen, P., 1993. Protein phosphatase 2A1 is the major enzyme in vertebrate cell extracts that dephosphorylates several physiological substrates for cyclin-dependent protein kinases. *Molecular Biology of the Cell*, 4(7), pp.669–677.
- Fischer, E.H. and Krebs, E.G., 1955. Conversion of phosphorylase b to phosphorylase a in muscle extracts. *Journal of Biological Chemistry*, pp.121–132.
- Fisher, D.L. and Nurse, P., 1996. A single fission yeast mitotic cyclin B p34cdc2 kinase promotes both S-phase and mitosis in the absence of G1 cyclins. *The EMBO Journal*, 15(4), pp.850–860.
- Fragkos, M., Ganier, O., Coulombe, P. and Méchali, M., 2015. DNA replication origin activation in space and time. *Nature Reviews Molecular Cell Biology*, 16(6), pp.360–374.
- Fu, C., Ward, J.J., Loiodice, I., Velve-Casquillas, G., Nedelec, F.J. and Tran, P.T., 2009. Phospho-Regulated Interaction between Kinesin-6 Klp9p and Microtubule Bundler Ase1p Promotes Spindle Elongation. *Developmental Cell*, 17(2), pp.257–267.
- Gautier, J., Norbury, C., Lohka, M., Nurse, P. and Maller, J., 1988. Purified maturation-promoting factor contains the product of a Xenopus homolog of the fission yeast cell cycle control gene cdc2. *Cell*, 54(3), pp.433–439.

- Gavet, O. and Pines, J., 2010. Progressive Activation of CyclinB1-Cdk1 Coordinates Entry to Mitosis. *Developmental Cell*, 18(4), pp.533–543.
- Geil, C., Schwab, M. and Seufert, W., 2008. A Nucleolus-Localized Activator of Cdc14 Phosphatase Supports rDNA Segregation in Yeast Mitosis. *Current Biology*, 18(13), pp.1001–1005.
- Geng, Y., Yu, Q., Sicinska, E., Das, M., Schneider, J.E., Bhattacharya, S., Rideout, W.M., III, Bronson, R.T., Gardner, H. and Sicinski, P., 2003. Cyclin E Ablation in the Mouse. *Cell*, 114(4), pp.431–443.
- Ghaemmaghami, S., Huh, W.-K., Bower, K., Howson, R.W., Belle, A., Dephoure, N., O'Shea, E.K. and Weissman, J.S., 2003. Global analysis of protein expression in yeast. *Nature*, 425(6959), pp.737–741.
- Gharbi-Ayachi, A., Labbe, J.C., Burgess, A., Vigneron, S., Strub, J.M., Brioude, E., Van-Dorselaer, A., Castro, A. and Lorca, T., 2010. The Substrate of Greatwall Kinase, Arpp19, Controls Mitosis by Inhibiting Protein Phosphatase 2A. *Science*, 330(6011), pp.1673–1677.
- Glotzer, M., Murray, A.W. and Kirschner, M.W., 1991. Cyclin is degraded by the ubiquitin pathway. *Nature*, 349(6305), pp.132–138.
- Godfrey, M., Touati, S.A., Kataria, M., Jones, A., Snijders, A.P. and Uhlmann, F., PP2A^{Cdc55} phosphatase imposes phosphothreonine-specific ordering of cell cycle phosphorylation. In revision.
- Goldman, A., Roy, J., Bodenmiller, B., Wanka, S., Landry, C.R., Aebersold, R. and Cyert, M.S., 2014. The Calcineurin Signaling Network Evolves via Conserved Kinase-Phosphatase Modules that Transcend Substrate Identity. *Molecular Cell*, 55(3), pp.422–435.
- Grallert, A., Boke, E., Hagting, A., Ben Hodgson, Connolly, Y., Griffiths, J.R., Smith, D.L., Pines, J. and Hagan, I.M., 2014. A PP1-PP2A phosphatase relay controls mitotic progression. *Nature*, pp.1–19.
- Gray, C.H., Good, V.M., Tonks, N.K. and Barford, D., 2003. The structure of the cell cycle protein Cdc14 reveals a proline-directed protein phosphatase. *The EMBO Journal*, 22(14), pp.3524–3535.
- Gruneberg, U., Glotzer, M., Gartner, A. and Nigg, E.A., 2002. The CeCDC-14 phosphatase is required for cytokinesis in the *Caenorhabditis elegans* embryo. *The Journal of Cell Biology*, 158(5), pp.901–914.
- Hall, M.C., Jeong, D.E., Henderson, J.T., Choi, E., Bremmer, S.C., Iliuk, A.B. and Charbonneau, H., 2008. Cdc28 and Cdc14 Control Stability of the Anaphase-promoting Complex Inhibitor Acml. *Journal of Biological Chemistry*, 283(16), pp.10396–10407.

- Hartwell, L.H., Culotti, J., Pringle, J.R. and Reid, B.J., 1974. Genetic Control of the Cell Division Cycle in Yeast: A model to account for the order of cell cycle events is deduced from the phenotypes of yeast mutants. *Science*, 183(4120), pp.46–51.
- Heim, A., Konietzny, A. and Mayer, T.U., 2015. Protein phosphatase 1 is essential for Greatwall inactivation at mitotic exit. *Nature Publishing Group*, 16(11), pp.1501–1510.
- Hertz, E.P.T., Kruse, T., Davey, N.E., Montoya, G., Olsen, J.V. and Nilsson, J., 2016. A Conserved Motif Provides Binding Specificity to the PP2A-B56 Phosphatase. [online] *Molecular Cell*.
- Hégarat, N., Vesely, C., Vinod, P.K., Ocasio, C., Peter, N., Gannon, J., Oliver, A.W., Novak, B. and Hochegger, H., 2014. PP2A/B55 and Fcp1 Regulate Greatwall and Ensa Dephosphorylation during Mitotic Exit. *PLoS Genetics*, 10(1), p.e1004004.
- Higuchi, T. and Uhlmann, F., 2005. Stabilization of microtubule dynamics at anaphase onset promotes chromosome segregation. *Nature Cell Biology*, 433(7022), pp.171–176.
- Hobiger, K. and Friedrich, T., 2015. Voltage sensitive phosphatases: emerging kinship to protein tyrosine phosphatases from structure-function research. *Frontiers in Pharmacology*, 6.
- Hochegger, H., Dejsuphong, D., Sonoda, E., Saberi, A., Rajendra, E., Kirk, J., Hunt, T. and Takeda, S., 2007. An essential role for Cdk1 in S phase control is revealed via chemical genetics in vertebrate cells. *The Journal of Cell Biology*, 178(2), pp.257–268.
- Hochegger, H., Takeda, S. and Hunt, T., 2008. Cyclin-dependent kinases and cell-cycle transitions: does one fit all? *Nature Reviews Molecular Cell Biology*, 9(11), pp.910–916.
- Hogan, E. and Koshland, D., 1992. Addition of extra origins of replication to a minichromosome suppresses its mitotic loss in *cdc6* and *cdc14* mutants of *Saccharomyces cerevisiae*. *Proceedings of the National Academy of Sciences*, 89(7), pp.3098–3102.
- Holt, L.J., Hutti, J.E., Cantley, L.C. and Morgan, D.O., 2007. Evolution of Ime2 Phosphorylation Sites on Cdk1 Substrates Provides a Mechanism to Limit the Effects of the Phosphatase Cdc14 in Meiosis. *Molecular Cell*, 25(5), pp.689–702.
- Holt, L.J., Krutchinsky, A.N. and Morgan, D.O., 2008. Positive feedback sharpens the anaphase switch. *Nature*, 454(7202), pp.353–357.
- Holt, L.J., Tuch, B.B., Villen, J., Johnson, A.D., Gygi, S.P. and Morgan, D.O., 2009. Global Analysis of Cdk1 Substrate Phosphorylation Sites Provides Insights into Evolution. *Science*, 325(5948), pp.1682–1686.
- Hu, F. and Aparicio, O.M., 2005. Swe1 regulation and transcriptional control restrict the activity of mitotic cyclins toward replication proteins in *Saccharomyces cerevisiae*. *Proceedings of the National Academy of Sciences*, 102(25), pp.8910–8915.

- Hu, F., Wang, Y., Liu, D., Li, Y., Qin, J. and Elledge, S.J., 2001. Regulation of the Bub2/Bfa1 GAP Complex by Cdc5 and Cell Cycle Checkpoints. *Cell*, 107(5), pp.655–665.
- Jackson, L.P., Reed, S.I. and Haase, S.B., 2006. Distinct Mechanisms Control the Stability of the Related S-Phase Cyclins Clb5 and Clb6. *Molecular and Cellular Biology*, 26(6), pp.2456–2466.
- Jaspersen, S.L. and Morgan, D.O., 2000. Cdc14 activates Cdc15 to promote mitotic exit in budding yeast. *Current Biology*, 10(10), pp.615–618.
- Jaspersen, S.L., Charles, J.F. and Morgan, D.O., 1999. Inhibitory phosphorylation of the APC regulator Hct1 is controlled by the kinase Cdc28 and the phosphatase Cdc14. *Current Biology*, 9(5), pp.227–236.
- Jensen, S., Geymonat, M., Johnson, A.L., Segal, M. and Johnston, L.H., 2002. Spatial regulation of the guanine nucleotide exchange factor Lte1 in *Saccharomyces cerevisiae*. *Journal of Cell Science*, 115(24), pp.4977–4991.
- Jin, F., Liu, H., Liang, F., Rizkallah, R., Hurt, M.M. and Wang, Y., 2008. Temporal control of the dephosphorylation of Cdk substrates by mitotic exit pathways in budding yeast. *Proceedings of the National Academy of Sciences*, 105(42), pp.16177–16182.
- Jin, F., Richmond, D. and Wang, Y., 2014. The multilayer regulation of the metaphase-to-anaphase transition. *Cell Cycle*, 8(5), pp.700–704.
- Johnson, L.N., Brown, N.R., Noble, M.E.M. and Endicott, J.A., 1999. The structural basis for specificity of substrate and recruitment peptides for cyclin-dependent kinases. *Nature Cell Biology*, 1(7), pp.438–443.
- Kalaszczynska, I., Geng, Y., Iino, T., Mizuno, S.-I., Choi, Y., Kondratiuk, I., Silver, D.P., Wolgemuth, D.J., Akashi, K. and Sicinski, P., 2009. Cyclin A Is Redundant in Fibroblasts but Essential in Hematopoietic and Embryonic Stem Cells. *Cell*, 138(2), pp.352–365.
- Kao, L., Wang, Y.T., Chen, Y.C., Tseng, S.F., Jhang, J.C., Chen, Y.J. and Teng, S.C., 2014. Global Analysis of Cdc14 Dephosphorylation Sites Reveals Essential Regulatory Role in Mitosis and Cytokinesis. *Molecular & Cellular Proteomics*, 13(2), pp.594–605.
- Kennelly, P.J. and Krebs, E.G., 1991. Consensus sequences as substrate specificity determinants for protein kinases and protein phosphatases. *The Journal of Biological Chemistry*, 266(24), pp.15555–15558.
- Kimura, M., Suzuki, H. and Ishihama, A., 2002. Formation of a Carboxy-Terminal Domain Phosphatase (Fcp1)/TFIIF/RNA Polymerase II (pol II) Complex in *Schizosaccharomyces pombe* Involves Direct Interaction between Fcp1 and the Rpb4 Subunit of pol II. *Molecular and Cellular Biology*, 22(5), pp.1577–1588.

- Kobayashi, J., Hirano, H. and Matsuura, Y., 2015. Crystal structure of the karyopherin Kap121p bound to the extreme C-terminus of the protein phosphatase Cdc14p. *Biochemical and Biophysical Research Communications*, 463(3), pp.309–314.
- Kosugi, S., Hasebe, M., Tomita, M. and Yanagawa, H., 2009. Systematic identification of cell cycle-dependent yeast nucleocytoplasmic shuttling proteins by prediction of composite motifs. *Proceedings of the National Academy of Sciences*, 106(25), pp.10171–10176.
- Kozar, K., Ciemerych, M.A., Rebel, V.I., Shigematsu, H., Zagozdzon, A., Sicinska, E., Geng, Y., Yu, Q., Bhattacharya, S., Bronson, R.T., Akashi, K. and Sicinski, P., 2004. Mouse Development and Cell Proliferation in the Absence of D-Cyclins. *Cell*, 118(4), pp.477–491.
- Kõivomägi, M., Örd, M., Iofik, A., Valk, E., Venta, R., Faustova, I., Kivi, R., Balog, E.R.M., Rubin, S.M. and Loog, M., 2013. Multisite phosphorylation networks as signal processors for Cdk1. *Nature Structural & Molecular Biology*, 20(12), pp.1415–1424.
- Kõivomägi, M., Valk, E., Venta, R., Iofik, A., Lepiku, M., Morgan, D.O. and Loog, M., 2011. Dynamics of Cdk1 Substrate Specificity during the Cell Cycle. *Molecular Cell*, 42(5), pp.610–623.
- Krasinska, L., de Bettignies, G., Fisher, D., Abrieu, A., Fesquet, D. and Morin, N., 2007. Regulation of multiple cell cycle events by Cdc14 homologues in vertebrates. *Experimental Cell Research*, 313(6), pp.1225–1239.
- Krebs, E.G. and Fischer, E.H., 1956. The phosphorylase b to a converting enzyme of rabbit skeletal muscle. *Biochimica et Biophysica Acta*, 20, pp.150–157.
- Krek, W., Ewen, M.E., Shirodhkar, S., Arany, Z., Kaelin, W.G., Jr and Livingston, D.M., 1994. Negative regulation of the growth-promoting transcription factor E2F-1 by a stably bound cyclin A-dependent protein kinase. *Cell*, 78(1), pp.161–172.
- Kroll, E.S., Hyland, K.M., Hieter, P. and Li, J.J., 1996. Establishing genetic interactions by a synthetic dosage lethality phenotype. *Genetics*, 143(1), pp.95–102.
- Kuilman, T., Maiolica, A., Godfrey, M., Scheidel, N., Aebersold, R. and Uhlmann, F., 2015. Identification of Cdk targets that control cytokinesis. *The EMBO Journal*, 34(1), pp.81–96.
- Lee, S.E., Jensen, S., Frenz, L.M., Johnson, A.L., Fesquet, D. and Johnston, L.H., 2001. The Bub2-dependent mitotic pathway in yeast acts every cell cycle and regulates cytokinesis. *Journal of Cell Science*, 114(12), pp.2345–2354.
- Li, L., Ernsting, B.R., Wishart, M.J., Lohse, D.L. and Dixon, J.E., 1997. A Family of Putative Tumor Suppressors Is Structurally and Functionally Conserved in Humans and Yeast. *Journal of Biological Chemistry*, 272(47), pp.29403–29406.

- Lin, H., Ha, K., Lu, G., Fang, X., Cheng, R., Zuo, Q. and Zhang, P., 2015. Cdc14A and Cdc14B Redundantly Regulate DNA Double-Strand Break Repair. *Molecular and Cellular Biology*, pp.MCB.00233–15.
- Loog, M. and Morgan, D.O., 2005. Cyclin specificity in the phosphorylation of cyclin-dependent kinase substrates. *Nature*, 434(7029), pp.104–108.
- López-Avilés, S., Kapuy, O., Novak, B. and Uhlmann, F., 2009. Irreversibility of mitotic exit is the consequence of systems-level feedback. *Nature*, 459(7246), pp.592–595.
- Lu, D., Hsiao, J.Y., Davey, N.E., Van Voorhis, V.A., Foster, S.A., Tang, C. and Morgan, D.O., 2014. Multiple mechanisms determine the order of APC/C substrate degradation in mitosis. *The Journal of Cell Biology*, 207(1), pp.23–39.
- Ma, S., Vigneron, S., Robert, P., Strub, J.M., Cianferani, S., Castro, A. and Lorca, T., 2016. Greatwall dephosphorylation and inactivation upon mitotic exit is triggered by PP1. *Journal of Cell Science*.
- Mah, A.S., Jang, J. and Deshaies, R.J., 2001. Protein kinase Cdc15 activates the Dbf2-Mob1 kinase complex. *Proceedings of the National Academy of Sciences*, 98(13), pp.7325–7330.
- Mailand, N., Gibbs-Seymour, I. and Bekker-Jensen, S., 2013. Regulation of PCNA–protein interactions for genome stability. *Nature Reviews Molecular Cell Biology*, 14(5), pp.269–282.
- Mailand, N., Lukas, C., Kaiser, B.K., Jackson, P.K., Bartek, J. and Lukas, J., 2002. Deregulated human Cdc14A phosphatase disrupts centrosome separation and chromosome segregation. *Nature Cell Biology*, 4(4), pp.318–322.
- Manchado, E., Guillamot, M., de Cárcer, G., Eguren, M., Trickey, M., García-Higuera, I., Moreno, S., Yamano, H., Cañamero, M. and Malumbres, M., 2010. Targeting Mitotic Exit Leads to Tumor Regression In Vivo: Modulation by Cdk1, Mastl, and the PP2A/B55 α , δ Phosphatase. *Cancer Cell*, 18(6), pp.641–654.
- Marianayagam, N.J., Sunde, M. and Matthews, J.M., 2004. The power of two: protein dimerization in biology. *Trends in Biochemical Sciences*, 29(11), pp.618–625.
- Masui, Y. and Markert, C.L., 1971. Cytoplasmic control of nuclear behavior during meiotic maturation of frog oocytes. *Journal of Experimental Zoology*, 177(2), pp.129–145.
- Mayer-Jaekel, R.E., Ohkura, H., Gomes, R., Sunkel, C.E., Baumgartner, S., Hemmings, B.A. and Glover, D.M., 1993. The 55 kd regulatory subunit of Drosophila protein phosphatase 2A is required for anaphase. *Cell*, 72(4), pp.621–633.
- Mayordomo, I. and Sanz, P., 2002. The *Saccharomyces cerevisiae* 14-3-3 protein Bmh2 is required for regulation of the phosphorylation status of Fin1, a novel intermediate

filament protein. *Biochemical Journal*, 365(1), pp.51–56.

McCloy, R.A., Parker, B.L., Rogers, S., Chaudhuri, R., Gayevskiy, V., Hoffman, N.J., Ali, N., Watkins, D.N., Daly, R.J., James, D.E., Lorca, T., Castro, A. and Burgess, A., 2015. Global Phosphoproteomic Mapping of Early Mitotic Exit in Human Cells Identifies Novel Substrate Dephosphorylation Motifs. *Molecular & Cellular Proteomics*, 14(8), pp.2194–2212.

McGrath, D.A., Balog, E.R.M., Kõivomägi, M., Lucena, R., Mai, M.V., Hirschi, A., Kellogg, D.R., Loog, M. and Rubin, S.M., 2013. Cks confers specificity to phosphorylation-dependent CDK signaling pathways. *Nature Structural & Molecular Biology*, 20(12), pp.1407–1414.

McGuffin, L.J., Bryson, K. and Jones, D.T., 2000. The PSIPRED protein structure prediction server. *Bioinformatics*, 16(4), pp.404–405.

Miller, D.P., Hall, H., Chaparian, R., Mara, M., Mueller, A., Hall, M.C. and Shannon, K.B., 2015. Dephosphorylation of Iqg1 by Cdc14 regulates cytokinesis in budding yeast. *Molecular Biology of the Cell*, 26(16), pp.2913–2926.

Milo, R., Jorgensen, P., Moran, U., Weber, G. and Springer, M., 2009. BioNumbers--the database of key numbers in molecular and cell biology. *Nucleic Acids Research*, 38(Database), pp.D750–D753.

Minshull, J., Blow, J.J. and Hunt, T., 1989. Translation of cyclin mRNA is necessary for extracts of activated *Xenopus* eggs to enter mitosis. *Cell*, 56(6), pp.947–956.

Mirchenko, L. and Uhlmann, F., 2010. Sli15INCENP Dephosphorylation Prevents Mitotic Checkpoint Reengagement Due to Loss of Tension at Anaphase Onset. *Current Biology*, 20(15), pp.1396–1401.

Mocciaro, A. and Schiebel, E., 2010. Cdc14: a highly conserved family of phosphatases with non-conserved functions? *Journal of Cell Science*, 123(17), pp.2867–2876.

Mocciaro, A., Berdoudo, E., Zeng, K., Black, E., Vagnarelli, P., Earnshaw, W., Gillespie, D., Jallepalli, P. and Schiebel, E., 2010. Vertebrate cells genetically deficient for Cdc14A or Cdc14B retain DNA damage checkpoint proficiency but are impaired in DNA repair. *The Journal of Cell Biology*, 189(4), pp.631–639.

Mochida, S. and Hunt, T., 2007. Calcineurin is required to release *Xenopus* egg extracts from meiotic M phase. *Nature*, 449(7160), pp.336–340.

Mochida, S., Ikeo, S., Gannon, J. and Hunt, T., 2009. Regulated activity of PP2A–B55 δ is crucial for controlling entry into and exit from mitosis in *Xenopus* egg extracts. *The EMBO Journal*, 28(18), pp.2777–2785.

Mochida, S., Maslen, S.L., Skehel, M. and Hunt, T., 2010. Greatwall Phosphorylates an Inhibitor of Protein Phosphatase 2A That Is Essential for Mitosis. *Science*, 330(6011),

pp.1670–1673.

Mohl, D.A., Huddleston, M.J., Collingwood, T.S., Annan, R.S. and Deshaies, R.J., 2009. Dbf2–Mob1 drives relocalization of protein phosphatase Cdc14 to the cytoplasm during exit from mitosis. *The Journal of Cell Biology*, 184(4), pp.527–539.

Monica, Della, R., Visconti, R., Cervone, N., Serpico, A.F., Grieco, D. and Hunter, T., 2015. Fcp1 phosphatase controls Greatwall kinase to promote PP2A-B55 activation and mitotic progression. *eLife*, 4, p.e10399.

Morgan, D.O., 2007. *The Cell Cycle: Principles of Control*. New Science Press.

Murray, A.W. and Kirschner, M.W., 1989. Cyclin synthesis drives the early embryonic cell cycle. *Nature*, 339(6222), pp.275–280.

Musacchio, A., 2015. The Molecular Biology of Spindle Assembly Checkpoint Signaling Dynamics. *Current Biology*, 25(20), pp.R1002–R1018.

Nigg, E.A., 1991. The substrates of the cdc2 kinase. *Seminars in Cell Biology*, 2(4), pp.261–270.

Oikonomou, C. and Cross, F.R., 2011. Rising Cyclin-CDK Levels Order Cell Cycle Events. *PLOS ONE*, 6(6), p.e20788.

Ovejero, S., Ayala, P., Bueno, A. and Sacristan, M.P., 2012. Human Cdc14A regulates Wee1 stability by counteracting CDK-mediated phosphorylation. *Molecular Biology of the Cell*, 23(23), pp.4515–4525.

Pabbisetty, K.B., Yue, X., Li, C., Himanen, J.P., Zhou, R., Nikolov, D.B. and Hu, L., 2007. Kinetic analysis of the binding of monomeric and dimeric ephrins to Eph receptors: Correlation to function in a growth cone collapse assay. *Protein Science*, 16(3), pp.355–361.

Pagliuca, F.W., Collins, M.O., Lichawska, A., Zegerman, P., Choudhary, J.S. and Pines, J., 2011. Quantitative Proteomics Reveals the Basis for the Biochemical Specificity of the Cell-Cycle Machinery. *Molecular Cell*, 43(3), pp.406–417.

Palani, S., Meitinger, F., Boehm, M.E., Lehmann, W.D. and Pereira, G., 2012. Cdc14-dependent dephosphorylation of Inn1 contributes to Inn1–Cyt3 complex formation. *Journal of Cell Science*, 125(13), pp.3091–3096.

Pereira, G., 2003. Separase Regulates INCENP-Aurora B Anaphase Spindle Function Through Cdc14. *Science*, 302(5653), pp.2120–2124.

Pereira, G., Manson, C., Grindlay, J. and Schiebel, E., 2002. Regulation of the Bfa1p–Bub2p complex at spindle pole bodies by the cell cycle phosphatase Cdc14p. *The Journal of Cell Biology*, 157(3), pp.367–379.

- Pédelacq, J.-D., Cabantous, S., Tran, T., Terwilliger, T.C. and Waldo, G.S., 2005. Engineering and characterization of a superfolder green fluorescent protein. *Nature Biotechnology*, 24(1), pp.79–88.
- Pfleger, C.M. and Kirschner, M.W., 1992. The KEN box: an APC recognition signal distinct from the D box targeted by Cdh1. *Genes & Development*, 14, pp.655–665.
- Potapova, T.A., Daum, J.R., Pittman, B.D., Hudson, J.R., Jones, T.N., Satinover, D.L., Stukenberg, P.T. and Gorbsky, G.J., 2006. The reversibility of mitotic exit in vertebrate cells. *Nature*, 440(7086), pp.954–958.
- Queralt, E. and Uhlmann, F., 2008. Separase cooperates with Zds1 and Zds2 to activate Cdc14 phosphatase in early anaphase. *The Journal of Cell Biology*, 182(5), pp.873–883.
- Queralt, E., Lehane, C., Novak, B. and Uhlmann, F., 2006. Downregulation of PP2A^{Cdc55} Phosphatase by Separase Initiates Mitotic Exit in Budding Yeast. *Cell*, 125(4), pp.719–732.
- Richardson, H.E., Wittenberg, C., Cross, F. and Reed, S.I., 1989. An essential G1 function for cyclin-like proteins in yeast. *Cell*, 59(6), pp.1127–1133.
- Richter, K., Muschler, P., Hainzl, O. and Buchner, J., 2001. Coordinated ATP Hydrolysis by the Hsp90 Dimer. *Journal of Biological Chemistry*, 276(36), pp.33689–33696.
- Rogers, S., McCloy, R., Watkins, D.N. and Burgess, A., 2015. Mechanisms regulating phosphatase specificity and the removal of individual phosphorylation sites during mitotic exit. *Inside the Cell*, pp.n/a–n/a.
- Rossio, V. and Yoshida, S., 2011. Spatial regulation of Cdc55–PP2A by Zds1/Zds2 controls mitotic entry and mitotic exit in budding yeast. *The Journal of Cell Biology*, 193(3), p.445.
- Saito, R.M., Perreault, A., Peach, B., Satterlee, J.S. and van den Heuvel, S., 2004. The CDC-14 phosphatase controls developmental cell-cycle arrest in *C. elegans*. *Nature*, 6(8), pp.777–783.
- Santamaría, D., Barrière, C., Cerqueira, A., Hunt, S., Tardy, C., Newton, K., Cáceres, J.F., Dubus, P., Malumbres, M. and Barbacid, M., 2007. Cdk1 is sufficient to drive the mammalian cell cycle. *Nature*, 448(7155), pp.811–815.
- Schmitz, M.H.A., Held, M., Janssens, V., Hutchins, J.R.A., Hudecz, O., Ivanova, E., Goris, J., Trinkle-Mulcahy, L., Lamond, A.I., Poser, I., Hyman, A.A., Mechtler, K., Peters, J.-M. and Gerlich, D.W., 2010. Live-cell imaging RNAi screen identifies PP2A-B55[α] and importin-[β]1 as key mitotic exit regulators in human cells. *Nature Cell Biology*, 12(9), pp.886–893.
- Schwab, M., Lutum, A.S. and Seufert, W., 1997. Yeast Hct1 Is a Regulator of Clb2

Cyclin Proteolysis. *Cell*, 90(4), pp.683–693.

Schwede, T., Kopp, J., Guex, N. and Peitsch, M.C., 2003. SWISS-MODEL: an automated protein homology-modeling server. *Nucleic Acids Research*, 31(13), pp.3381–3385.

Schwob, E. and Nasmyth, K., 1993. CLB5 and CLB6, a new pair of B cyclins involved in DNA replication in *Saccharomyces cerevisiae*. *Genes & Development*, 7(7a), pp.1160–1175.

Shirayama, M., Tóth, A., Gálová, M. and Nasmyth, K., 1999. Access : APC^{Cdc20} promotes exit from mitosis by destroying the anaphase inhibitor Pds1 and cyclin Clb5 : Nature. *Nature*, 402(6758), pp.203–207.

Shou, W., Azzam, R., Chen, S.L., Huddleston, M.J., Baskerville, C., Charbonneau, H., Annan, R.S., Carr, S.A. and Deshaies, R.J., 2002. Cdc5 influences phosphorylation of Net1 and disassembly of the RENT complex. *BMC Molecular Biology*, 3(1), p.1.

Shou, W., Sakamoto, K.M., Keener, J., Morimoto, K.W., Traverso, E.E., Azzam, R., Hoppe, G.J., Feldman, R.M.R., DeModena, J., Moazed, D., Charbonneau, H., Nomura, M. and Deshaies, R.J., 2001. Net1 Stimulates RNA Polymerase I Transcription and Regulates Nucleolar Structure Independently of Controlling Mitotic Exit. *Molecular Cell*, 8(1), pp.45–55.

Skoufias, D.A., Indorato, R.-L., Lacroix, F., Panopoulos, A. and Margolis, R.L., 2007. Mitosis persists in the absence of Cdk1 activity when proteolysis or protein phosphatase activity is suppressed. *The Journal of Cell Biology*, 179(4), pp.671–685.

Songyang, Z., Blechner, S., Hoagland, N., Hoekstra, M.F., Piwnica-Worms, H. and Cantley, L.C., 1994. Use of an oriented peptide library to determine the optimal substrates of protein kinases. *Current Biology*, 4(11), pp.973–982.

Stegmeier, F. and Amon, A., 2004. Closing Mitosis: The Functions of the Cdc14 Phosphatase and Its Regulation. *Annual Review of Genetics*, 38(1), pp.203–232.

Stegmeier, F., Visintin, R. and Amon, A., 2002. Separase, Polo Kinase, the Kinetochore Protein Slk19, and Spo12 Function in a Network that Controls Cdc14 Localization during Early Anaphase. *Cell*, 108(2), pp.207–220.

Stern, B. and Nurse, P., 1996. A quantitative model for the cdc2 control of S phase and mitosis in fission yeast. *Trends in Genetics*, 12(9), pp.345–350.

Strausfeld, U., Labbe, J.C., Fesquet, D., Cavadore, J.C., Picard, A., Sadhu, K., Russell, P. and Dorée, M., 1991. Dephosphorylation and activation of a p34cdc2/cyclin B complex in vitro by human CDC25 protein. *Nature*, 351(6323), pp.242–245.

Sullivan, M. and Uhlmann, F., 2003. A non-proteolytic function of separase links the onset of anaphase to mitotic exit. *Nature Cell Biology*, 5(3), pp.249–254.

- Sullivan, M., Higuchi, T., Katis, V.L. and Uhlmann, F., 2004. Cdc14 Phosphatase Induces rDNA Condensation and Resolves Cohesin-Independent Cohesion during Budding Yeast Anaphase. *Cell*, 117(4), pp.471–482.
- Sullivan, M., Holt, L. and Morgan, D.O., 2008. Cyclin-Specific Control of Ribosomal DNA Segregation. *Molecular and Cellular Biology*, 28(17), pp.5328–5336.
- Suzuki, K., Sako, K., Akiyama, K., Isoda, M., Senoo, C., Nakajo, N. and Sagata, N., 2015. Identification of non-Ser/Thr-Pro consensus motifs for Cdk1 and their roles in mitotic regulation of C2H2 zinc finger proteins and Ect2. *Scientific Reports*, 5, p.7929.
- Tanguay, P.-L., Rodier, G. and Meloche, S., 2010. C-terminal domain phosphorylation of ERK3 controlled by Cdk1 and Cdc14 regulates its stability in mitosis. *Biochemical Journal*, 428(1), pp.103–111.
- Taylor, G.S., Liu, Y., Baskerville, C. and Charbonneau, H., 1997. The Activity of Cdc14p, an Oligomeric Dual Specificity Protein Phosphatase from *Saccharomyces cerevisiae*, Is Required for Cell Cycle Progression. *Journal of Biological Chemistry*, 272(38), pp.24054–24063.
- Tonks, N.K., 2006. Protein tyrosine phosphatases: from genes, to function, to disease. *Nature Reviews Molecular Cell Biology*, 7(11), pp.833–846.
- Traverso, E.E., Baskerville, C., Liu, Y., Shou, W., James, P., Deshaies, R.J. and Charbonneau, H., 2001a. Characterization of the Net1 Cell Cycle-dependent Regulator of the Cdc14 Phosphatase from Budding Yeast. *Journal of Biological Chemistry*, 276(24), pp.21924–21931.
- Traverso, E.E., Baskerville, C., Liu, Y., Shou, W., James, P., Deshaies, R.J. and Charbonneau, H., 2001b. Characterization of the Net1 Cell Cycle-dependent Regulator of the Cdc14 Phosphatase from Budding Yeast. *Journal of Biological Chemistry*, 276(24), pp.21924–21931.
- Traverso, E.E., Baskerville, C., Liu, Y., Shou, W., James, P., Deshaies, R.J. and Charbonneau, H., 2001c. Characterization of the Net1 Cell Cycle-dependent Regulator of the Cdc14 Phosphatase from Budding Yeast. *Journal of Biological Chemistry*, 276(24), pp.21924–21931.
- Tyers, M., 1996. The cyclin-dependent kinase inhibitor p40SIC1 imposes the requirement for Cln G1 cyclin function at Start. *Proceedings of the National Academy of Sciences*, 93(15), pp.7772–7776.
- Tyson, J.J. and Novak, B., 2011. Cell Cycle: Who Turns the Crank? *Current Biology*, 21(5), pp.R185–R187.
- Ubersax, J.A., Woodbury, E.L., Quang, P.N., Paraz, M., Blethrow, J.D., Shah, K., Shokat, K.M. and Morgan, D.O., 2003. Targets of the cyclin-dependent kinase Cdk1. *Nature*, 425(6960), pp.859–864.

- Uhlmann, F., 2016. SMC complexes: from DNA to chromosomes. *Nature Reviews Molecular Cell Biology*, 17(7), pp.399–412.
- Uhlmann, F., Lottspeich, F. and Nasmyth, K., 1999. Sister-chromatid separation at anaphase onset is promoted by cleavage of the cohesin subunit Scc1. *Nature*, 400(6739), pp.37–42.
- van Hemert, M.J., Deelder, A.M., Molenaar, C., Steve, A. and van Heusden, G.P.H., 2003. Self-association of the Spindle Pole Body-related Intermediate Filament Protein Fin1p and Its Phosphorylation-dependent Interaction with 14-3-3 Proteins in Yeast. *Journal of Biological Chemistry*, 278(17), pp.15049–15055.
- Van Roey, K., Uyar, B., Weatheritt, R.J., Dinkel, H., Seiler, M., Budd, A., Gibson, T.J. and Davey, N.E., 2014. Short Linear Motifs: Ubiquitous and Functionally Diverse Protein Interaction Modules Directing Cell Regulation. *Chemical Reviews*, 114(13), pp.6733–6778.
- Vazquez-Novelle, M.D., Mailand, N., Ovejero, S., Bueno, A. and Sacristan, M.P., 2010. Human Cdc14A Phosphatase Modulates the G2/M Transition through Cdc25A and Cdc25B. *Journal of Biological Chemistry*, 285(52), pp.40544–40553.
- Vigneron, S., Brioudes, E., Burgess, A., Labbé, J.-C., Lorca, T. and Castro, A., 2009. Greatwall maintains mitosis through regulation of PP2A. *The EMBO Journal*, 28(18), pp.2786–2793.
- Virchow, R.L.K., 1858. *Cellular pathology*. John Churchill.
- Visintin, C., Tomson, B.N., Rahal, R., Paulson, J., Cohen, M., Taunton, J., Amon, A. and Visintin, R., 2008. APC/C-Cdh1-mediated degradation of the Polo kinase Cdc5 promotes the return of Cdc14 into the nucleolus. *Genes & Development*, 22(1), pp.79–90.
- Visintin, R., Craig, K., Hwang, E.S., Prinz, S., Tyers, M. and Amon, A., 1998. The Phosphatase Cdc14 Triggers Mitotic Exit by Reversal of Cdk-Dependent Phosphorylation. *Molecular Cell*, 2(6), pp.709–718.
- Visintin, R., Hwang, E.S. and Amon, A., 1999. Cfi1 prevents premature exit from mitosis by anchoring Cdc14 phosphatase in the nucleolus : Article : Nature. *Nature*, 398(6730), pp.818–823.
- Visintin, R., Stegmeier, F. and Amon, A., 2003. The Role of the Polo Kinase Cdc5 in Controlling Cdc14 Localization. *Molecular Biology of the Cell*, 14(11), pp.4486–4498.
- Wakula, P., Beullens, M., Ceulemans, H., Stalmans, W. and Bollen, M., 2003. Degeneracy and Function of the Ubiquitous RVXF Motif That Mediates Binding to Protein Phosphatase-1. *Journal of Biological Chemistry*, 278(21), pp.18817–18823.
- Walter, D., Hoffmann, S., Komseli, E.-S., Rappsilber, J., Gorgoulis, V. and Sørensen,

- C.S., 2016. SCFCyclin F-dependent degradation of CDC6 suppresses DNA re-replication. *Nature Communications*, 7, p.10530.
- Wan, J., Xu, H. and Grunstein, M., 1992. CDC14 of *Saccharomyces cerevisiae*. Cloning, sequence analysis, and transcription during the cell cycle. *Journal of Biological Chemistry*, 267(16), pp.11274–11280.
- Wang, J., Wang, Z., Yu, T., Yang, H., Virshup, D.M., Kops, G.J.P.L., Lee, S.H., Zhou, W., Li, X., Xu, W. and Rao, Z., 2016. Crystal structure of a PP2A B56-BubR1 complex and its implications for PP2A substrate recruitment and localization. *Protein & Cell*, 7(7), pp.516–526.
- Wang, W.Q., Bembenek, J., Gee, K.R., Yu, H., Charbonneau, H. and Zhang, Z.Y., 2004. Kinetic and Mechanistic Studies of a Cell Cycle Protein Phosphatase Cdc14. *Journal of Biological Chemistry*, 279(29), pp.30459–30468.
- Wäsch, R. and Cross, F.R., 2002. APC-dependent proteolysis of the mitotic cyclin Clb2 is essential for mitotic exit. *Nature*, 418(6897), pp.556–562.
- Wienken, C.J., Baaske, P., Rothbauer, U., Braun, D. and Duhr, S., 2010. Protein-binding assays in biological liquids using microscale thermophoresis. *Nature Communications*, 1(7), p.100.
- Williams, B.C., Filter, J.J., Blake-Hodek, K.A., Wadzinski, B.E., Fuda, N.J., Shalloway, D., Goldberg, M.L. and Pines, J., 2014. Greatwall-phosphorylated Endosulfine is both an inhibitor and a substrate of PP2A-B55 heterotrimers. *eLife*, 3, p.e01695.
- Wilmes, G.M., Archambault, V., Austin, R.J., Jacobson, M.D., Bell, S.P. and Cross, F.R., 2004. Interaction of the S-phase cyclin Clb5 with an 'RXL' docking sequence in the initiator protein Orc6 provides an origin-localized replication control switch. *Genes & Development*, 18(9), pp.981–991.
- Wlodarchak, N. and Xing, Y., 2016. PP2A as a master regulator of the cell cycle. *Critical Reviews in Biochemistry and Molecular Biology*, 51(3), pp.162–184.
- Wolf, F., Wandke, C., Isenberg, N. and Geley, S., 2006. Dose-dependent effects of stable cyclin B1 on progression through mitosis in human cells. *The EMBO Journal*, 25(12), pp.2802–2813.
- Wolfe, B.A. and Gould, K.L., 2004. Fission yeast Clp1p phosphatase affects G2/M transition and mitotic exit through Cdc25p inactivation. *The EMBO Journal*, 23(4), pp.919–929.
- Wolfe, B.A., McDonald, W.H., Yates, J.R., III and Gould, K.L., 2006. Phospho-Regulation of the Cdc14/Clp1 Phosphatase Delays Late Mitotic Events in *S. pombe*. *Developmental Cell*, 11(3), pp.423–430.
- Woodbury, E.L. and Morgan, D.O., 2006. Cdk and APC activities limit the spindle-

stabilizing function of Fin1 to anaphase. *Nature Cell Biology*, 9(1), pp.106–112.

Woodbury, E.L. and Morgan, D.O., 2007. The Role of Self-association in Fin1 Function on the Mitotic Spindle. *Journal of Biological Chemistry*, 282(44), pp.32138–32143.

Wu, J., Cho, H.P., Rhee, D.B., Johnson, D.K., Dunlap, J., Liu, Y. and Wang, Y., 2008. Cdc14B depletion leads to centriole amplification, and its overexpression prevents unscheduled centriole duplication. *The Journal of Cell Biology*, 181(2), pp.475–483.

Wu, J.Q., Guo, J.Y., Tang, W., Yang, C.-S., Freel, C.D., Chen, C., Nairn, A.C. and Kornbluth, S., 2009. PP1-mediated dephosphorylation of phosphoproteins at mitotic exit is controlled by inhibitor-1 and PP1 phosphorylation. *Nature*, 11(5), pp.644–651.

Yeong, F.M., Lim, H.H., Padmashree, C.G. and Surana, U., 2000. Exit from Mitosis in Budding Yeast. *Molecular Cell*, 5(3), pp.501–511.

Yoshida, S. and Toh-e, A., 2002. Budding yeast Cdc5 phosphorylates Net1 and assists Cdc14 release from the nucleolus. *Biochemical and Biophysical Research Communications*, 294(3), pp.687–691.

Zhai, Y., Yung, P.Y.K., Huo, L. and Liang, C., 2010. Cdc14p resets the competency of replication licensing by dephosphorylating multiple initiation proteins during mitotic exit in budding yeast. *Journal of Cell Science*, 123(22), pp.3933–3943.